

Biologie



Heba Dosoki

**The Role of NADPH Oxidase in the Pathogenesis of
Systemic Sclerosis**

2015

Biologie

**The Role of NADPH Oxidase in the Pathogenesis
of Systemic Sclerosis**

INAUGURAL-DISSERTATION

zur Erlangung des akademischen Grades

Doktorin der Naturwissenschaften (Dr. rer. nat.) im Fachbereich Biologie

der Mathematisch-Naturwissenschaftlichen Fakultät

der Westfälischen Wilhelms-Universität Münster

vorgelegt von

Heba Dosoki

aus Ägypten

- 2015 -

„Gedruckt mit Unterstützung des Deutschen Akademischen
Austauschdienstes“

Dekan:	Prof. Dr. Wolf-Michael Weber
Erster Gutachter:	Prof. Dr. med. Markus Böhm
Zweiter Gutachter:	Prof. Dr. rer. nat. Bruno Moerschbacher
Tag der mündlichen Prüfung:	07.12.2015
Tag der Promotion:	18.12.2015

Abstract

Systemic sclerosis (SSc) is a complex autoimmune disease with an incompletely understood pathogenesis that involves vascular damage, autoimmune-mediated inflammation, and fibrosis. These latter processes are heavily regulated by transforming growth factor-beta1 (TGF- β_1), as it induces activation of fibroblasts. We hypothesized (1) that distinct NADPH oxidase (Nox) isoforms, especially Nox4, may regulate TGF- β_1 -mediated activation of human dermal fibroblasts (HDFs), (2) that Nox4 expression is present in SSc fibroblasts, and (3) that suppressing Nox activity in general, or Nox4 specifically, attenuates experimentally induced skin fibrosis. To test these hypotheses, we first performed a detailed expression analysis of all Nox isoforms and adaptor proteins at the RNA and protein levels, and we found that Nox4 is the major Nox isoform expressed by HDFs. Stimulation of normal HDFs with TGF- β_1 resulted in a time- and dose-dependent induction of Nox4 at mRNA and protein levels. This effect was mechanistically dependent on Smad signalling and was also associated with increased NADPH activity. Immunofluorescence analysis using laser confocal microscopy studies further revealed that Nox4 localizes to the endoplasmic reticulum as demonstrated by double staining with protein disulfide isomerase. Nox4 expression was maintained in SSc fibroblasts. Our final set of experiments investigated the effects of inhibiting Nox/Nox4 activity *in vitro* and *in vivo*. Interestingly, pharmacologically inhibiting Nox enzyme activity *in vitro* by DPI, a Nox inhibitor, not only suppressed TGF- β_1 -mediated expression of collagen type I, but it also suppressed the induction of both α -smooth muscle actin and fibronectin 1, two established myofibroblasts markers. We confirmed this finding in other *in vitro* models. Finally, we also explored Nox inhibition *in vivo* using the bleomycin mouse model of SSc. We found that pharmacologically inhibiting Nox activity using DPI or treating mice with Nox4 siRNA lead to significantly reduced collagen content, skin fibrosis and expression of myofibroblasts markers. Overall, these findings show that Nox4 is a key intracellular mediator of fibroblast activation. Moreover, targeting Nox4 may be a novel therapeutic strategy for treating fibrotic skin diseases such as SSc.

Acknowledgment

Above all, I am really thankful to Allah for his infinite blessings, sustenance and providence. Thanks Allah for accepting my prayers, protecting me and keeping me on track during hard times. Thanks Allah for all those kind people you put on my way. There are no words to fully express the deepest gratitude I feel towards everyone who has supported me throughout this incredible journey. I have been extremely fortunate to come across so many people willing to help me achieve this milestone.

First and foremost, I would like to extend my deepest gratitude and appreciation to my supervisor (Doktorvater) **Prof. Dr. Markus Böhm** for giving me the opportunity to undertake this research work. He has always been knowledgeable, compassionate, and encouraging to my research ideas. He provides me with endless guidance and supports me through the difficult periods. He was always there, really thank you for everything!

I would like to thank my lab members **Dr. Agatha, Dr. Nina, Mara** and **Eva** for their discussion, patience and help. All of them provide valuable input to the work and helped me to develop important technical skills to become an independent researcher.

I am grateful to **Prof. Dr. Claus Kerkhoff** for his valuable guidance and suggestions that has often led me to the right direction or even helped me in solving *in situ* technical problems. Endless thanks for his recommendation letters for DAAD and valuable revision of this thesis. Thank you for being around.

I would like to thank my thesis committee **Prof. Dr. Bruno Moerschbacher** and **Prof. Dr. Jörg Kudla** for their effort and support to read and evaluate my thesis. A very special thank you to **Prof. Dr. Hans Schnittler**, our collaborator, and to his laboratory team in University of Münster. I am also very grateful to our collaborator **Dr. Katrin Schröder** in Goethe University of Frankfurt.

I was fortunate to be a part of wonderful department. I learned much from my colleagues and have wonderful memories. I thank all members of the cell biology department who have always been supportive during my study.

I would like to offer special thanks to the German academic exchange service (**DAAD**) and the ministry of higher education in Egypt for the continuous financial support during my stay in Germany.

I must offer my deepest appreciation and very special and infinite thanks to my amazing parents **Salah Eldeen Dosoki** and **Neamat Elabrashy** who raised me to be responsible, independent and taught me to value education. They are always loving me and being supportive to my decisions. Their love and encouragement have made me grow up as the person I am today. Thank you mom and dad, I will make you all proud of me. I would like to thank my twin brother **Mohamed** and my sisters, **Asmaa, Shima** and **Somia** for their honest love, faithful encouragement and endless care for my mother during my stay abroad. Without their prayers and loving support, I would not be where I am today.

I would like to say “Thanks a lot” to my friends Nihal Elnhas, Carolin Pundt, Muna Taha, Rana Siblini, Aziza Ögel, Samar Tarish and Asmaa Elnagar for their faithful prayers, encouragement and for keeping me smile deep from my heart.

*Dedicate to the spirit of my Father and my Mother who
made me the person I am today*

"There is no disease that Allah has created, except that He also has created its treatment."

(Prophet Mohamed)

List of abbreviations

Name	
AD	Actinomycin D
AP1	Activating protein 1
APS	Ammoniumpersulfat
BLM	Bleomycin
BSA	Bovine serum albumin
CaCo2	Human colon carcinoma cell line
cAMP	Adenylyl cyclase pathway,
CRE	cAMP-response- element
CTGF	Connective tissue growth factor
CV	Crystal violet
DAPI	4', 6-Diamidino-2-phenylindol
DMSO	Dimethylsulfoxid
DPI	Diphenyleneiodonium
ECL	Enhanced chemiluminescence
ECM	Extracellular matrix
EGCG	Epigallocatechin-3-gallate
EMT	Epithelial mesenchymal transition
EndoMT	Endothelial-mesenchymal transition)
ERK	Extracellular signal-regulated kinases
FAD	Flavin Adenine dinucleotide
FCS	Fetal calf serum
GSH	Glutathione
H&E	Hematoxylin and eosin
HDFs	Human dermal fibroblasts
HNKs	Normal human keratinocytes
HPR	Horseshoe-peroxidase
HUVEC	Human Umbilical Vein Endothelial Cells
IFN- β	Interferon- β
IPF	Idiopathic pulmonary fibrosis
JAK	Janus kinase
JNK	Jun N-terminal kinase
LPS	Lipopolysaccharid
MAPK	Mitogen activated protein kinase
MNC	Human peripheral blood monocytes
MNC	Human peripheral blood monocytes
MPO	Myeloperoxidase
MTR	MitoTracker Deep Red
NAC	N-acetyl-cysteine
NF- κ B	Nuclear factor-kappaB
NOX	NADPH oxidase
Nrf2	Nuclear factor (erythroid-derived 2)-like 2
PBS	Phosphate buffered saline
PDGF	Platelets-derived growth factor
PDI	Protein disulfide isomerase
PICP	Procollagen Type I C-Peptide
Poldip2	DNA polymerase-delta interacting protein 2
PTPs	Protein tyrosine phosphatases
PVDF	Polyvinylidenedifluorid
ROS	Reactive oxygen species
RPMI	Rosewell Park Memorial Institute
SOD	Superoxide dismutase

List of Abbreviations

SOH	reactive sulfenic acid
Sp3	Sp3 transcription factor
SSc	Systemic sclerosis
TBST	Tris buffered saline with Tween pH 8,0
TEMED	N,N,N',N'-Tetramethylethylenediamin
TGF- β	Transforming growth factor- β
TKs5	Tyrosine kinase substrate 5
TM	Transmembrane domains
TNF- α	Tumor necrosis factor alpha
Tween 20	Polyoxyethylensorbitanmonolaureat
UPR	Unfolded protein response
XTT	2, 3-Bis-(2-methoxy-4-nitro-5-sulfophenyl)-2H-tetrazolium-5-carboxanilid
α -MSH	Alpha-melanocyte stimulating hormone
α -SMA	Alpha smooth muscel actin

Table of Contents

Abstract	I
Acknowledgment	II
Dedication	III
List of abbreviations	V
List of Figures	XII
List of Tables	XV
1. Introduction	1
1.1. Systemic sclerosis	1
1.1.1. Definition and epidemiology	1
1.1.2. The pathogenesis of systemic sclerosis	1
1.1.3. Skin fibrosis in SSc.....	2
1.1.4. Players of skin fibrosis in SSc	3
1.1.5. Experimental model of systemic sclerosis.....	8
1.2. Reactive oxygen species.....	9
1.2.1. Sources of reactive oxygen species generation	9
1.2.2. ROS in cell signaling.....	10
1.2.3. Antioxidant studies in <i>vitro</i> , <i>vivo</i> and clinical trials	11
1.3. NADPH oxidases (NOXs)	12
1.3.1. The family of NADPH oxidases.....	12
1.3.4. Tissue distribution and subcellular localization	14
1.4. NADPH oxidase 4 (Nox4)	15
1.4.1. Structure, function and regulation of Nox4	15
1.4.2. Tissue distribution and subcellular localization	17
1.4.3. Physiological and pathological role of Nox4	18
1.4.4. Pathological role of Nox4 in fibrotic disorders	19
1.5. NADPH oxidase inhibition	20
2. Aim of the study	23
3. Materials and Methods	24
3.1. Materials	24
3.1.1. Chemicals	24
3.1.2. Stimulants and pharmacological inhibitors	25
3.1.3. Media and Buffers	25

3.1.4. DNA ladder and protein markers.....	27
3.1.5. Consumables and kits	28
3.1.6. Primers.....	28
3.1.7. Antibodies.....	30
3.1.8. Instruments and Laboratory equipment.....	31
3.1.9. Animals.....	32
3.1.10. Software and computer programmes.....	32
3.1.11. Cells, cell lines and cell culture reagents.....	33
3.2. Methods.....	33
3.2.1. Cell biological methods.....	33
3.2.2. Molecular biological methods	35
3.2.3. Biochemical methods	38
3.2.4. Immunological methods	41
3.2.5. Cytotoxicity assays.....	41
3.2.6. Confocal immunofluorescences microscopy.....	42
3.2.7. Assessment of dermal thickness.....	43
3.2.8. Determination of collagen protein content ex vivo.....	43
3.2.9. In <i>silico</i> promoter analysis.....	43
3.2.10. Measurement of NADPH oxidase activity assay	43
3.2.11. Statistical analysis.....	44
4. Results.....	45
4.1. Detection of Nox isoforms and adaptor proteins in HDFs.....	45
4.1.1. Expression of Nox4 isoform and its adaptor proteins in normal HDFs	45
4.1.2. Expression of Nox4 isoform and its adaptor proteins in affected skin and HDFs from SSc patients.....	46
4.1.3. Expression of other Nox isoforms, cytosolic subunits and adaptor proteins in normal nHDFs	48
4.1.4. Expression of additional Nox isoform and adaptor proteins in HDFs from SSc patients.....	49
4.2. Subcellular localization of Nox4 in HDFs	51
4.3. Induction of Nox4 expression and NADPH oxidase activity by TGF- β_1 in HDFs	53
4.3.1. TGF- β_1 -upregulates Nox4 expression at mRNA level.....	53
4.3.2. TGF- β_1 upregulates Nox4 expression at protein level.....	54
4.3.3. TGF- β_1 enhances NADPH oxidase activity	56

4.4. Functional characterization of Nox4 in TGF- β_1 -mediated activation of HDFs	57
4.4.1. Effect of the pharmacological inhibitor DPI on cell viability and metabolic activity in nHDFs.....	57
4.4.2. Effect of the pharmacological inhibitor VAS2870 on cell viability in nHDFs	57
4.4.3. Pharmacological inhibition of NADPH oxidase by DPI reduces TGF- β_1 -mediated fibroblast activation	58
4.4.4. VAS2870 does not reduce TGF- β_1 -mediated fibroblast activation.....	60
4.4.5. Genetic knockdown of Nox4 neutralizes TGF- β_1 -mediated fibroblast activation	61
4.5. Regulation of Nox4 expression by TGF- β_1 in HDFs	62
4.5.1. <i>In silico</i> promoter analysis of the human Nox4 gene	62
4.5.2. Nox4 expression is depend on canonical smad3 signaling pathway in HDFs	63
4.6. Pharmacological inhibition of NADPH oxidase activity by DPI reduces cutaneous fibrosis in the bleomycin mouse model of scleroderma.....	65
4.7. Nox4 is an emerging novel target for antifibrotic agents.....	67
5. Discussion.....	69
5.1. Nox4 is abundant in SSc HDFs.....	69
5.2. Nox4 is colocalized with endoplasmic reticulum in HDFs.....	71
5.3. Nox4 expression is regulated by TGF- β_1 in HDFs.....	73
5.4. Nox4 expression is regulated by the Smad2/3 pathway in HDFs	74
5.5. Nox4 inhibition prevented experimentally induced skin fibrosis in the bleomycin mouse model of scleroderma.....	75
5.6. α -MSH suppressed TGF- β_1 -mediated Nox4 gene expression in HDFs	75
6. Conclusion & Future perspectives	78
7. Pharmacological inhibition of Nox4 by GKT137831 reduces TGF- β_1 -mediated fibroblast activation.....	80
8. References.....	82
9. Appendix Figures.....	102
10. Curriculum Vita	104

List of Figures

Figure 1. Cellular and molecular pathways underlying fibrosis in systemic sclerosis.....	2
Figure 2 . Overview of the origin of myofibroblasts.	4
Figure 3. Schematic overview of the signal transduction of TGF- β_1 signaling pathway.....	7
Figure 4. Schematic digram showing the various sources of ROS generation, cellular responses and its pathophysiological effects.....	10
Figure 5. The NADPH oxidase enzyme family.....	14
Figure 6. The structure and regulatory subunits and proteins of Nox4.....	16
Figure 7. Exon structures of Nox4 splice variants compared to prototype Nox4.....	27
Figure 8. Expression analysis of Nox4 and its adaptors in HDFs.....	46
Figure 9. Expression of the Nox4 and its adaptors was preserved in affected skin as well as in HDFs of patients with SSc.....	47
Figure 10. Expression analysis of additional Nox isoforms, adaptor proteins as well as Rac1 and Rac2 in normal nHDFs by endpoint RT-PCR analysis.....	49
Figure 11. Expression analysis of additional Nox isoforms, adaptor proteins as well as Rac 1 and Rac2 in HDFs from patients with SSc by endpoint RT-PCR.....	50
Figure 12. Subcellular localization of Nox4 in cultured HDFs.....	51
Figure 13. Nox4 did not co-localize with mitochondria, lysosomes or focal adhesion in nHDFs.....	52
Figure 14. TGF- β_1 -induced Nox4 mRNA expression in HDFs.....	54
Figure 15. TGF- β_1 induces Nox4 protein expression in nHDFs.....	55
Figure 16. Increase of NADPH enzyme activity by TGF- β_1	56
Figure 17. Effect of DPI on metabolic activity and cell viability of nHDFs as measured by crystal violet assay and XTT assay.....	57
Figure 18. Effect of VAS2870 on metabolic activity and cell viability of nHDFs as measured by crystal violet assay and XTT test.....	58
Figure 19. Effect of DPI on TGF- β_1 -mediated activation of dermal fibroblasts.....	59
Figure 20. Effect of VAS2870 on TGF- β_1 -mediated activation of dermal fibroblasts.....	60
Figure 21. Effect of genetic inhibition of Nox4 on TGF- β_1 -mediated activation of dermal fibroblasts.....	62

Figure 22. Mechanisms of TGF- β_1 -mediated Nox4 expression in nHDFs.....63

Figure 23. Mechanisms of TGF- β_1 -mediated Nox4 expression in nHDFs.....64

Figure 24. The NADPH oxidase inhibitor DPI attenuated BLM-induced skin fibrosis.66

Figure 25. α -MSH suppresses TGF- β_1 -mediated Nox4, Collagen and myofibroblast marker genes expression in HDF.....68

Figure 26. Schematic illustration of the proposed interaction between TGF- β_1 -mediated Nox4 induction, α -MSH-signaling, collagen expression and fibroblast activation.....77

Figure 27. Effect of pharmacological inhibition of Nox4 via GKT137831 on TGF- β_1 mediated activation of dermal fibroblasts.81

Appendix Figure 1. Expression analysis of additional Nox isoforms, adaptor proteins as well as Rac1 and Rac2 in normal adult HDFs by endpoint RT-PCR analysis.....102

Appendix Figure 2. Confirmation the specificity of the Nox antibody.....103

List of Tables

Table 1. Animal models of systemic sclerosis.....	9
Table 2. Tissue distribution of Nox family NADPH oxidase	4
Table 3. List of the most common NADPH oxidase inhibitors	21
Table 4. List of chemicals and biochemical reagents used in this study.....	24
Table 5. Stimulants and pharmacological inhibitors.....	25
Table 6. List of sera used in this study.....	25
Table 7. List of buffers and solutions used in this study.....	26
Table 8. List of human PCR primers, amplicons sizes, and references for endpoint RT-PCR and real-time RT-PCR.	28
Table 9. List of murine PCR primers for real-time RT-PCR and amplicons sizes.....	29
Table 10. List of targeted human siRNA sequences	30
Table 11. List of primary antibodies used in this study	30
Table 12. List of secondary antibodies used in this study.....	30
Table 13. List of laboratory equipments used in this study	31
Table 14. List of human and mouse cell used in this study	33
Table 15. Components of separating gel.....	39
Table 16. Components of stacking gel.....	40

1. Introduction

1.1. Systemic sclerosis

1.1.1. Definition and epidemiology

Systemic sclerosis (SSc) is an autoimmune disease characterized by immune dysregulation, microvascular damage inflammation, extensive fibrosis of the skin and internal organs. SSc is associated with mortality and is challenging to treat due to the lack of effective antifibrotic therapies. There is a great variability and heterogeneity between patients with SSc (Bhattacharyya, Wei et al. 2012, Stern and Denton 2015). According to the location of skin fibrosis, SSc is classified into two major clinical subtypes: limited cutaneous systemic sclerosis (lcSSc) and diffuse cutaneous systemic sclerosis (dcSSc). In lcSSc, fingers, distal extremities, hand and face are involved, whereas in dcSSc, skin fibrosis extends to proximal limbs and trunk. Moreover renal, cardiac and pulmonary failure may be occur more often (Maitre, Hours et al. 2004).

The etiology of systemic sclerosis is not completely understood. Beside genetic predispositions environmental triggers such as pollution, exposure to silica or organic solvents, infection with cytomegalovirus have been reported to be involved in the pathogenesis of SSc (Hunzelmann and Brinckmann 2010, Viswanath, Phiske et al. 2013). The development of SSc is sex dependent as women are five times more prone to develop the disease than men. The incidence of SSc estimates 14-21 per million per year in both America and southern Europe and 100 per million in northern Europe and Great Britain, respectively (Mayes, Lacey et al. 2003).

1.1.2. The pathogenesis of systemic sclerosis

The pathogenesis of SSc is complex and remains incompletely understood. It involves a complex interplay between immune system, vasculature and connective tissue system resulting in excessive production of extracellular matrix (ECM) and progressive fibrosis that is considered to be a hallmark of SSc (**Figure 1**). This interplay is likely the driving mechanism and initiates the disease development. The primary event is vascular injury that involves the endothelium and is initiated by viral infection, autoantibodies, toxins, or oxidative stress (Katsumoto, Whitfield et al. 2011). Endothelial damage then stimulates the release of chemokines, the generation of reactive oxygen species (ROS), the production of platelets-derived growth factors which causes a loss in the integrity of the endothelial lining and promotes recruitment and proliferation of immune cells. Under normal condition,

immune cells act in a coordinate manner and participate in the healing process and tissue repair. But under disease conditions, cells suffer from repeated injury leading to accumulation of macrophages, recruitment of lymphocytes and activation of T cells at the site of injury. Consequently, endothelial-derived chemokines and growth factors recruit and activate both mesenchymal progenitor cells and resident fibroblasts. In addition, profibrotic cytokines produced by activated T cells promote the activation of fibroblasts and their differentiation into persistent myofibroblasts. Pathological myofibroblasts finally produce excessive amounts of collagen and other ECM proteins which eventually lead to tissue contraction, permanent scarring and tissue fibrosis (Varga and Abraham 2007).

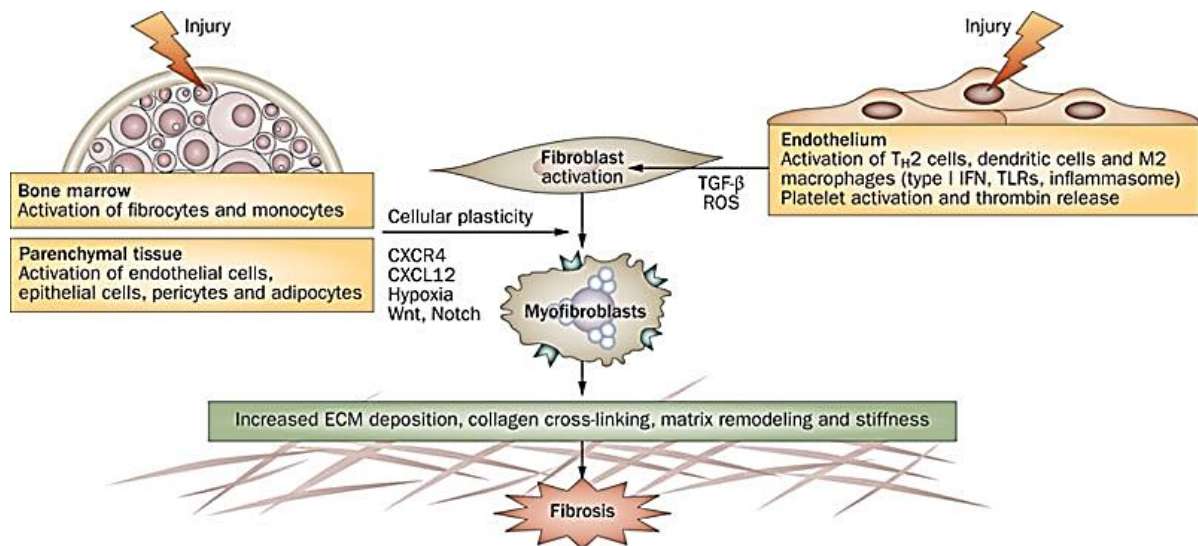


Figure 1. Cellular and molecular pathways underlying fibrosis in systemic sclerosis. (Bhattacharyya, Wei et al. 2012).

1.1.3. Skin fibrosis in SSc

Fibrosis is a distinct pathologic hallmark of SSc and is characterized by the extensive accumulation of fibrous matrix consisting of collagen, elastin and fibronectin. The accumulation leads to the disruption of the normal tissue architecture. Collagen type I is the most abundant protein, constituting about 85 % of skin collagens, and is composed of glycine and proline rich two- α 1(I) and one- α 2(I) chains (van der Rest and Garrone 1991). Pro COL1A1 and COL1A2 polypeptide chains are synthesized by fibroblasts and osteoblasts.

1.1.4. Players of skin fibrosis in SSc

1.1.4.1. Fibroblast and myofibroblasts

The main effector cells in fibrosis are fibroblasts and their contractile counterpart, the myofibroblasts. Actually, the number of fibroblast/myofibroblast foci are considered to be a major prognostic factor in SSc patients (Jinnin 2010). The origins of activated fibroblasts within the fibrotic process are diverse (**Figure 2**). Firstly, fibroblasts are cells of mesenchymal origin which orchestrate the production of a wide variety of ECM proteins, and cytokines as well as growth factors such as platelets-derived growth factor (PDGF), transforming growth factor β_1 (TGF- β_1), connective tissue growth factor (CTGF), and interferon- β (IFN- β) (Denton, Black et al. 2006, Rajkumar, Shiwen et al. 2006, Kisseleva and Brenner 2008). Activation is associated with the appearance of α -smooth muscle actin (α -SMA) and altered ECM secretion. In response to injury, resident fibroblasts can be activated and then migrate into the injured area, where they proliferate and differentiate into myofibroblasts in response to profibrotic cytokines produced by the infiltrating inflammatory cells (Rajkumar, Shiwen et al. 2006). Kuwahara et al showed that perivascular accumulation of macrophages preceded both TGF- β_1 expression and fibroblast proliferation (Kuwahara, Kai et al. 2004). Activated myofibroblasts themselves express TGF- β_1 and other profibrotic substances which self-induce the ongoing fibrotic process (Desmouliere, Geinoz et al. 1993).

There is growing evidence that myofibroblasts also originate from other cell types such as epithelial cells which transdifferentiate by a process known as epithelial mesenchymal transition (EMT) and most recently, endothelial cells that transdifferentiate by a process known as endothelial-mesenchymal transition (EndoMT). These processes have been shown to be involved in renal fibrosis, pulmonary fibrosis and liver fibrosis (Wells 2010, Chapman 2011, Fragiadaki and Mason 2011). Additionally, fibrocytes are a distinct population of leukocytes with characteristics of fibroblasts (Bellini and Mattoli 2007, Mathai, Gulati et al. 2010). These cells are recruited to sites of tissue injury by chemotaxis and play an important role in tissue repair by the production of matrix proteins. Excessive matrix protein generation may also cause pathological fibrogenesis. Microvascular pericytes have also been suggested to contribute to the development of fibrosis (Rajkumar, Sundberg et al. 1999). The balance between matrix formation and degradation is disrupted in fibrotic diseases, usually due to the increased production and the decreased degradation of extracellular matrix proteins (Razzaque and Taguchi 2003). Altered number and function of myofibroblasts are implicated in diseases associated with increased ECM deposition (Tamby,

Chanseaud et al. 2003). In SSc fibroblasts, transcription of collagen genes remains unregulated over several passages (Ihn, Yamane et al. 2005). In addition, these cells overexpress many cytokines such as TGF- β_1 and monocyte chemoattractant protein 1 and TGF- β_1 receptors (Yamane, Ihn et al. 2002).

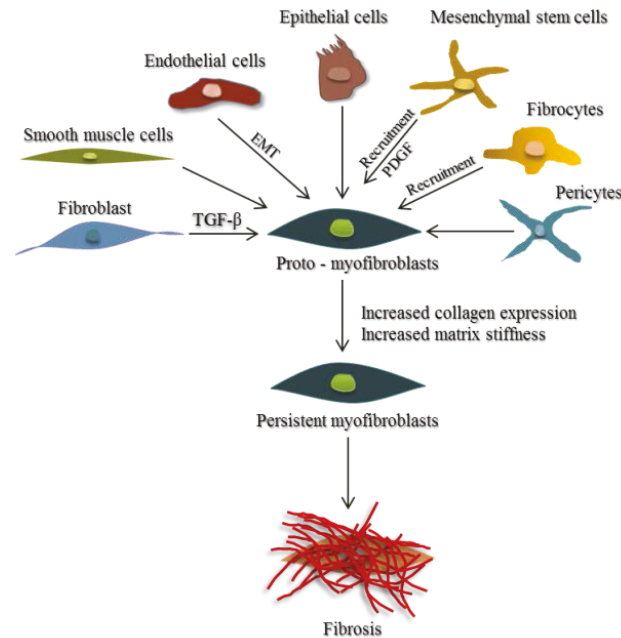


Figure 2 . Overview of the origin of myofibroblasts.

1.1.4.2. Oxidative stress

Oxidative stress is defined as a pathological imbalance between the production of reactive oxygen species (ROS) and the antioxidant defense. The imbalance may cause oxidative damage to critical biomolecules including DNA, lipids and proteins (Hybertson, Gao et al. 2011). Under physiological condition, ROS are produced either as a part of the host defense mechanism against pathogens via NADPH oxidase (Nox2) in phagocytes or produced in a small amount to act as a second messenger in virtually cellular signaling pathways. In contrast, under several pathological conditions such as type 2 diabetes, inflammation and fibrosis, ROS are produced in excessive amounts which lead to many cellular harmful effects such as protein oxidation, lipid peroxidation and DNA damage (Delanian and Lefaix 2004, Yarnold and Brotons 2010). Oxidative stress in skin disease results from both increased generation of ROS and decreased antioxidant defense. This stress therefore contributes to the induction of profibrotic mediators such as TGF- β_1 which in turn

leads to the induction of fibroblast proliferation and differentiation into myofibroblasts, the deposition of ECM proteins as well as the induction of several pro-fibrotic genes including TGF- β_1 and CTGF which results in excessive tissue remodeling and fibrogenesis (Bickers and Athar 2006, Rinnerthaler, Bischof et al. 2015).

In 1993, Dr. Murrell hypothesized that the pathogenesis of SSc is linked to oxidative stress (Murrell 1993). Recently, several studies have shown permanent overproduction of ROS by various cells in SSc, suggesting the involvement of oxidative stress in SSc pathogenesis (Servettaz, Guilpain et al. 2007). Another study showed that sera from SSc patients with pulmonary hypertension lead to oxidative stress-induced activation of collagen synthesis in human pulmonary smooth muscle cells (Chaisson and Hassoun 2013). Moreover, oxidative stress is also involved in several pathogenic states including fibrotic pulmonary disorders such as idiopathic pulmonary fibrosis, liver fibrosis, cardiovascular diseases and chronic kidney disease. Different plasma markers of oxidative stress, i. e. protein carbonyls, nitrosothiols, malondialdehyde, and 8-isoprostane are found to be elevated in patients with SSc (Tsou, Balogh et al. 2014). Additionally, several studies have reported the contribution of oxidative stress in the progression of fibrosis in mice (Gabrielli, Svegliati et al. 2012).

1.1.4.3. The TGF- β_1 signaling and its role in fibrosis

TGF- β_1 is a multifunctional cytokine and member of the TGF- β superfamily. It is recognized as a master regulator not only of physiological wound healing and tissue repair, but also of pathological fibrosis as seen in SSc (Leask and Abraham 2004). It is a 25 kDa polypeptide which is involved in various biological processes such as immune modulation, tumor suppression and promotion, tissue regeneration, wound healing, homeostasis, proliferation and differentiation of cells, apoptosis, adhesion, migration, inflammation and response to injury (O'Sullivan and Levin 2003, Hneino, Francois et al. 2012, Massague 2012). Its mRNA and protein expression is up regulated during the pathogenesis of various diseases including kidney fibrosis, cardiac fibrosis, liver cirrhosis and pulmonary fibrosis as well as cancers. Furthermore, it is secreted by various cell types including fibroblasts, T cells, monocytes and macrophages, platelets and many cell types also possess surface receptors specific for TGF- β_1 . Three mammalian TGF- β isoforms (TGF- β_1 -3) have been identified (Rotzer, Roth et al. 2001). TGF- β_1 is the most abundantly expressed isoform whereas TGF- β_2 was first described in human glioblastoma cells and is also expressed by neurons and astroglial cells in embryonic nervous system (Rotzer, Roth et al. 2001).

The SMAD pathway is the canonical signaling pathway that is activated directly by TGF- β_1 cytokines and plays an important role in regulation of collagen synthesis. However recent studies have also suggested the potential relevance of non-Smad pathways (Akhmetshina, Palumbo et al. 2012). Briefly, the Smad family consists of five receptor-activated Smads (Smad1-5 and 8), one common mediator Smad (Smad4) and two inhibitory Smads (Smad6 and 7) (ten Dijke and Arthur 2007). Once TGF- β_1 bind to its heterodimer receptor, the TGF β type 1 receptor (TGF β -R1) is activated resulting in the phosphorylation of the Smad proteins (Smad2/3). That phosphorylation is the critical step in the initiation of the TGF- β_1 signals. Upon phosphorylation, Smad2 and 3 form complexes with the Co-Smad, Smad4, followed by the translocation to the nucleus where they could act as transcription factors or rather activate the transcription of specific target genes. Smad6 and Smad7 antagonize TGF- β_1 signaling by both hindering Smad2/3 phosphorylation and nuclear translocation of R-Smad/Smad4 (Moustakas and Heldin 2009, Ikushima and Miyazono 2010) (**Figure 3**).

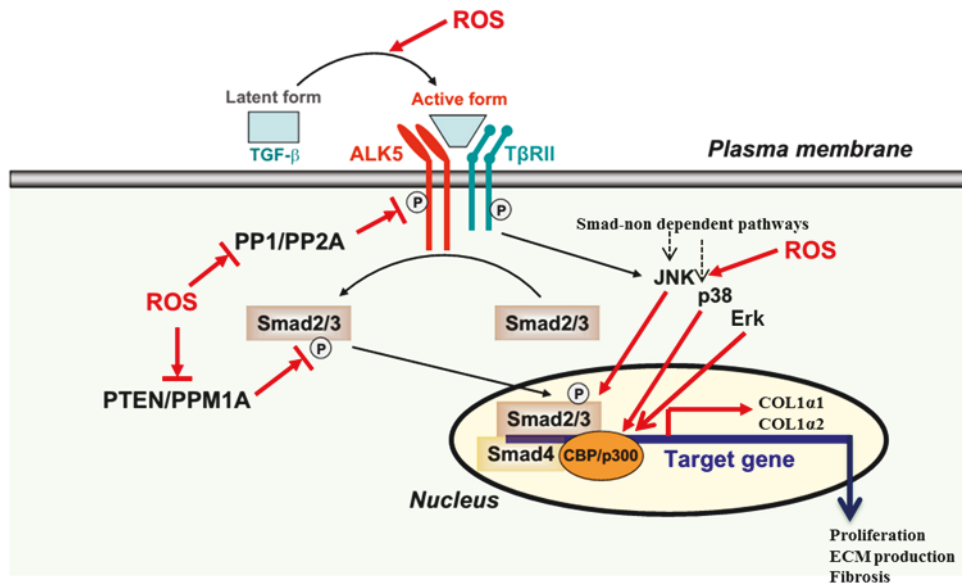


Figure 3. Schematic overview of the signal transduction of TGF-β₁ signaling pathway.

TGF-β signaling is transduced through Smad pathway. TGF-β ligand binds to TGFBR2 and TGFBR1. TGFBR2 phosphorylates (P) TGFBR1, which subsequently phosphorylates and activates Smad2 and Smad3 forming a Smad complex with Smad4 and translocate into the nucleus. In the nucleus, the Smad complex interacts with other DNA-binding transcription factors, and co-activators and co-repressors, binds to the promoter regions of TGF-β target genes and regulates the transcription of target genes. TGF-β can also activate other non-canonical Smad-independent pathways via ROS including c-jun N-terminal kinase (JNK), p38 and Extracellular signal-regulated kinases (ERK). PTEN, Phosphatase and Tensin Homolog deleted on Chromosome 10; PPM1A, Protein phosphatase 1A; ALK5, The TGFβ type I receptor kinase (modified from Jiang, Liu et al. 2014).

The generation of TGF-β₁ is elevated in SSc fibroblasts, as well as in monocyte/macrophages and other infiltrating inflammatory cells (Verrecchia, Mauviel et al. 2006). Microarray studies have demonstrated that TGF-β₁-dependent genes are overexpressed in skin biopsies from patients with SSc (Sargent, Milano et al. 2009). Elevated expression of both TGF-β₁ receptors and TGF-β₁-activating integrins in SSc fibroblasts suggests that sustained autocrine TGF-β₁ stimulation contributes to the maintenance of the activated SSc fibroblast phenotype (Yamane, Ihn et al. 2002). Impaired Smad7 expression or function has been demonstrated in SSc fibroblasts (Varga and Abraham 2007). TGF-β₁ activation is attributed to ROS production by activating NADPH oxidases and inhibiting antioxidants such as glutathione system, establishing a vicious cycle in which ROS activate TGF-β₁ and in turn, activated TGF-β₁ promotes ROS production (Jiang, Liu et al. 2014). Indeed, TGF-β₁ has also

been reported to reduce antioxidant system such as glutathione level which plays a cytoprotective role in oxidative damage (Liu and Gaston Pravia 2010). TGF- β_1 -deficient mice develop numerous autoimmune disorders and are more susceptible to cancer (Hahm, Im et al. 2000). Blockade of autocrine TGF- β_1 signaling with antibodies was unable to normalize Smad subcellular distribution, suggesting that elevated nuclear Smad import was due to alterations downstream of the TGF receptors (Mori, Chen et al. 2003). There are some experimental anti-fibrotic drugs such as Pirfenidone that attempt to target the activation and proliferation of fibroblasts. These drugs were recently approved for the treatment of idiopathic pulmonary fibrosis in Europe and Japan (van Laar and Varga 2015). The anti-cancer drug paclitaxel attenuated Smad activation in SSc tissue grafts in a transplantation model in vivo. Strategies such as antisense oligonucleotides and antibodies targeting TGF- β_1 were effectively applied in various animal models. For example, Giri and colleagues showed that administration of TGF- β_1 antibodies could reduce bleomycin-induced lung fibrosis in mice (Giri, Hyde et al. 1993). Topical application of a peptide inhibitor of TGF- β_1 has been shown to ameliorate skin fibrosis in bleomycin-induced SSc (Dotor and Pablos 2008). In contrast, targeted inhibition with anti-TGF- β_1 antibodies has not been shown to be successful in diffuse SSc. Unfortunately, a randomized clinical trial of human recombinant TGF- β_1 performed by Denton (Denton, Merkel et al. 2007) failed to improve the symptoms in SSc patients. However, owing to its pleiotropic effects on a wide range of cell types, it is still crucial to use TGF- β_1 as an anti-fibrotic target and thus selective blockade of downstream mediators to TGF- β_1 signaling may represent an alternative approach.

1.1.5. Experimental model of systemic sclerosis

Several experimental animal models of skin fibrosis, such as tight skin (Tsk) mouse, Tsk2 mouse, and bleomycin (BLM) induced murine SSc, sclerodermatous graft versus-host disease (Scl-GvHD) mouse exogenous injections of TGF- β_1 and CTGF-induced murine fibrosis model have been reviewed in detail (Yamamoto 2010). The features of those experimental models are summarized in **Table 1**. The BLM mouse model is a well-established model of SSc in which mice develop localized skin fibrosis after repeated intradermal or subcutaneous injections of BLM into the shaved back skin (Yamamoto, Takagawa et al. 1999). BLM is a chemotherapeutic agent and exhibits skin and lung fibrosis as a common side effect. In this mouse model, the sequence of histopathological changes in the skin closely resembles to that seen in SSc including upregulated TGF- β_1 expression and accumulation of α -SMA expressing myofibroblasts (Yamamoto 2006). In vitro, BLM

upregulates collagen and induces TGF- β_1 mRNA expression in cultured rat lung (Yamamoto and Nishioka 2005) and human skin fibroblasts (Yamamoto, Eckes et al. 2000). Also, BLM enhances gene expression of ECM proteins as well as fibrogenic cytokines which may contribute to the induction of fibrosis. Interestingly, superoxide and hydroxyl radicals are generated after bleomycin administration (Yamamoto and Katayama 2011). P47^{phox}-deficient mice exhibited lower level of free radical production through NADPH-oxidase and reduced bleomycin-induced lung fibrosis (Varga and Abraham 2007).

Table 1: Animal models of systemic sclerosis

Mouse model	Characters				
	Skin fibrosis	Skin sclerosis	Lung fibrosis	Increased collagen	TGF- β_1 upregulation
BLM-induced Mouse	+	+	+	+	+
TSK mouse	+	-	+	+	+
Scl-GvHD mouse	+	-	+	+	+
Growth factor injected mouse	+	-	+	+	+
UCD-200 chicken	+	+	+	+	+

1.2. Reactive oxygen species

1.2.1. Sources of reactive oxygen species generation

ROS are small chemically reactive molecules derived from oxygen with one or more unpaired electrons in the outer orbitals. They are classified into the following oxygen radicals: superoxide ($O_2^{\bullet-}$), hydroxyl (OH^{\bullet}), peroxy (RO_2^{\bullet}), alkoxy (RO^{\bullet}) and non-radicals such as hypochlorous acid (HOCl), ozone (O_3), and hydrogen peroxide (H_2O_2). The non-radicals are either oxidizing agent and or easily converted into radical forms. Long time ago, it was known that ROS have an essential role in the host defense mechanism by killing microbes or inactivating microbial virulence factors but recently, another properties have been emerged. ROS has been showed to participate in virtually all intracellular cellular signaling pathways such as inhibition of phosphatases, activation of kinases, angiogenesis and regulation of matrix metalloproteinases (Scandalios 2005, Valko, Leibfritz et al. 2007, Armitage, Wingler et al. 2009). Excessive production of ROS is involved in many pathological disorders such as carcinogenesis, neurodegeneration, atherosclerosis, ischemia,

fibrosis, cancer and diabetes. ROS are produced by different sources including mitochondria, endoplasmic reticulum, peroxisomes, microsomes, cytochrome P-450, lipoxygenase, xanthine oxidoreductase, and nitric oxide synthase (NOS) (Rahman 2007) (**Figure 4**). However, the NADPH oxidase was the only enzyme whose primary biological function is the production of ROS. For instance, mitochondria produce superoxide anions ($O_2^{\bullet-}$) at the complex I and complex III of the electron transport chain through releasing superoxide into both the matrix side of mitochondria and the inner membrane of mitochondria (Drose and Brandt 2012). However, how mitochondria produce ROS is still incompletely understood due to the complexity of mammalian mitochondrial complex. In the ER, ROS are generated as part of oxidative protein folding process (Ushio-Fukai 2008, Bhandary, Marahatta et al. 2012).

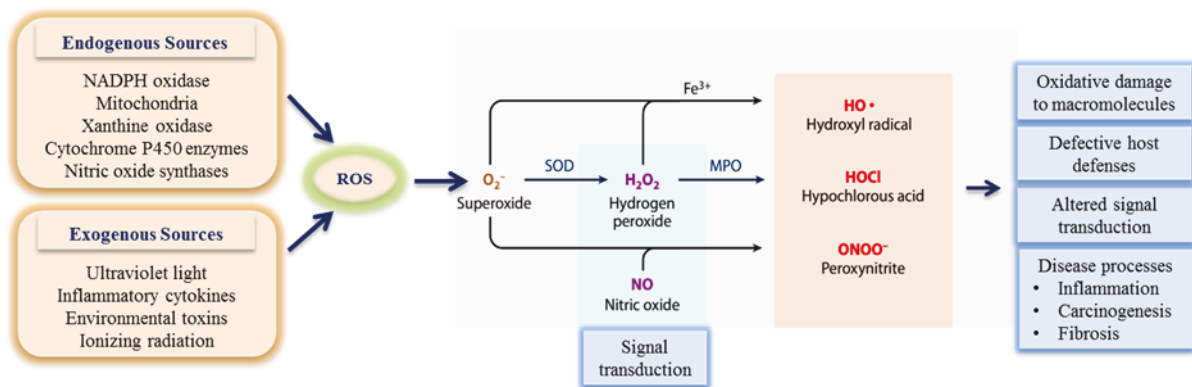


Figure 4. Schematic diagram showing the various sources of ROS generation, cellular responses and its pathophysiological effects. ROS are produced from different exogenous and endogenous sources. ROS may participate in the regulation of redox sensitive pathways like ($O_2^{\bullet-}$, H_2O_2 and NO) which have a moderate reactivity. Other ROS also generated in the biological system like ($HO\bullet$, HOCL and $ONOO^-$) which are highly reactive. Excessive ROS production triggers many pathophysiological effects within the cell (modified from Finkel and Holbrook 2000, Lambeth and Neish 2014).

1.2.2. ROS in cell signaling

ROS have essential roles in cellular signaling through many different mechanisms. ROS were first observed to increase tyrosine phosphorylation after growth factor stimulation. In addition, ROS can directly affect kinase signaling through the redox-dependent modification of a reactive Cys residue within a particular receptor leading to receptor activation. Cysteine residues are target amino acids of H_2O_2 mediated cell signaling

(Holmstrom and Finkel 2014). ROS can modulate redox-reactive Cys residues through switching between oxidation and reduction. Oxidation of these residues forms reactive sulfenic acid (SOH) which leads to conformational changes in target proteins. Subsequently, SOH forms disulfide bonds or is further oxidized to sulfinic (-SO₂H) or sulfonic (-SO₃H) acid (Babalola, Mamalis et al. 2014). These intermediate products can be reversed by reducing system including glutathione (Gth) and the thioredoxin (Trx) system. Both Trx and GSH redox systems have been shown to regulate cell signaling and metabolic pathways differently and independently during diverse stressful conditions (Chung, Wang et al. 2013, Babalola, Mamalis et al. 2014). Furthermore, redox states of Trx and GSH have been used as indicators of oxidative stress and are described to physically interact with different transcription factors (Holmstrom and Finkel 2014). It should be noted that many transcription factors seem to be redox-sensitive such as activator protein 1 (AP1) and Nuclear factor (erythroid-derived 2)-like 2 (Nrf2) (Liu, Colavitti et al. 2005, Pendyala and Natarajan 2010).

1.2.3. Antioxidant studies in vitro, vivo and clinical trials

Cells have the ability to eliminate excess of ROS by various antioxidant defense systems either enzymatically by superoxide dismutase (SOD), catalase, peroxiredoxins and cytosolic glutathione peroxidase (GSH) or by non-enzymatic scavenging compounds such as tocopherols (vitamin E), ascorbate (vitamin C), glutathione, selenium and carotene (Valko, Leibfritz et al. 2007). The localization of these antioxidant enzymes is cell type specific. The most important of these antioxidant enzymes is superoxide dismutase, which exists in three major cellular forms: copper zinc (CuZnSOD, SOD1) in the cytosol, manganese (MnSOD, SOD2) in the mitochondria, and extracellular (SOD3) in the interstitial spaces of tissues and extracellular fluids of many cell types and tissues (Nozik-Grayck, Suliman et al. 2005, Valko, Leibfritz et al. 2007). Other antioxidant enzymes play an important role in the regulation of cellular H₂O₂ like GSH-Px in cytoplasm and catalase which is mainly found in peroxisomes (Vives-Bauza, Starkov et al. 2007). SOD catalyzes two molecules of superoxide to produce H₂O₂ by a chemical reaction called dismutation. Catalase and GSH convert hydrogen peroxide into water. In the presence of iron, superoxide and H₂O₂ react to generate hydroxyl radicals. Neutrophils in inflamed areas produces hypochlorous acid (HOCl), H₂O₂ and chloride by the phagocyte-specific enzyme myeloperoxidase (MPO) (Winterbourn and Hampton 2008).

Many studies reported that SSc patients exhibit a reduced total antioxidant activity, antioxidative vitamins (ascorbic acid, α -tocopherol, and β -carotene), and minerals (zinc,

selenium) (Sfrent-Cornateanu, Mihai et al. 2008). Recently, attempts have been made to find antioxidative molecules either nutritional or pharmacological ones to neutralize or reduce the oxidative stress in cells that are involved in SSc pathogenesis, in particular in endothelial cells and proliferating fibroblasts. For instance, N-acetyl-cysteine (NAC) has been used as an antioxidant, and its effect in SSc was examined in various studies (Yildirim, Kotuk et al. 2005) (Failli, Palmieri et al. 2002). Treatment of dermal fibroblast from SSc patients with NAC reduced the generation of H₂O₂, collagen type I expression and cell proliferation. Other natural antioxidants are now emerging in the field, such as polyphenols from green tea extracts, namely epigallocatechin-3-gallate (EGCG). TGF- β ₁-induced collagen, fibronectin and α -SMA expression was down-regulated after the treatment with EGCG in SSc fibroblasts (Dooley, Shi-Wen et al. 2010), indicating its potential anti-fibrotic effects. Interestingly, EGCG can beneficially inhibit ROS production in vivo models (Pini, Shemesh et al. 2010).

Additionally, many antioxidants mechanisms are involved in the reduction of intracellular ROS production. For example, Nrf2 is activated in response to oxidative stress which results in the induction of many cytoprotective genes. Interestingly, Nrf2-deficient mice displayed the upregulation of ECM genes in response to hypoxia (Saw, Yang et al. 2014), and increased BLM-induced lung fibrosis (Cho, Reddy et al. 2004) has been also observed. Nonetheless, Nrf2 exerts a crucial role in attenuating pulmonary fibrosis through the improvement of antioxidant capacity in mice (Kikuchi, Ishii et al. 2010). Overall, Nrf2 might be targeted as a potential therapy in SSc.

To date, several clinical trials have been reported that the administration of antioxidants might be harmful rather than beneficial and this may be due several reasons including lack of specificity, low oral bioavailability, potency, poor trial design, duration of administration, or lack of relevant biomarkers of oxidation (Galli, Battistoni et al. 2012, Ciofu and Lykkesfeldt 2014, Grygiel-Gorniak and Puszczewicz 2014). Therefore, alternative strategies targeting the enzyme responsible for ROS generation in such fibrotic disease (likely SSc) by developing specific Nox inhibitors are currently emerging. Such agents could represent novel antifibrotic therapeutic strategies.

1.3. NADPH oxidases (NOXs)

1.3.1. The family of NADPH oxidases

The nicotinamide adenine dinucleotide phosphate (NADPH) oxidase (Nox) was first discovered in phagocytic cells. Currently, seven distinct Nox isoforms have been identified in

human: Nox1-5 and dual oxidase: Duox1-2. All Nox isoforms consists of six highly conserved transmembrane domains (TM). These domain including two heme binding regions and the cytoplasmic COOH terminus that contains the binding sites for both Flavin Adenine Dinucleotide (FAD) and NADPH and N-terminus (Geiszt 2006, Bedard and Krause 2007). The classical phagocytic Nox isoform consists of two plasma membrane associated proteins, the catalytic subunit gp91^{phox} (namely Nox2) together with the regulatory units p22^{phox} forming cytochrome b558 complex. The remaining oxidase components reside in the cytosol and include other regulatory subunits p40^{phox}, p47^{phox}, p67^{phox} and the small GTPase Rac1/2 (Figure 5). Upon stimulation, p47^{phox} is phosphorylated and forms a complex with the other cytosolic subunits. This complex translocate to the cell membrane where it assembles with cytochrome b558 to constitute the active enzyme which transfers electrons from the reduced substrate NADPH to FAD, then to the first and second heme redox centers and finally to molecular oxygen to produce superoxide, however this key catalytic subunit also requires the assembly of the five subunits for activation (Cross and Segal 2004). All Nox isoforms release different type of ROS whereas Nox1, 2 and 5 produce superoxide while Nox4 and Duox1/2 produce mainly hydrogen peroxide. Notably, the amount and duration of ROS production is significantly less than that of the phagocyte Nox enzyme (Kawahara and Lambeth 2007). These variations may influence the activation mechanisms of individual isoforms. Additionally, it has been reported that all Nox isoforms bind to one or more cytosolic or regulatory proteins which essential for their function (Li and Shah 2003, Bedard, Lardy et al. 2007). Nox1 activity requires p22^{phox}, Noxo1 (or possibly p47^{phox} in some cases) and Noxa1, and the small GTPase Rac. Nox2 requires p22^{phox}, p47^{phox}, p67^{phox}, and Rac. Nox3 requires p22^{phox} and Noxo1. In contrast, Nox4 requires p22^{phox} in some cells but usually it is constitutively active without the requirement for other subunits, this isoform is discussed in details in the chapter 1.4. Unlike Nox1-Nox4, Nox5, Duox1/2 are activated by Ca²⁺ and do not appear to require other activator or organizer subunits (Rizvi, Heimann et al. 2012) (Figure 5).

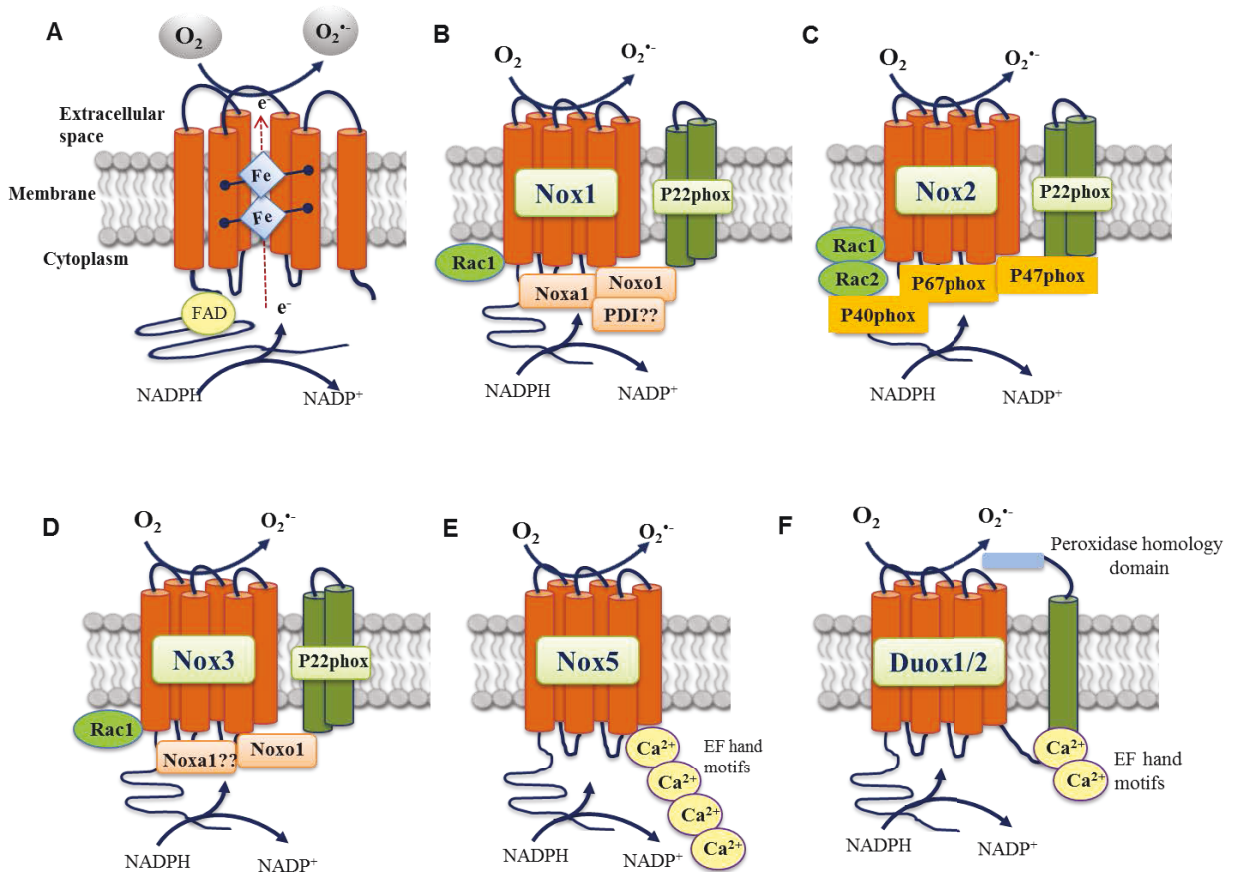


Figure 5. The NADPH oxidase enzyme family. (A) The core structure of the NADPH oxidase. (B-E) The structure and subunit composition of Nox1, Nox2, Nox3, Nox5 and Duox1/2.e-, electron: FAD, flavin adenine dinucleotide: Fe, Hem group. Details are described in the text.

1.3.4. Tissue distribution and subcellular localization

Nox enzymes are widely distributed in many cell types and tissues and the rate of expression is cell and tissue-dependent. They are expressed in a small number of tissues at high levels but show intermediate to low-level expression in many other tissues (**Table 2**). Nox2 is abundant in phagocytes; however, it also appears to be widely expressed in a large number of tissues including thymus, small intestine, colon, spleen, pancreas, ovary, placenta, prostate, and testis. Nox4 was initially discovered in the kidney. Currently, Nox5 is restricted to humans and absent in rodents which hindered studies of Nox5 in mouse. Nox enzymes also display wide subcellular localization within different cellular compartments. In phagocytes, Nox2 localizes to both intracellular and plasma membrane (Bae, Oh et al. 2011). In non-

phagocytic cells, the subcellular distribution depends on the cell type. For example, in smooth muscle cells, Nox2 is localized with the perinuclear cytoskeleton. In neurons, Nox2 is localized in the membranes of synaptic sites (Tejada-Simon, Serrano et al. 2005). Nox4 is suggested to be localized in intracellular membranes.

Table 2. Tissue distribution of Nox family NADPH oxidase

Enzyme	Other names	Regulatory factors	High level of expression	Intermediate or low expression
Nox1	Mox1, gp91-2	Noxo1, Noxa1 and p22 ^{phox}	Colon	Aortic smooth muscle, uterus, prostate, endothelium, osteoclasts and retinal pericytes
Nox2	gp91 ^{phox} , CYBB	p22 ^{phox} , p47 ^{phox} , p67 ^{phox} , p40 ^{phox} , Rac1-2	Phagocytes	lymphocytes, neurons, endothelium, cardiomyocytes, hematopoietic stem cells, skeletal muscle, hepatocytes, smooth muscle cells
Nox3	gp91-3	Noxo1, Noxa1??	Inner ear	Sensory epithelia, fetal spleen, brain
Nox4	Renox, KOX, KOX	p22 ^{phox} , Poldip2??	Kidney, blood vessels, fibroblasts,	Osteoclasts, smooth muscle cells, hematopoietic stem cells, keratinocytes, melanoma cells, neurons
Nox5	-	Calcium	Lymphoid tissue, testis	Endothelium, smooth muscle, pancreas, placenta, ovary, uterus, stomach, various fetal tissues
Duox1	ThOx1	Calcium	Thyroid	Airway epithelia, tongue epithelium, cerebellum, testis
Duox2	ThOx2	Calcium	Thyroid	Salivary and rectal glands, gastrointestinal epithelia, airway epithelia, uterus, gall bladder, pancreatic islets

1.4. NADPH oxidase 4 (Nox4)

1.4.1. Structure, function and regulation of Nox4

The human Nox4 gene is located on chromosome 11. Nox4 is a 67 kDa protein sharing 39% amino acid identity with Nox2. Nox4 comprises six membrane- α -helices connected by five loops, namely loops A-E, and a dehydrogenase (DH) domain that contains the binding sites for FAD and NADPH as illustrated in **Figure 6**. The A,C and E-loops face the outer space of the membrane while B and D loops Face the cytoplasm side of the membrane where DH domain is located (Yoshida and Tsunawaki 2008). Unlike other Nox isoforms, Nox4 is constitutively active and it produces mainly H₂O₂ through the highly conserved histidine residue in the E-loop (Takac, Schroder et al. 2011) and superoxide (Boudreau, Emerson et al. 2009). According to the recent model proposed by Nisimoto (Nisimoto, Diebold et al. 2014), two molecules of oxygen were sequentially reduced to superoxide then two molecules of superoxide dismutated spontaneously by SOD into H₂O₂ and oxygen.

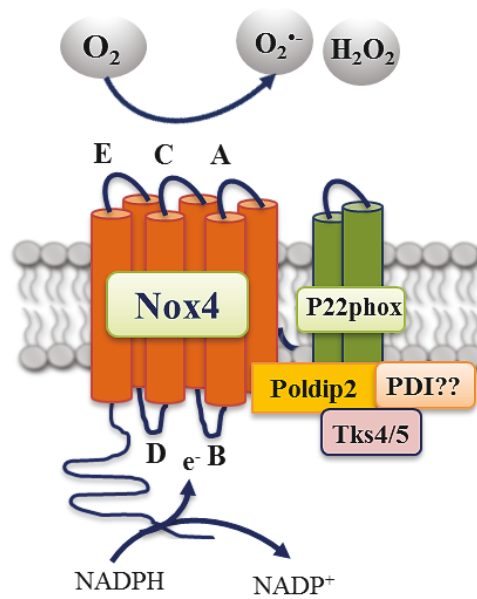


Figure 6. The structure and regulatory subunits and proteins of Nox4. Details are described in the text.

At the mRNA level, Nox4 undergo alternative splicing generating 4 splice variants, NoxB, NoxC, NoxD and NoxE in addition to the prototype Nox4A (Goyal, Weissmann et al. 2005), as illustrated in **Figure 7**. Nox4 is associated with p22^{phox} and does not require any regulatory subunits for ROS production.

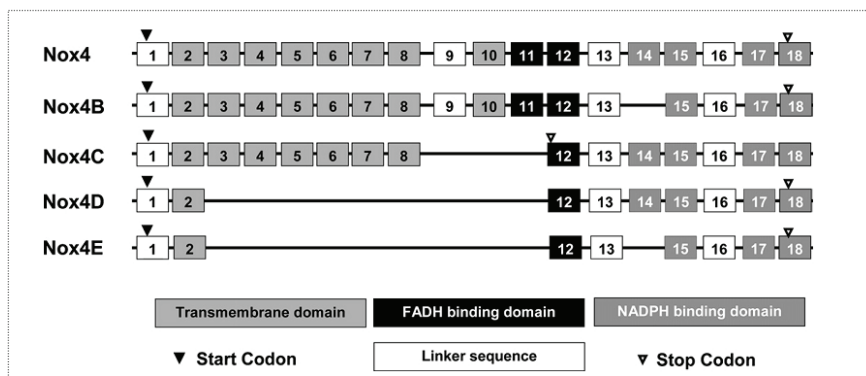


Figure 7. Exon structures of Nox4 splice variants compared to prototype Nox4. The numbers in box represent the exon number and the black lines represent introns (Goyal, Weissmann et al. 2005).

The regulation of Nox4 activity is quite complex and occurs at the transcriptional and post-transcriptional level. Several studies also suggest possible N-glycosylation of the

canonical protein (65kDa) during the posttranslational maturation, increasing its molecular weight (75-80 kDa). Unlike other Nox isoforms, Nox4 is solely regulated via its expression level, and its activation depends on its interaction with p22^{phox} (Ambasta, Kumar et al. 2004). Nevertheless, recent studies have demonstrated that the modulation of Nox4 activity occurred by proteins such as the DNA polymerase-delta interacting protein 2 (Poldip2)(Lyle, Deshpande et al. 2009), tyrosine kinase substrate 5 (TKs5)(Diaz, Shani et al. 2009) the protein disulfide isomerase (PDI) (Janiszewski, Lopes et al. 2005), although the exact mechanisms in SSc cells need to be elucidated. Several cytokines and growth factor have been reported to modulate Nox4 expression such as TGF- β_1 , TNF- α , PDGF and LPS in different cell types. Additionally, various transcription factors including Smad2/3 (Sturrock, Cahill et al. 2006), E2F (Zhang, Sheppard et al. 2008), Nrf2 (Pendyala, Moitra et al. 2011), NF- κ B (Manea, Tanase et al. 2010), HIF-1 α (Diebold, Petry et al. 2010, Lassegue and Griendling 2010), Sp3 and Sp1 (Katsuyama, Hirai et al. 2011), c-jun and STAT3 (Manea, Tanase et al. 2010) have been identified to bind to the Nox4 promoter thereby regulating its expression. Nox4 is consistently upregulated by TGF- β_1 in all cell types tested (Brown and Griendling 2009, Lassegue and Griendling 2010). Nox4 may also be involved in the regulation of redox-sensitive pathways (MAPK, TGF- β_1 , Nrf2/KEAP1) through hydrogen peroxide (H₂O₂) production which has been reported to act as a second messenger in physiological conditions (Konior, Schramm et al. 2014). Moreover, histone deacetylases (Siuda, Zechner et al. 2012), histone modification (Sanders, Liu et al. 2015) and miRNAs (Varga, Kupai et al. 2013) have been proposed to affect Nox4 expression at the posttranscriptional level.

1.4.2. Tissue distribution and subcellular localization

Nox4 displays a wide tissue expression suggesting a number of diverse functions ranging from oxygen sensing to fibrotic processes. Nox4 mRNA is essentially found in renal tissue (fetal and adult) and in diverse tissues (pancreas, lung, placenta, ovary, testis, muscles and fetal tissues in general). At the cellular level, Nox4 mRNA is found in various cell types including smooth muscle cells, endothelial cells, fibroblasts, adipocytes, cardiomyocytes, neurons, and keratinocytes. Nox4 is also found in hematopoietic stem cells (Piccoli, Ria et al. 2005), osteoclasts(Yang, Zhang et al. 2004), melanoma cells (Brar, Kennedy et al. 2002), neurons (Kleinschnitz, Grund et al. 2010), keratinocytes (Chamulitrat, Stremmel et al. 2004), adipocyte (Kanda, Hinata et al. 2011), embryonic stem cells (Bartsch, Bekhite et al. 2011), chondrocytes (Grange, Nguyen et al. 2006), hepatic stellate cells (Ikeda, Ishii et al. 2011),

epithelial cells (Carnesecchi, Deffert et al. 2011), and podocytes (Piwkowska, Rogacka et al. 2011).

Although Nox4 has been reported to be localized at intracellular membranes even its subcellular localization is still in debate. It has been described in the endoplasmic reticulum (ER) of cardiomyocyte where Nox4 interacts with the protein disulfide isomerase (PDI), in the nuclei of human airway smooth muscle cells, in the plasma membrane of HEK 293 cells, and in the mitochondria of mesangial cells of the kidney cortex (Janiszewski, Lopes et al. 2005). In other studies, Nox4 was also described to translocate to the plasma membrane after interacting with its partner component p22^{phox} in different cell types (Laurindo, Fernandes et al. 2008, von Lohneysen, Noack et al. 2008). It has been hypothesized that the specific physiological role may depend on its intracellular localization and/or its ability to produce H₂O₂, a stable and diffusible signaling molecule (Takac, Schroder et al. 2011). Notably, the localization of Nox4 in intracellular membranes is dependent upon the presence of signal sequences specific to the ER (Chen, Kirber et al. 2008), to mitochondria (Ago, Kuroda et al. 2010) and to the nucleus (Matsushima, Kuroda et al. 2013). Alternative splicing of Nox4 mRNA, post-translational modifications has been recently suggested to direct Nox4 synthesis in different subcellular compartments (Anilkumar, San Jose et al. 2013). However, the intracellular localization of Nox4 may influence its downstream targets.

1.4.3. Physiological and pathological role of Nox4

Nox4 has an important role in a variety of physiological and pathological conditions in different cell types. It has been showed that Nox4 play a physiological role in anti-inflammatory response in neurons, senescence of human endothelial cells, oxygen sensing in HEK293 cells, migration in vascular smooth muscle cells, insulin regulation in adipocytes; proliferation in preadipocytes, osteoclastogenesis and bone resorption in osteoclasts, and apoptosis in cerebral microvascular endothelial cells (Guo and Chen 2015).

Nevertheless, several studies reported the involvement of Nox4 activation in various pathological conditions, notably cardiovascular disease, diabetes, atherosclerosis, kidney and lung fibrosis. In both fibroblasts and smooth muscle cells, Nox4 mRNA is increased by hypoxia, and knockdown of Nox4 decreases cell proliferation (Li, Tabar et al. 2008, Ismail, Sturrock et al. 2009). TGF- β ₁ also induces Nox4 expression and ROS production in HPASMC (Sturrock, Cahill et al. 2006). In addition, Nox4 is involved in TGF- β ₁-induced epithelial-to-mesenchymal transition and migration of breast epithelial cells. Interestingly,

knock-down of Nox4 by siRNA Nox4 gene ameliorates bleomycin-induced pulmonary fibrosis in mice by decreasing ECM protein accumulation (Hecker, Vittal et al. 2009).

1.4.4. Pathological role of Nox4 in fibrotic disorders

Nox enzymes have been implicated in the pathogenesis of fibrosis at different pathological conditions such as diabetic nephropathy, pulmonary fibrosis, cardiac hypertrophy, and pancreatic fibrosis (Barnes and Gorin 2011, Bhattacharyya, Wei et al. 2011). Indeed, several growth factors which participate in SSc pathogenesis including TGF- β_1 , PDGF, angiotensin II and endothelin 1 have been shown to modulate the expression of Nox protein, in particular Nox4 (Gorin, Ricono et al. 2003, McCann, Disting et al. 2008, Amara, Goven et al. 2010, Kim, Kim et al. 2011). For example, in heart, TGF- β_1 stimulates Nox4-mediated generation of ROS leading to increased expression of ECM proteins such as collagen and fibronectin (Rocic and Lucchesi 2005). Nox4 is upregulated in lungs of patients with idiopathic pulmonary fibrosis (IPF) as well as in kidney and liver fibrosis (Amara, Goven et al. 2010, Bondi, Manickam et al. 2010). Nox4 expression is robustly increased in pulmonary fibroblasts from patients with idiopathic pulmonary fibrosis and also in rodent models. Inhibition of Nox4 using genetic or pharmacological approaches prevents lung fibrosis (Hecker, Vittal et al. 2009) and suggests a prominent role for Nox4 in the pathogenesis of pulmonary fibrosis. Additionally, Nox4-derived ROS reversibly inactivate cysteine-dependent serine/threonine protein tyrosine phosphatases (PTPs) resulting in the increased activity of various kinases including c-jun amino-terminal kinase (JNK), mitogen-activated protein kinases (MAPKs), Janus kinase (JAK), c-Src, and extracellular signal-regulated kinases (ERKs) (Anilkumar, Weber et al. 2008). Furthermore, fibroblasts isolated from lungs of patients with IPF generated increased H₂O₂ in response to TGF- β_1 , and induced death of the respiratory epithelial cells (Sakai and Tager 2013). In vivo, p47^{phox}-deficient mice are protected against bleomycin-induced lung and liver fibrosis (Manoury, Nenan et al. 2005, Levin, Petrasek et al. 2012). Indeed, Nox has been reported to be involved in many skin disorders as hypertrophic scars and keloids fibroproliferative disorder in which Nox upregulates pyridinoline cross-link formation in collagen (Wan and Evans 1999, Wan, Wu et al. 2002, De Felice, Wilson et al. 2009). Nox4-dependent generation of ROS has recently been postulated to be involved in the fibrotic process in SSc. However, experimental findings supporting the involvement for Nox4 in the fibrotic progress in SSc are still lacking.

1.5. NADPH oxidase inhibition

Given the fact that oxidative stress is involved in the pathogenesis of many fibrotic diseases, many efforts have been dedicated to discover and develop effective isoform-specific Nox inhibitors (**Table 3**). Inhibition of Nox could be achieved through several strategies: by decreasing gene or protein expression via siRNA techniques; by inhibiting the assembly of the cytosolic component that may prevent the activation of Nox enzymes, by post-translational modification of the oxidase itself and/or its upstream activators by disrupting Nox-mediated cell signaling, by competitive inhibition of Nox enzymes with molecules mimicking NADPH structure; and by inhibiting the phosphorylation of the p47^{phox} subunit (Altenhofer, Kleikers et al. 2012, Schramm, Matusik et al. 2012, Rodino-Janeiro, Paradela-Dobarro et al. 2013, Babalola, Mamalis et al. 2014).

Table 3. List of the most common NADPH oxidase inhibitors

Name	Proposed mechanism of action	Reference
Apocynin	Inhibits association of p47 ^{phox} with membrane-bound heterodimer	(t Hart, Simons et al. 1990)
DPI	abstracts electrons from FAD and then prevents electron flow through the flavocytochrom and block the activity	(Stuehr, Fasehun et al. 1991)
GKT137831/ GKT136901	They might act as a competitive inhibitor to Nox enzyme but the mechanism is still under investigation	(Gianni, Taulet et al. 2010)
N-acetyl-L-cysteine	Increases SOD2 activity caused decreased oxidative stress	(Moon, Kang et al. 2006)
(PHTE)(2)NQ (a tellurium-based catalyst 2,3 bis (phenyltellanyl)naphthoquinone)	Reduces the intracellular level of ROS, reveals cytotoxic activity in hyperproliferative fibroblasts	(Marut, Kavian et al. 2012)
Pulmbagin	Inhibits Nox-derived ROS; the mechanism is still unknown	(Ding, Chen et al. 2005)
VAS2870	Directly interacts with the Nox complex and inhibit its assembly	(Tsai and Jiang 2010)

Diphenylene iodonium (DPI) is very potent inhibitor of NADPH oxidases. It inhibits NADPH oxidases and other FAD-containing enzymes (Wind et al., 2010). Notably, it was found that DPI also inhibits the production of ROS in a variety of other cell types including white blood cells, epithelial cells of the gut and fibroblast that express different Nox isoforms as Nox1, Nox2 and Nox4. As a rule of thumb, if the signal is not blocked by DPI, this usually means that the ROS are not derived from Nox (Maghzal, Krause et al. 2012). Thus, DPI is a useful tool for studying Nox enzymes in vitro. Thus, interpretation of in vitro results with

DPI needs to be combined with data from other techniques such as gene ablation of Nox isoforms. In a BLM-lung fibrosis model, administration of DPI 1 mg/kg resulted in a decrease of superoxide anion production measured by lucigenin enhanced chemiluminescence, as well as attenuation of lung and intestinal injury (Abdelrahman, Mazzon et al. 2005). Caution should be taken when using DPI for inhibiting ROS production in vivo as it lacks specificity and has cytotoxic effects at certain doses thereby limiting the use of DPI in clinical trials. Therefore, only a small number of studies have been published in which the potential beneficial effects of DPI was examined in in vivo animal models.

Apocynin is an orally natural active agent that can block NADPH oxidase assembly but requires a reaction with peroxidase for its activation, and therefore does not work immediately (Abdelrahman, Mazzon et al. 2005). Apocynin reduces ROS production when tested in animal models of arthritis, asthma and hypertension (Schramm, Matusik et al. 2012). In addition, apocynin acts to lower ROS levels in non-phagocytic cells by functioning as an antioxidant rather than a Nox inhibitor and therefore its use is currently limited. By contrast, apocynin acts at the level of the p47^{Nox} subunit thereby preventing its association with the membrane-bound heterodimeric Nox-p22^{Nox} complex (Drummond, Selemidis et al. 2011).

VAS2870 and **VAS3947** (Vasopharm) are cell permeable thiotriazolo pyrimidine compounds that are reported as rapid and reversible inhibitors of NADPH oxidase activity. VAS2870 has also been shown to efficiently reduce ROS generation in vitro. It was effective in inhibiting PDGF-stimulated cell migration and PMA-dependent stimulation of superoxide production from NADPH oxidase in human phagocytes (ten Freyhaus, Huntgeburth et al. 2006, Wind, Beuerlein et al. 2010). However, the mechanism has not yet been fully established. There is currently no information on the in vivo effects of VAS2870 in either normal or diseased animal models. GKT137831 and GK136901 are very recent Nox1/4 inhibitors (Genkyotex) and have drawn considerable attention. Indeed, recent reports have demonstrated that NADPH oxidase activity, p38MAP kinase activity as well as TGF- β ₁-induced fibronectin generation were attenuated in mouse proximal tubular cells after GKT136901 administration (Sedeek, Callera et al. 2010). Similar, it has been shown that GKT137831 attenuated hypoxia-induced pulmonary vascular cell proliferation in mice, suggesting its value in pulmonary hypertension (Green, Murphy et al. 2012). Interestingly, Hecker et al. demonstrated that myofibroblasts phenotype was reversed following treatment with the Nox4-selective small-molecule inhibitor GKT137831 (Hecker, Logsdon et al. 2014). GKT137831 and GK136901 have unique features more than other identified Nox inhibitors.

They display high oral bioavailability, lack of off-target effects and show a good safety profile in vivo. Therefore, GKT137831, has been applied in phase II clinical studies in patients with diabetic nephropathy revealing promising data in several other disease models, including atherosclerosis (Di Marco, Gray et al. 2014), idiopathic pulmonary fibrosis (Hecker, Cheng et al. 2012) and liver fibrosis (Jiang, Chen et al. 2012).

2. Aim of the study

SSc is a complex chronic disease with a high rate of morbidity and mortality without any effective therapies to date. A better understanding of the molecular mechanism that underlies the pathogenesis of SSc will provide a novel approach for an effective treatment for this disease. TGF- β_1 appears as a master regulator not only of collagen synthesis and pathological extracellular matrix remodeling but also being responsible for fibroblast activation and differentiation into a profibrotic myofibroblast phenotype. In addition, there is growing evidence that oxidative stress may also contribute to tissue damage in SSc. One of the major sources of ROS generation is the multicomponent membrane-bound Nox. However, the precise molecular interplay between TGF- β_1 and NADPH oxidase remains largely unexplored in human dermal fibroblasts. Therefore, the present study has been performed to explore the role of NADPH oxidase in the context of TGF- β_1 signaling within fibrotic disorders especially skin fibrosis.

According to our preliminary data we have hypothesized that NADPH oxidase 4 (Nox4) represents an intracellular nodal point that orchestrates collagen synthesis, differentiation of dermal fibroblasts into a profibrotic myofibroblast phenotype, and thus dermal fibrosis. To verify that hypothesis we set up the following specific aims:

Aim 1: To investigate the expression of Nox4 and related Nox isoforms and cytosolic co-factors in both human dermal fibroblasts and scleroderma fibroblasts.

Aim 2: To determine whether Nox4 modulates activation and differentiation of fibroblasts to myofibroblasts in response to TGF- β_1 .

Aim 3: To evaluate whether pharmacological or genetic inhibition of Nox4 suppress dermal fibroblasts differentiation into a profibrotic myofibroblast phenotype.

Aim 4: To analyze whether the neuropeptide α -melanocyte stimulating hormone (α -MSH) has an inhibitory effect on TGF- β_1 -mediated Nox4 expression.

Aim 5: To determine whether pharmacological Nox inhibitors affect experimentally induced skin fibrosis in a bleomycin animal model of scleroderma

3. Materials and Methods

3.1. Materials

3.1.1. Chemicals

Table 4: List of chemicals and biochemical reagents used in this study

Chemical	Manufacture
Acetic acid	Sigma-Aldrich, Taufkirchen
Acetone	Sigma-Aldrich, Taufkirchen
Acrylamide	Carl Roth, Karlsruhe
Agarose	Biozym, Hessisch Oldendorf
Ammonium persulfate (APS)	Sigma-Aldrich, Taufkirchen
Bromophenol blue	Merck, Darmstadt
Chloroform	Merck, Darmstadt
DAPI	Sigma-Aldrich, Taufkirchen
DMSO (Dimethylsulfoxide)	Sigma-Aldrich, Taufkirchen
DPBS w/o Ca ²⁺ or Mg ²⁺	Merck, Darmstadt
ECL	Carl Roth, Karlsruhe
EDTA	Applichem, Darmstadt
Ethanol	Sigma-Aldrich, Taufkirchen
EGTA	Sigma-Aldrich, Taufkirchen
Ethidium bromide	Sigma-Aldrich, Taufkirchen
Glycine	Carl Roth, Karlsruhe
GoTaq polymerase	Promega, Mannheim
HCl	Carl Roth, Karlsruhe
Hydrogen peroxide solution, 30%	Carl Roth, Karlsruhe
Isopropyl alcohol	Carl Roth, Karlsruhe
KH ₂ PO ₄	MERCK, Darmstadt
L-Glutamine	Sigma-Aldrich, Taufkirchen
Lipofectamin 2000	Invitrogen, UK
Luciginin	Enzo, Lörrach
Methanol	Carl Roth, Karlsruhe
DABCO / Mowiol 4-88	Carl Roth, Karlsruhe
NADH	Sigma-Aldrich, Taufkirchen
NaHCO ₃	MERCK, Darmstadt
NaH ₄ Cl	MERCK, Darmstadt
NaCO ₃	Carl Roth, Karlsruhe
Nitrocellulose	Millipore, Bedford, MA, USA
Penicillin/Streptomycin (10,000 U/ml, 10 mg/ml)	Gibco, Darmstadt
Protease inhibitor cocktail tablets	Roche Diagnostics GmbH, Mannheim
RedSafe	iNtron biotechnology, Freiburg
RNAse free Water	Qiagen, Hilden

Material and Methods

Sodium Dodecylsulfate (SDS)	Sigma-Aldrich, Taufkirchen
Sucrose	Sigma-Aldrich, Taufkirchen
SYBR Green Rox Mix	Thermo Fisher Scientific, Epsom, Surrey, UK
TEMED	Sigma-Aldrich, Taufkirchen
Triton X-100	Sigma-Aldrich, Taufkirchen
Tris (HCl)	Carl Roth, Karlsruhe
Triton-X-100	Sigma-Aldrich, Taufkirchen
Trizol reagent	iNtron biotechnology, Freiburg
Trypsin 0.25 %	Gibco, Karlsruhe
Tween 20	Sigma-Aldrich, Taufkirchen
Trizol (peqGOLD-Trifast)	PeqLab, Erlangen, Deutschland
Trypan blue	Sigma-Aldrich, Taufkirchen
β -Mercaptoethanol	Carl Roth, Karlsruhe

3.1.2. Stimulants and pharmacological inhibitors

Table 5: List of stimulants and pharmacological inhibitors used in this study

Name	Manufacture
α -MSH	Calbiochem, Schwalbach
Actinomycin D	Sigma-Aldrich, Taufkirchen
Bleomycin	Sigma-Aldrich, Taufkirchen
Cycloheximide	Sigma-Aldrich, Taufkirchen
Diphenyleiodonium	Sigma-Aldrich, Taufkirchen
SIS3	Calbiochem, Schwalbach
TGF- β_1 (Human)	Peprtech, Hamburg
TGF- β_1 (murine)	eBioscience, Frankfurt am Main
VAS2870	Sigma-Aldrich, Taufkirchen

3.1.3. Media and Buffers

3.1.3.1. Sera

Table 6: List of sera used in this study

Name	Manufacturer
Bovine Serum Albumin (BSA)	PAA, Pasching, Austria
Fetal Bovine Serum (FBS)	PAA, Pasching, Austria
Normal goat serum	Dako, Glostrup, Denmark

3.1.3.2. Media

All cell culture media used in this study were purchased from Gibco (Karlsruhe)

- **Dulbecco's Modified Eagle Medium** (Advanced DMEM/F-12) was supplemented with 2 mM L-glutamine, 5 % FCS, 1 % penicillin (50 U/ml) and streptomycin (50 µg/ml).
- **Roswell Park Memorial Institute Medium** (RPMI1640) was supplemented with 2 mM L-glutamine, 10 % FCS, 1 % penicillin (50 U/ml) and streptomycin (50 µg/ml).

3.1.3.3. Buffers

Table 7: List of buffers and solutions used in this study

Name	Components
DNA loading buffer (6x)	0.25 % Bromophenol blue 0.25 % Xylene cyanol 30.0 % Glycerol 100.0 mM EDTA Adjusted with HCl to pH 8.0
Blotting buffer	25 mM Tris base 192 mM glycine 10 % methanol pH adjusted with HCl to 7.6
Laemmli sample buffer (2x)	100 mM Tris-HCl, pH 6.8 4 % SDS 20 % Glycerol 0.2 % Bromophenol blue 10 % β-Mercaptoethanol H ₂ O up to 10 ml
Lysis buffer (Immunoprecipitation buffer)	50 mM HEPES, pH adjusted to 7.5 150 mM NaCl 10 % Glycerol 1 % Triton-X-100 1.5 mM MgCl ₂ 1 mM EGTA 100 mM NaF 10 mM Pyrophosphate 0.01 % NaN ₃ H ₂ O up to 100 ml pH 7.5 (adjusted using HCl)
Phosphates buffered salt solution	0.2 g KCl 1.44 g Na ₂ HPO ₄ 0.24 g KH ₂ PO ₄ H ₂ O up to 1000 ml pH 7.4 (adjusted using HCl)

Material and Methods

Running buffer	25 mM Tris 192 mM glycine 1 % SDS
Separating gel buffer	1.5 M Tris HCl 13.9 mM SDS H ₂ O up to 500 ml pH 8.8 adjusted with HCl
Stacking gel buffer	1.25 M Tris HCl 13.9 SDS H ₂ O up to 500 ml pH 6.8 adjusted with HCl
Stripping buffer	7 M Guanidine hydrochloride solution 50 mM Glycine (pH 10.8) 0.05 mM EDTA 100 mM KCl 20 mM β-Mercaptoethanol
TBE-buffer	8.9 mM Tris, pH (8.2) 8.9 mM boric acid 0.25 mM EDTA
TBS-buffer	10 mM Tris, pH (7.5) 150 mM NaCl
TBST-buffer	20 mM Tris, pH (7.5) 500 mM NaCl 0.05 % Tween 20 0.2 % Triton X
Transfer buffer	25 mM Tris, pH (8.3) 150 mM glycine 10 % methanol

3.1.4. DNA ladder and protein markers

Name	Manufacture
PageRuler™ Prestained Protein Ladder	Thermo Scientific, Sankt Leon-Rot
GeneRuler™ 50 bp DNA ladder	Fermentas, Sankt Leon-Rot
GeneRuler™ 100 bp DNA ladder	Fermentas, Sankt Leon-Rot
GeneRuler™ 1000 bp DNA ladder	Fermentas, Sankt Leon-Rot

3.1.5. Consumables and kits

Name	Manufacture
BCA Protein Assay Reagent A and B	Thermo Scientific, Sankt Leon-Rot
RNeasy Mini Kit	Qiagen, Hilden
Revert Aid TM cDNA Synthesis Kit	Fermentas, Sankt Leon-Rot
procollagen I C-peptide ELISA	Takara Bio Europe, SAS

3.1.6. Primers

Table 8: List of human PCR primers, amplicons sizes and references for endpoint RT-PCR and real-time RT-PCR.

a) Endpoint RT-PCR primers

Target Gene	Forward/Reverse	Primer Sequence	Product size	Reference
Nox1	Forward	5'TTCACCAATTCCCAGGATTGAAGTGGATG-3'	230	Loughlin et al.,2010
	Reverse	5'-GACCTGTCACGATGTCAGTGGCCTTGTC-3'		
Nox2	Forward	5'-TGGGCTGTGAATGAGGGGCT-3'	385	Jones et al.,1994
	Reverse	5'-TGACTCGGGCATTACACAC-3'		
Nox4	Forward	5'-CTGGAGGAGCTGGCTCGCCAACGAAGG-3'	512	Loughlin et al.,2010
	Reverse	5'-GATCATGAGGAATAGCACCACCAC-3'		
Nox5	Forward	5'-ATCAAGCGGCCCCCTTTTTTCAC-3'	240	O'Brien et al., 2009
	Reverse	5'-CTCATTGTACACTCCTCGACAGC-3'		
Duox1	Forward	5'-ATCGCCACCTACCAGAACATC-3'	316	Cui et al.,2010
	Reverse	5'-CAGTGCATCCACATCTTCAGC-3'		
p22^{phox}	Forward	5'-GTTTGTGTGCCTGCTGGAGT-3'	316	O'Brien et al., 2009
	Reverse	5'-TGGGCGGCTGCTTGATGGT-3'		
p40^{phox}	Forward	5'-GGACATAGCTCTGAATTACC-3'	174	Zhan et al., 1996
	Reverse	5'-GGCATCGTGTGTAGACCCT-3'		
p47^{phox}	Forward	5'-ACCCAGCCAGCACTATGTGT-3'	767	Jones et al.,1994
	Reverse	5'-AGTAGCCTGTGACGTCGTCT-3'		
p67^{phox}	Forward	5'-CGAGGGAACCAGCTGATAGA-3'	712	Jones et al.,1994
	Reverse	5'-CATGGGAACACTGAGCTTCA-3'		
Poldip2	Forward	5'-TTTGGTGCCTACTCCATTGTGG-3'	65	This study
	Reverse	5'-CAAGTTCTCCAAACGGATACAG-3'		
Rac1	Forward	5'-GTAAAATACCTGGAGTGCT-3'	120	Cui et al.,2010
	Reverse	5'-CAGCAGGCATTTTCTCTTCC-3'		
Rac2	Forward	5'-TCTCTGGCAAGCAGGAC-3'	165	Cui et al.,2010
	Reverse	5'-GTGGAAGCATCTACCCG-3'		

b) Real-time RT-PCR primers

Target Gene	Forward/ Reverse	Primer Sequence	Product size	References
Nox4	Forward	5'-CAGAAGGTTCCAAGCAGGAG-3'	128	Craig et al.,2011
	Reverse	5'-GTTGAGGGCATTACCAGAT-3'		
p22^{phox}	Forward	5'-TTTGGTGCCTACTCCATTGTGG-3'	199	This study
	Reverse	5'-TCATGTACTTCTGTCCCCAGCG-3'		
Poldip2	Forward	5'-TTTGGTGCCTACTCCATTGTGG-3'	65	This study
	Reverse	5'-CAAGGTTCTCCAAACGGATACAG-3'		
Fibronectin1	Forward	5'-GTGCCCCACTCTCGGAATTC-3'	160	This study
	Reverse	5'-CAGCAACAACCTCCAGGTCCC-3'		
α-SMA	Forward	5'-GACCGAATGCAGAAGGAGAT-3'	98	Stegemann et al.,2013
	Reverse	5'-CCACCGATCCAGACAGAGTA-3'		
SMAD3	Forward	5'-GAGTAGAGACACCAGTTCTA-3'	234	This study
	Reverse	5'-TTTGGAGAACCTGCGTCCAT-3'		
COL(I)α1	Forward	5'-CAGCCGCTTACCTACAGC-3'	250	Böhm et al.,2004
	Reverse	5'-AATCACTGTCTTGCCCCAGG-3'		
COL(I) α2	Forward	5'-GATTGAGACCCTTCTTACTCTGAA-3'	230	Böhm et al.,2004
	Reverse	5'-GGGTGGCTGAGTCTCAAGTCA-3'		
β-actin	Forward	5'-AAGGAGAAGCTGTGCTACGTC-3'	128	This study
	Reverse	5'-AACCCTCATTGCCAATGGTG-3'		

Table 9: List of murine PCR primers for real-time RT-PCR, amplicons sizes and references.

Target Gene	Forward/ Reverse	Primer Sequence	Product size	References
Fibronectin1	Forward	5'-ACCGACAGTGGTGTGGTCTA-3'	130	Hecker et al., 2009
	Reverse	5'-CACCATAAGTCTGGGTCACG-3'		
α-SMA	Forward	5'-GTCCCAGACATCAGGGAGTAA-3'	102	Hecker et al., 2009
	Reverse	5'-TCGGATACTTCAGCGTCAGGA-3'		
Nox4	Forward	5'-AGATGTTGGGGCTAGGATTG-3'	137	Hecker et al., 2009
	Reverse	5'-TCTCCTGCTTGAACCTTCT-3'		
COL(I)α1	Forward	5'-ACTGGE TACATCAGCCCCGAACC-3'	145	Stegemann et al.,2013
	Reverse	5'-GACATTAGGCGCAGGAAGGTC-3'		
COL(I) α2	Forward	5'-CAGGCCCAACCTGTAAACACC-3'	147	Stegemann et al.,2013
	Reverse	5'-CTGAGTTGCCATTTCTTGGAG-3'		
β-actin	Forward	5'-TTGCTGACAGGATGCAGAAG-3'	147	Stegemann et al.,2013
	Reverse	5'-TGATCCACATCTGCTGGAAG-3'		

Table 10: List of targeted human siRNA sequences

Target Gene	No:	Target siRNA Sequence
SMAD3 Gene ID:4088	1	CAACAGGAAUGCAGCAGUG
	2	GAGUUCGCCUCAAUAUGA
	3	GGACGCAGGUUCUCCAAAC
	4	UUAGAGACAUCAAGUAUGG
Nox4 Gene ID:50507	1	ACUAUGAUAUUCUUCUGGUA
	2	GAAAUUAUCCCAAGCUGUA
	3	GGGCUAGGAUUGUGUCUAA
	4	GAUCACAGCCUCUACAUAU
Non-targeting ON-TARGET plus control		UGGUUUACAUGUUGUGUGA

* All siRNAs sequences and transfection reagent used in this study were purchased from Thermo Scientific Dharmacon, Germany.

3.1.7. Antibodies

3.1.7.1. Primary antibodies

Table 11: List of primary antibodies used in this study

Antibody	Application	Dilution	Catalog #	Manufacture
Rabbit anti- Nox4	Western Blotting	1:500	110-58849	Novus
Rabbit anti- P22 ^{phox}	Western Blotting	1:1000	Ab-75941	Abcam
Rabbit anti- Poldip2	Western Blotting	1:800	Ab-68663	Abcam
Mouse anti-β-actin	Western Blotting	1:1000	Sc-47778	Santa Cruz
Mause anti-Vinculin	Immunofluorescence	1:100	Sc-5573	Santa Cruz
Mouse anti-α-tubulin	Western Blotting	1:1000	Sc-8035	Santa Cruz
Mause anti-LAMP2	Immunofluorescence	1:200	Sc-8101	Santa Cruz
Mause anti-Fibronectin 1	Western Blotting	1:400	Ab-6328	Abcam
Mause anti-Fibronectin 1	Immunofluorescence	1:200	Ab-6328	Abcam
Mause anti-α-SMA	Western Blotting	1:100	M0851	Dako
Mause anti-α-SMA	Immunofluorescence	1:100	M0851	Dako
Mause anti-PDI	Immunofluorescence	1:100	NB300-517	Novus

3.1.7.2. Secondary antibodies**Table 12:** List of secondary antibodies used in this study

Antibody	Application	Dilution	Catalog #	Manufacturer
Anti-rabbit IgG HRP-linked (ECL)	Western Blotting	1:10.000	NA9340V	GE Healthcare
Anti-Mouse IgG HRP-linked (ECL)	Western Blotting	1:10.000	NA9310V	GE Healthcare
Rabbit IgG isotype control	Immunofluorescence	1:500	Sc-2027	Santa Cruz
Mouse IgG isotype control	Immunofluorescence	1:200	400101	BioLegend
Alexa 488 goat-anti-rabbit	Immunofluorescence	1:1000	A-11070	Invitrogen
Alexa 568 goat-anti-rabbit	Immunofluorescence	1:1000	A-11036	Invitrogen

3.1.8. Instruments and Laboratory equipment**Table 13:** List of laboratory equipments used in this study

Name	Company
Analytical balance	Sartorius
Laminar flow station (Herasafe)	Omnilab-Labcenter GmbH, Bremen
Liquid nitrogen	Tec-lab, Hessen
Polyacrylamide gel electrophoresis chambers	Biometra GmbH, Göttingen
Agarose gel electrophoresis chambers	Biorad, München
Magnetic stirrer	IKA, Labor technique
Micropipette	Pipetus, Hirschman
pH-meter 766	Calimatic
Microplate reader ELx808	BioTek, Bad Friedrichshall
Sonicator IKA	Bandelin
Stander Power supply (P25T)	Biometra,
TissueLyser II	Qiagen, Hilden, Deutschland
Vortexer	Scientific Industries Inc., New York, USA
Centrifuge Megafuge	Eppendorf, Hamburg
Centrifuge MiniSpin plus	Eppendorf, Hamburg
Centrifuge: 5415R	Eppendorf, Hamburg
Thermocycler	Eppendorf, Hamburg
Thermomixer	Eppendorf, Hamburg
Geldocumentation system	FUSION-FX7 Advance™, Peqlab, Erlangen
Blotting chamber semi dry	Roth, Karlsruhe,
Incubator Function Line	Heraeus, Hanau
Cryostat CM 1950	Leica, Wetzlar

3.1.9. Animals

An established mouse model for scleroderma, originally described by Yamamoto et al., (1999) was used for evaluating the anti-fibrogenic effect of diphenyleiiodonium (DPI) *in vivo*. Six- to eight-week-old female C3H/HeJ (The Jackson Laboratory, USA) mice were randomly divided into 4 groups (7 mice per group) as follows: BLM (10 µg), DPI (40 µg), BLM plus DPI and NaCl (negative control). Mice received daily subcutaneous injections of bleomycin (10 µg) or filter-sterilized 0.9 % saline into the dorsal shaved skin. DPI (2 mg/kg) was daily administered by intraperitoneal (IP) injections. After 4 weeks of injection, mice were sacrificed and skin biopsies were collected under sterile conditions and processed for RNA extraction followed by real-time PCR for measurement of collagen type I and routine H&E histochemistry. Mice were housed under controlled conditions with free access to food (standard rat chow diet) and water. All experimental animal procedures were performed under approval of the local veterinary authorities (District Government and District Veterinary Office, university of Münster, Germany) (8.87-51.04.20.09.384).

3.1.10. Software and computer programmes

3.1.10.1. Online Tools and databases

- BLAST (Basic Local Alignment Search Tool): <http://www.ncbi.nlm.nih.gov/BLAST>
- ClustalW (multiple sequence alignments): <http://www.ebi.ac.uk/Tools/clustalw/index.html>
- Ensembl Genome Browser: <http://www.ensembl.org/index.html>
- Genomatix (MatInspector, etc.): <http://www.genomatix.de/>
- NCBI (National Center of Biotechnology Information): <http://www.ncbi.nlm.nih.gov/>
- AliBaba 2.1: <http://www.gene-regulation.com/pub/programs/alibaba2/index.html>
- PROMO: http://alggen.lsi.upc.es/cgi-bin/promo_v3/promo/promoinit.cgi?dirDB=TF_8.3

3.1.10.2. Software

Name	Company
Zen2011, Carl Zeiss software	Carl Zeiss, Göttingen
Endnote X4	Thomson Reuters, Carlsbad, USA
Origin	Additive GmbH, Friedrichsdorf
Adobe Illustrator C5	Adobe Systems GmbH, München
Adobe Photoshop C6	Adobe Systems GmbH, München

3.1.11. Cells, cell lines and cell culture reagents

Table 14: List of human and mouse cell used in this study

Name	Species	Description	Source
nHDF	Human	Normal human dermal fibroblast	Tebu-bio,
aHDF	Human	Adult human dermal fibroblast	Tebu-bio,
SScHDF	Human	HDF from SSc patients	were received from SSc patients, WWU Münster (UKM) Clinic
HUVEC	Human	Human Umbilical Vein Endothelial Cells	Provided by Prof. H. Schnittler, were isolated from Fresh human umbilical cords, WWU Münster (UKM) Clinic
MNC	Human	Mononuclear Cells	Promocell,
NHK	Human	Normal human keratinocytes	Promocell,
CaCo2	Human	human colon epithelial cancer cell line	Promocell,
Nox4-/-	Mouse	Fibrosarcoma cells	Supplied by Prof. K. Schröder

3.2. Methods

3.2.1. Cell biological methods

3.2.1.1. Cultivation of cells

Primary cells and cell lines used in this study are listed in **Table 14**. The human dermal fibroblasts (HDFs) were cultured and maintained at 37 °C in a humidified 5% CO₂ atmosphere in RPMI 1640 medium supplemented with 10 % fetal bovine serum, 1 % penicillin/streptomycin and 1% L-glutamine. The fibroblasts were to a maximal passage 6-7. After reaching 80 % confluency, cells were washed once with PBS (without Ca²⁺ and Mg²⁺) and detached from surface by incubation with trypsin/EDTA solution at 37 °C. After 5 min incubation, trypsinization process was inactivated by adding serum containing culture medium. Cell number and viability were determined using Trypan blue Solution (1:1) using the Neubauer chamber hemocytometer.

3.2.1.2. Freezing of cells and storage

Cells were gently detached from culture tissue flask using trypsin/EDTA solution. Subsequently, they were pelleted by centrifugation at 1200 rpm for 5 min and resuspended in 1.5 ml RPMI 16 medium containing 20 % (v/v) FCS, 10 % (v/v) dimethyl sulfoxide (DMSO). The cell suspension was transferred to 1.5 ml cryo-vials which were stored at -80 °C overnight and then transferred to liquid nitrogen at 180 °C for long term storage.

Frozen cryo-vials were quickly thawed at 37 °C in a water bath. The cells were pelleted at 1200 rpm for 5 min and subsequently resuspended in fresh RPMI 1640 medium supplemented with 10 % FCS, 1 % Penicillin/Streptomycin und 1 % L-glutamine at a density of 1×10^6 cells/cm². Culture medium was replaced the following day to remove residual DMSO.

3.2.1.3. Generation of Nox4^{-/-}-deficient murine fibroblasts

Nox4^{-/-} mice were generated by targeted deletion of the translation initiation site and of exons 1 and 2 of the Nox4 gene (Schröder, Zhang et al. 2012) and backcrossed into C57Bl/6J for more than 10 generations. To induce fibrosarcomas the chemical carcinogen methylchoanthrene was injected subcutaneously into the right flank of the mice. In case tumors reached a diameter of 1.5 cm or 150 days after methylchoanthrene injection mice were sacrificed and if present the tumor tissue was used for cell isolation. Fibrosarcoma cells were isolated using the tumor dissociation kit for mouse and the gentle MACS Dissociator (Miltenyi Biotec), following the manufactures instructions. Shortly, tumor tissue was homogenized enzymatically, erythrocytes were lysed and eventually cells were cultured in Dulbecco's Modified Eagle's Medium+ glutaMAX (Gibco) supplemented with 5 % FCS , 1 % penicillin (50 U/ml) and streptomycin (50 µg/ml) in a humidified atmosphere of 5 % CO₂ at 37 °C. Erythrocyte depletion buffer consisted of 155 mM NH₄Cl, 10 nM NaHCO₃ and 100 nM EDTA in double distilled water, pH=7.4. All animal experiments were approved by the local governmental authorities (F28/46) and were performed in accordance with the animal protection guidelines.

3.2.1.4. Generation of skin samples and HDFs from patients with SSc

Samples from lesional skin were received from SSc patients undergoing routine diagnostic biopsies. Samples from n=3 patients (age: 33-67; 2 females, 1 male; biopsy sites: finger, neck, abdomen; ANA phenotype: 2 anti-SCL70, 1 anti-CENP-B) were immediately frozen in liquid nitrogen and further processed for total RNA preparation as indicated below. HDFs from lesional skin of n=3 SSc patients were established and maintained as previously reported (Stegemann et al., 2013). The patient characteristics were: age: 50-72; 2 females, 1 male; biopsy site: dorsal lower arm; ANA phenotype: 1 anti-SCL70, 1 anti-CENP-B, 1 ANA-negative. All patients fulfilled the ACR criteria for diagnosis of SSc. Studies were approved by the Local Ethical Committee of the University of Münster, Germany (2013-020-f-S).

3.2.2. Molecular biological methods

3.2.2.1. RNA isolation

Total cellular RNA extraction from individual cell types was carried out with the RNeasy mini kit (Qiagen, Hilden, Germany), according to the manufacturer's instructions. Briefly, medium was aspirated; adherent cells were washed once with PBS and scraped in lysis buffer. After centrifugation for 2 min at 13.000 rpm the homogenized cell lysate was mixed with 400 μ l 70 % ethanol and centrifuged for 2 min at 13.000 rpm 3 times. After several washing steps through RNeasy spin column, total RNA from the membrane was eluted with high purity by using 40 μ l of RNase free H₂O and centrifuge for 1 min at 8600 rpm. To eliminate potential DNA contamination, RNA (1 μ g) was mixed with H₂O and 10 μ l of DNase (Promega (1 U/ μ l) to a final volume of 100 μ l and incubated for 90 min at 37 °C and 10 min at 65 °C. The concentration of the RNA was determined by the optical density of the sample at wavelengths of 260 and 280 nm using spectrophotometer. An OD₂₆₀ of 1 corresponded to a RNA concentration of 40 μ g/ml. The purity of the RNA solution was evaluated measuring an aqueous solution of RNA via UV absorption at 260 nm and 280 nm. The ratio of OD₂₆₀/280 ratio should be between 1.8 to 2.0. The RNA was stored at -20 °C until further use for the cDNA synthesis and subsequent RT-PCR. Before RNA isolation from murine and human samples, frozen tissues were homogenized in tubes containing homogenization beads and placed in homogenizer (Thermo Scientific, Sweden) for 1 min at 2000 rpm. Total RNA was isolated using Trizol reagent according to a modified acid guanidium thiocyanate-phenol-chloroform extraction method (Chomczynski & Sacchi 1987). Shortly, 1 ml of Trizol reagent was added to 50-100 mg homogenized tissue and incubated for 5 min at room temperature (RT) to permit the complete dissociation of nucleoprotein complexes. Then, 200 μ l of chloroform was added per 1 ml of TRIZOL Reagent. The tubes were shaken vigorously for 15 seconds then incubated at room temperature for 2 to 3 min. Samples were centrifuged at 13,000 rpm for 15 min at 4 °C. After centrifugation, the mixture was separated into a lower phase, phenol chloroform phase, an interphase, and an upper aqueous phase. The aqueous phase was transferred to a fresh tube and 500 μ l isopropyl alcohol was added to allow precipitation of RNA. Samples were incubated at 4 °C overnight and were then centrifuged at 13,000 rpm for 10 min at 4 °C. After centrifugation, the pellets were washed twice with 70% cold ethanol and were centrifuged again at 13,000 rpm for 5 min at 4 °C. The supernatant was removed and the RNA pellets were kept 5 min at room temperature to air dry. Finally, RNA

pellets were dissolved in 20 µl RNase-free water at 60 °C for 5-10 min to help dissolving and subsequently and stored at -20 °C until use.

3.2.2.2. cDNA synthesis and reverse transcription

RNA was reverse transcribed into first-strand cDNA using the Revert Aid™ cDNA Synthesis Kit (Fermentas Life Sciences). 1 µg of template RNA was first incubated with 1 µl of oligo (dT)₁₈ primer (0.5 µg/µl) and the volume was made up to 12 µl with RNase free water. The reaction mixture was gently vortexed then incubated for 5 min at 65 °C in the thermoblock. Immediately after incubation, the tube was briefly centrifuged and placed on ice. The following reaction mixture was added in the indicated order: (4.2 µl of 5 x reaction buffer, 2 µl of 10 mM dNTP mix, 1 µl of RevertAid reverse transcriptase and 1 µl RiboLock™ Ribonuclease Inhibitor). The total volume was made up to 20 µl with RNase free water. The tubes were mixed gently, briefly centrifuged and incubated at 42 °C for 60 mins in a thermal cycler. The reaction was then terminated by heating at 70 °C for 10 mins and the resulting cDNA was used for RT-PCR analysis or stored at -20 °C until further use.

3.2.2.3. Polymerase chain reaction (PCR)

a) Semi-quantitative RT-PCR

Endpoint polymerase chain reaction (PCR) was used to amplify specific DNA-fragments. For all PCR reactions a master mix was prepared contained the following components : 1-3 µl of cDNA products; 5 µl 5X PCR buffer, 0.5 µl of 10 mM dNTPs, 3 µL of each primer (40 pmol); 0.125 µl of Promega GoTaq polymerase (5 U/µl) and RNA free water up to 25 µl. All the primer sequences used in this study are listed in **Table 8-9**. Our oligonucleotide primers were designed using Primer Express (Perkin- Elmer Life Sciences, Courtaboeuf, France) and generated by Biozyme or those cited in earlier studies. The specificity of the sequences was verified using the Blast Nucleotide software available at the National Center for Biotechnology Information.

The number of cycles and the program condition were optimized for each gene separately to ensure that no artefacts of the PCR reaction were generated. Reactions were performed in a Thermocycler for generally 33-35 cycles using the following standard amplification Program:

Initial denaturation	94 °C, 5 min	} Repeated 33-35 times
Denaturation	94 °C, 1 min	
Annealing	T _m -4 °C, 1 min x °C,	

Elongation 72 °C, 1 min/kb DNA

Termination 72 °C, 10 min

Cooling to 4 °C

The optimal annealing temperature (OAT) of the primers was calculated for each individual primer and is averaged for the primer pair according to the following formula described in (Sambrook et al. 1999):

$$\text{OAT} = T_m - 4 \text{ } ^\circ\text{C}$$

Where T_m is the melting temperature of the DNA, which is calculated from the G/C content, and is calculated by:

$$T_m = 4(\text{G}+\text{C}) + 2(\text{T}+\text{A}) \text{ } ^\circ\text{C}$$

We usually performed a negative control containing RNA instead of cDNA to rule out genomic DNA contamination. After cycling the reaction was diluted 1:5 by adding 80 μl nucleases free water to the 20 μl reaction mixture product. Samples were stored at -20 °C until further use.

b) Quantitative real-time RT-PCR

Real-time PCR analysis was performed with SYBR Green ROX PCR Master Mix Reagent (Thermo Fisher Scientific). The real-time PCR mixture was prepared according to the manufacturer's protocol. Briefly, reaction mix was made by mixing 10 μl of SYBR green, 4.6 μl of water, 0.4 μl of the primer mix (10 μM working solution). Each well of 96 well plates should have 5 μl of cDNA at the appropriate dilution and 20 μl of the RT-PCR reaction mix. The final volume per well should be 25 μl . Reactions were carried out for 40 cycles (95 °C for 15 s and 60 °C for 60 s) in duplicates using an ABI-prism 7300 sequence detector (Applied Biosystems). Relative expression of the gene of interest (the n-fold expression) is carried out or calculated according to The delta Ct ($2^{-\Delta\Delta\text{Ct}}$) method (Livak and Schmittgen, 2001) where Delta Ct (ΔCt) values were calculated by subtracting the mean Ct of the housekeeping gene from the mean Ct of the gene of interest. β -actin was used as an internal standard (housekeeping gene) and triplicate measurements were performed for each sample.

3.2.2.4. DNA gel electrophoresis

Amplified PCR products were separated on a 1.5% agarose gel (1X TBE buffer) containing 0.5 mg/ml Red safe together with a DNA marker for the appropriate fragment length. The electrophoresis was performed for around 1 h with 5 V/cm and DNA bands were visualized by UV light. Gel Images were captured by chemiluminescence imager (FUSION-FX7 Advance™).

The size of DNA fragments was determined by comparison with a DNA marker for the appropriate fragment length

3.2.2.5. siRNA transfection and gene knock-down

HDFs were transfected with small interference RNA (siRNA) against Nox4 and SMAD3 or non-targeting ON-TARGET plus control siRNA#2 according the manufacturer's protocols. Sequences of siRNAs used in this study have been described before in **Table 10**. Briefly, 250,000 cells were seeded in a 3.5 cm cell culture plate with RPMI1640 medium containing serum without antibiotic for 24 h, HDFs were cultured to 60-70 % confluence. For each plate, 10 μ L siRNA (siRNA was diluted in sterile nucleases free water to a final concentration of 25 nM) and 4 μ l transfection reagent in 200 μ l transfection medium (serum and antibiotic free RPMI 1640 medium) were prepared and incubated for 5 min at RT. Both preparations were mixed and incubated for 20 min at RT. Transfection complex was added drop wise to cell medium. After 48 hrs of incubation, transfection medium was removed and a new fresh RPMI 1640 medium containing 0 % serum and antibiotic added for further 24 hrs deprivation prior to treatments. Subsequently, cells were stimulated with or without TGF- β_1 as indicated and harvested for RNA extraction. Specific silencing of targeted genes was confirmed by RT-PCR analysis.

3.2.3. Biochemical methods

3.2.3.1. Preparation of cell extract

3.2.3.1.1. Preparation of cell lysate using hot lysis method

Prior to lysis, cells were grown to 70-80 % confluence and treated with stimulants or inhibitors according to the experimental design. Cells were washed with cold PBS and harvested by scraping in hot 6 x SDS sample buffer using a rubber policeman. This was followed by sonication for 2 x 5 sec and incubation at 95 $^{\circ}$ C for 5 min. Equal amounts of protein (30 μ g/lane) were separated by sodium dodecyl sulphate-polyacrylamide gel electrophoresis.

3.2.3.1.2. Preparation of cell lysates using immunoprecipitation buffer (IP).

After cell treatments, they were washed with ice cold PBS and harvested by scraping in PBS followed by centrifugation at maximum speed for 5 mins at 4 $^{\circ}$ C. Subsequently, cell pellets were resuspended in IP buffer and were incubated for 60 min on ice. After incubation in ice, samples were sonicated for 2 x 5 sec and centrifuged at 14,000 rpm for 10 mins at 4 $^{\circ}$ C. The supernatant

was transferred into a fresh microcentrifuge tube and the pellet was discarded. The protein concentrations of the lysates were determined using Bradford method as described later in (3.2.3.2). 30-50 µg of protein sample was mixed with 6x SDS sample buffer containing β-mercaptoethanol and then heated at 95 °C for 5 min. The samples were stored at -20 °C until further use.

3.2.3.2. Protein determination

Total protein concentration was measured using Bradford methods (Bradford 1976). Protein sample (5 µl) was dissolved in 100 µl of diluted Bradford reagents and then incubated for 5 min at room temperature. As a blank, 5 µl of the IP buffer were dissolved in 100 µl of diluted Bradford reagents the samples were mixed by pipetting gently. After incubation, the samples were transferred to cuvettes and absorbance was measured using spectrophotometer at 595 nm.

3.2.3.3. SDS-Polyacrylamide Gel Electrophoresis (SDS-PAGE)

Protein samples were separated on vertical, discontinuous SDS-polyacrylamide gel as described previously (Sambrook, 1990). According to the molecular weight of the protein of interest, the acrylamide concentration was adjusted to 10 % or 12 % at constant voltage of approx. 90 V in the stacking gel (**Table 16**) and at 120-130 V in the separating Gel (**Table 15**). The molecular weight of All proteins examined in this study ranges between 70:19 kDa (Nox4: 67 kDa, P22^{phox}:19 kDa, Poldip2: 42 kDa, β-actin: 43 kDa and α-tubulin: 55 kDa). The run of the gel was controlled by separation of pre-stained molecular weight marker as a size reference.

Table 15: Components of separating gel

Seperating gel components	Volume (5 ml)
<i>10%</i>	
H ₂ O	1.9
30 % Acrylamide-Mix	1.7
1.5 M Tris (pH 8.8)	1.3
10 % SDS	0.05
10 % Ammonium persulfate	0.05
TEMED	0.002
<i>12%</i>	
H ₂ O	1.6
30 % Acrylamide-Mix	2.0

1.5 M Tris (pH 8.8)	1.3
10 % SDS	0.05
10 % Ammonium persulfate	0.05
TEMED	0.002

Table 16: Components of stacking gel

Stacking gel components	Volume (2ml)
5%	
H ₂ O	1.4
30% Acrylamide-Mix	0.33
1.5 M Tris (pH 8.8)	0.25
10% SDS	0.02
10% Ammonium persulfate	0.02
TEMED	0.002

3.2.3.4. Western immunoblotting

After separation on SDS gels, proteins were blotted onto polyvinylidene difluoride membranes (PVDF) (Immobilon-P, 0.45 μ m, Millipore) according to Towbin Methods (Towbin et al., 1979). PVDF membranes were activated in methanol for 15 sec and equilibrated in blotting buffer for 15 min at room temperature. Gel and membrane were placed with three layers of Whatman paper in the electroblotting chamber. The semi-dry electroblotting was performed at a constant current of approx. 200 mA for 1 hr. After proteins transfer, the PVDF membrane was washed using 2 x TBST buffer and then blocked with 10 % BSA/TBST at 4 °C. After blocking, the membrane was incubated with the primary antibody diluted in the same buffer overnight at 4 °C at the appropriate concentration as described earlier in **Table 11**. The next day, the PVDF membrane was washed with 2 x TBST buffer three times for 5 mins and subsequently incubated with the appropriate secondary antibody conjugated to Horse Radish Peroxidase (HRP) enzyme for 30 min. The membrane was washed with 2 x TBST buffer three times for 5 min. Protein bands were visualized on the membrane using enhanced chemiluminescence (ECL). The ECLplus reaction mixture (Enhanced Luminol Reagent and Oxidizing Reagent) was prepared according to the manufacturer's instruction (Roti-Lumin-Kit) and incubated with nitrocellulose membrane for 1 min, and signals were detected with the Amersham Hyperfilm ECL (GE Healthcare). The film was placed in developer solution (G153, AGFA) until black bands appeared, washed in 1 % acetic acid and finally placed in fixer solution (G35A, AGFA) for a couple of mins. After

fixation, the film was washed in water and dried. Densitometric analysis was performed using the Image J software. To assure equal loading, membranes were stripped for 10-15 min at room temperature, and reprobed with an antibody against β -actin (Santa Cruz) or α -tubulin.

3.2.4. Immunological methods

3.2.4.1. ELISA

A commercially available Enzyme-linked immunosorbent assay (ELISA kit, TaKaRa) was used to measure the procollagen I C-peptide (PICP) secretion. Briefly, 250,000 cells per well were seeded into 12-well tissue culture plates. HDFs were deprived of FCS for two days and subsequently stimulated with TGF- β_1 alone or in combination with DPI. Cell culture supernatants were harvested after 48 hrs, and centrifuged at 2500 rpm for 5 min to remove pellet debris. The resulting supernatant was transferred into fresh microcentrifuge tubes and samples were centrifuged and frozen at -80 °C until use. At the time of measurement, samples were thawed on ice. The assay was performed according to the manufacturer's instructions, in 96 well plates precoated with Procollagen Type I C-Peptide (PIP) antibody. First, 100 μ l of lyophilized horseradish peroxidase (POD) conjugated murine monoclonal antibody solution were added to each well, and subsequently add 20 μ l sample or standard of known concentrations. The samples were carefully mixed and then incubated for 3 hrs at 37 °C followed by washing 4 times with ca. 400 μ l of PBS. Samples were then incubated with 100 μ l of substrate solution for 15 mins at room temperature in the dark, after which, 100 μ l of stop solution (1 N H₂SO₄) was added to terminate the reaction. The optical density was measured with a microplate reader at 450 nm. The concentration of procollagen I C-peptide in the supernatants were determined against a standard curve from the standard procollagen I C-peptide samples used on the same 96 well plate

3.2.5. Cytotoxicity assays

Cytotoxicity was evaluated using both crystal violet staining method and XTT test after treatment with different Nox inhibitors.

3.2.5.1. Crystal violet assay

Crystal violet (CV), a triphenylmethane dye (4-[(4-dimethylaminophenyl)-phenyl-methyl]-N,N-dimethyl-aniline) and was used to determine cell viability after treatment with DPI or VAS2870

Nox inhibitor. HDFs were seeded into 12-well culture plates at a density of 7,000 cells per well and cultivated for 24 hrs at 37 °C. After incubation, DPI or VAS2870 (dissolved in DMSO) was added at various concentrations as indicated and incubated 16 hrs at 37 °C. After this period, the medium was removed and the cells were washed with 1 x PBS and then stained with 0.1 % crystal violet solution in methanol with gentle shaking for 20 min at room temperature. Stained cells were carefully washed three times with 1 x PBS water until a clear background was visible and were left to dry overnight. CV was dissolved using lysis buffer (10 % methanol and 10 % acetic acid) for 15 min at room temperature with gentle shaking. Absorbance was measured spectrophotometrically at 590 nm by an automated microplate reader ELx808 (BioTek, Bad Friedrichshall, Germany). The experiments were repeated three times.

3.2.5.2. XTT test

XTT is 2, 3-Bis-(2-methoxy-4-nitro-5-sulfophenyl)-2H-tetrazolium-5-carboxanilid. XTT kit was provided from Roche Diagnostics (Karlsruhe) was used to determine cell proliferation after treatment with the Nox inhibitor. Briefly, 10,000 cells per well were seeded into 96-well tissue culture plates and incubated up to 24 hrs. After incubation, DPI or VAS2870 (dissolved in DMSO) was added at various concentrations as indicated and incubated 16 hrs at 37 °C. 50 µl XTT-labelling reagent and 1 µl electron coupling reagent were mixed and 50 µl from that mixture was added to each well containing 100 µl culture media (final concentration: 0,3 mg/ml) and incubated for 4-24 hrs at 37 °C. Absorbances were recorded at 490 nm by an automatic microplate reader ELx808 (BioTek, Bad Friedrichshall, Germany). Similar results were found in three independent experiments with four replicates for each dose.

3.2.6. Confocal immunofluorescences microscopy

HDFs were seeded on gelatin-coated glass coverslips in RPMI 1640 medium, after setting the experimental condition, cells were fixed with methanol at -20 °C or with 4% paraformaldehyde for 15 min, then washed for 5 min with PBS and blocked with 5 % goat serum. After blocking, cells were incubated for 1 hr at room temperature or overnight at 4 °C with the primary antibodies. Primary antibodies used in this study are listed in **Table 11**. In separate colocalization experiments, HDFs were loaded with MitoTracker Deep Red (MTR) (250 nmol/l, 30 min at 37 °C) (Invitrogen) followed by incubation with Nox4 antibody. After another washing step, the secondary corresponding fluor 488 or Alexa fluor 568 antibodies were applied (1:1000,

Invitrogen) for 1 hr at room temperature (**Table 12**). Nuclei were stained with 4', 6-diamidino-2-phenylindole (DAPI) (Fluka). Cells were mounted in fluorescence mounting medium (Roth) and observed under oil immersion 40 X or 63 X objective on an inverted LSM 780 confocal laser-scanning microscope (Carl Zeiss). Comparative IF images were acquired under the same microscopic setting. Results represent images from at least three independent experiments.

3.2.7. Assessment of dermal thickness.

4 µm sections of paraffin-embedded skin from mice treated with NaCl, bleomycin, DPI, or bleomycin plus DPI were de-paraffinized, rehydrated and then stained with hematoxylin and eosin (H&E) according to the standard protocols of our laboratory. Dermal thickness was determined using a Zeiss Axiophot microscope. Three measurements were performed for each microscopic field, and 5 different fields were analysed for each mouse (n= 3). Densitometric analysis was performed using ImageJ software.

3.2.8. Determination of collagen protein content ex vivo.

Mouse skin samples were weighed and incubated in 0.5M acetic acid in the presence of protease inhibitor cocktail (Roche Diagnostics). One milligram of pepsin (Sigma) per 500 µl 0.5M acetic acid was added to each sample, followed by incubation for 24 hrs at 4°C. After centrifugation, supernatants were precipitated with methanol/chloroform, after which 2X Laemmli sample buffer was added to dissolve the protein pellets. After normalization for wet weight, samples were subjected to SDS-PAGE and stained with 0.5 % Coomassie brilliant blue (Bio-Rad).

3.2.9. In silico promoter analysis

Coding promoter sequences of the human Nox4 gene (~ 4 kb upstream) were obtained from the ENSEMBL genomic database. The AliBaba 2.1/TRANSFAC 8.3 web based tool was used to predict the transcription factor binding sites in the sets of sequences. The stringency level was set to a value of 0.9, and the human promoter set of the Eukaryotic Promoter Database was chosen as third order background model.

3.2.10. Measurement of NADPH oxidase activity assay

HDFs (10⁶ cells per treatment) were seeded out in 10 cm diameter culture dishes. After deprivation from FCS for 24 hrs Cells were treated in the presence or absence of DPI, administered 1 h min before the stimulation with TGF-β₁ for further 24 hrs. Cells were washed

with ice cold PBS and harvested using scraping out of petri dish then centrifuged. Cell Pellets were homogenized with 100 strokes using a Dounce homogenizer on ice in lysis buffer containing 20 mM KH_2PO_4 (pH 7.0), 1 mM EGTA and protease inhibitor. Cell homogenate subjected to differential centrifugation to isolate membrane fraction. A total of 100 μl of membrane fraction (50 μg total protein) was immediately added to 900 μl of 50 mM phosphate buffer (pH 7) containing 1 mM EGTA, 150 mM sucrose, 500 μM lucigenin as an electron acceptor, and 100 μM NADH as an electron donor. Photon emission expressed as relative light units was measured every 25 s for 30 min in a microplate luminometer Centro LB960 (Berthold Technologies). There was no measurable activity in the absence of NADH. A buffer blank was subtracted from each reading before calculation of the data. The protocol used was optimised from (Abid et al., 2007).

3.2.11. Statistical analysis

All experiments were performed at least three times, unless stated otherwise. Results were expressed as means \pm SEM and deviations from normality were assessed by the Shapiro-Wilk test. Statistical significance in the differences between two mean values was determined by the student's t-test. Differences were considered as significant when $p < 0.05$.

4. Results

4.1. Detection of Nox isoforms and adaptor proteins in HDFs

4.1.1. Expression of Nox4 isoform and its adaptor proteins in normal HDFs

In a first set of experiments we performed a detailed expression analysis of the Nox4 isoform and its adaptor proteins in HDFs derived from both normal neonatal foreskin (nHDFs) and adult skin (aHDFs) (n=3 donors, each) by semi-quantitative RT-PCR analysis. Interestingly, HDFs derived from neonatal foreskin and adult HDFs constitutively express mRNA levels for Nox4. **Fig. 8A**, shows a representative analysis for one donor). Moreover, both cell types expressed steady-state levels of the Nox4 adapter proteins p22^{phox} and Poldip2, suggesting a functional Nox4 complex. State of the art negative controls of the utilized cDNA samples from nHDFs (RNA without RT) were negative. State of the art positive controls (human umbilical vein endothelial cells (HUVEC) were positive for Nox4 and its adapter proteins. These findings on HDF derived from neonatal foreskin and adult skin were confirmed in cells from two other donors.

Next, we verified that all components of a functional Nox4 complex are also present at protein level in nHDFs and aHDFs. Protein samples were subjected to SDS-PAGE followed by Western blot analysis. β -actin was used as internal control for equal protein loading. We detected Nox4, p22^{phox} and Poldip2 by Western immunoblotting in nHDFs (**Fig. 8B**) at the expected molecular weights. State of the art positive control HUVEC was used.

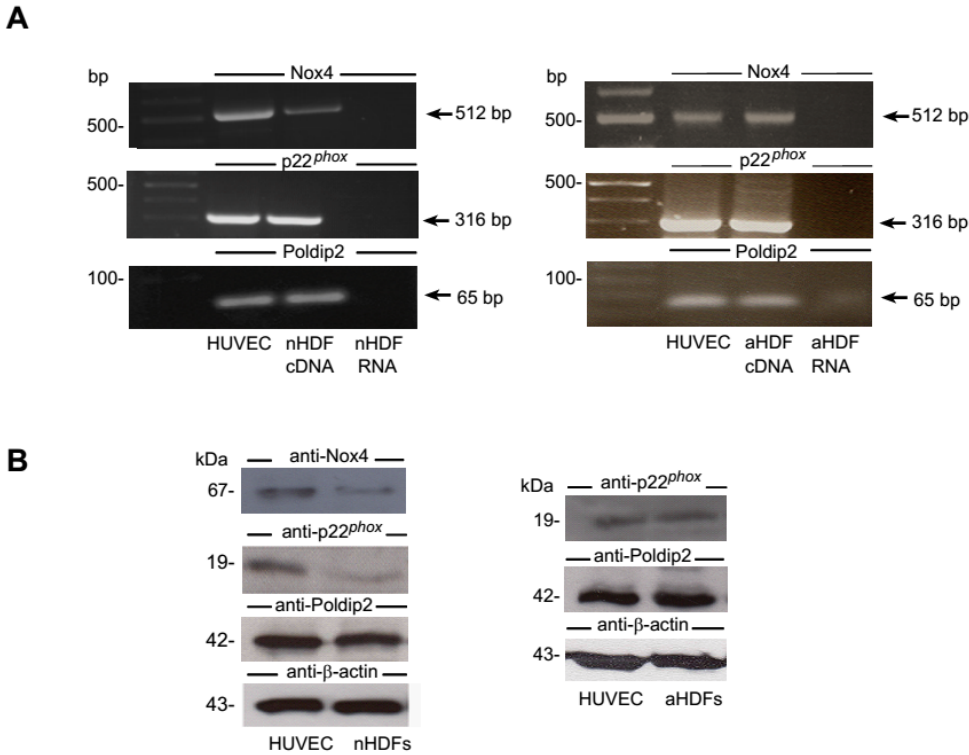


Figure 8. Expression analysis of Nox4 and its adaptors in HDFs. (A) Detection of Nox4 as well as its adaptors p22^{phox} and Poldip2 in nHDFs and aHDFs by endpoint RT-PCR analysis. State of the art positive and negative controls consisted of cDNA from HUVEC and HDF templates without RT. (B) Detection of Nox4, p22^{phox} and Poldip2 protein in nHDFs and aHDFs by Western blotting. Reprobing the membrane with an anti-β-actin antibody was used as control for equal protein loading. Data are representative images of n=3 donors of nHDFs with similar results. MW, molecular weight; bp, base pairs.

4.1.2. Expression of Nox4 isoform and its adaptor proteins in affected skin and HDFs from SSc patients

In another set of experiments we explored the expression pattern of the complete Nox4 complex in HDFs from SSc patients. The endpoint RT-PCR analysis demonstrated that diseased HDF constitutively expressed mRNA transcripts for Nox4 as well as its associated adaptor proteins p22^{phox} and Poldip2 (n=3; **Fig. 9A** and **B** show qualitative PCR analysis of 3 healthy donors and 3 SSc patients). Interestingly, quantitative RT-PCR analysis revealed that Nox4 mRNA expression was similar between normal adult and SSc HDF (**Fig. 9C**). Since levels of mRNA do not always directly correlate with protein levels, which can arise through differences in

Results

mRNA/protein stability or post-transcriptional/translational modifications (Yoshiko, Hirao et al. 2002), we evaluated Nox4 expression by Western immunoblotting analysis of total cell lysates from both adult HDFs and SSc HDFs. 30 μ g of protein was loaded per well and β -actin was used as a loading control (**Fig. 9D**). The Nox4 antibody detected a protein band at 67 kDa in both cell types; however, the protein band was more strongly abundant in at least 2 donors fibroblasts from SSc patients than in adult HDFs. In summary, these findings confirmed the presence of a complete Nox4 complex in SSc skin and HDFs from patients with SSc.

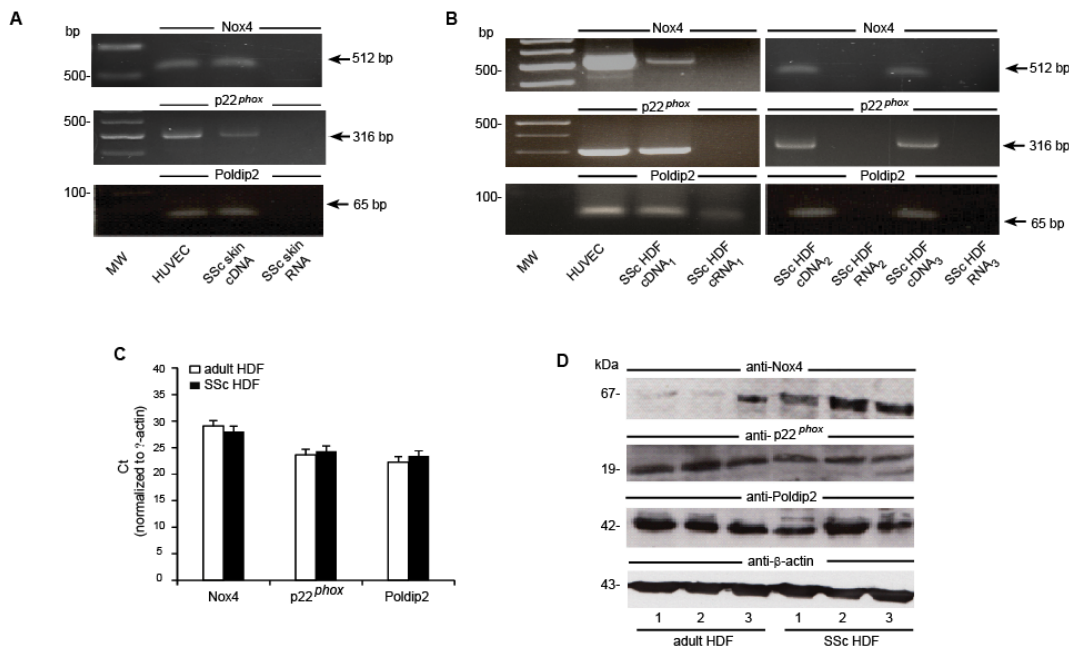


Figure 9. Expression of the Nox4 and its adaptors was preserved in affected skin as well as in HDFs of patients with SSc. (A) Detection of the Nox4 and its adaptors p22^{phox} and Poldip2 in SSc skin as shown by endpoint RT-PCR. State of the art positive and negative controls consisted of cDNA from HUVEC and HDFs templates without RT. Images were representative for skin samples (n=3) with identical results. (B) Detection of Nox4, p22^{phox} and Poldip2 in HDFs derived from SSc patients (n=3) by endpoint RT-PCR. State of the art positive and negative controls consisted of cDNA from HUVEC and HDF templates without RT. (C) Normal adult HDF (n=3) and SSc HDF (n=3) do not vary in Nox4, p22^{phox} and Poldip2 mRNA expression as shown by real-time RT-PCR. Depicted are Ct-values normalized to GAPDH. (D) Nox4 protein expression in adult HDF (n=3) and SSc HDF (n=3) as shown by Western immunoblotting.

4.1.3. Expression of other Nox isoforms, cytosolic subunits and adaptor proteins in normal nHDFs

To get first insights into the mRNA expression of other Nox isoforms and their adaptor proteins in healthy HDFs, we performed semi-quantitative RT-PCR analysis of HDFs derived from both nHDFs and aHDFs (n=3 donors, each). As shown in **Fig. 10**, these cells constitutively express steady-state levels of the small GTPases Rac1 and Rac2. Moreover, nHDFs and aHDFs express low level of Duox1 and Nox5. In contrast, Nox1, Nox2/gp91^{phox} (the prototypic phagocytic Nox isoform), Duox2, p40^{phox}, p47^{phox} and p67^{phox} were not detectable by semi quantitative RT-PCR. These findings on HDFs derived from neonatal foreskin were confirmed in cells from two other donors. Similarly, none of the other NOX components, i.e Nox2 or Nox3, p40^{phox}, p47^{phox} and p67^{phox} were detectable by semi-quantitative RT-PCR in aHDFs (**Appendix Fig. 1**). State-of-the-art negative controls of the utilized cDNA samples from HDFs (RNA without RT) were negative. State-of-the-art positive controls (human peripheral blood monocytes, CaCo2 cells) were positive for Nox1 and Nox2/gp91^{phox}. We did not examine Nox3 since Nox3 is selectively expressed in the inner ear (Banfi, Malgrange et al. 2004).

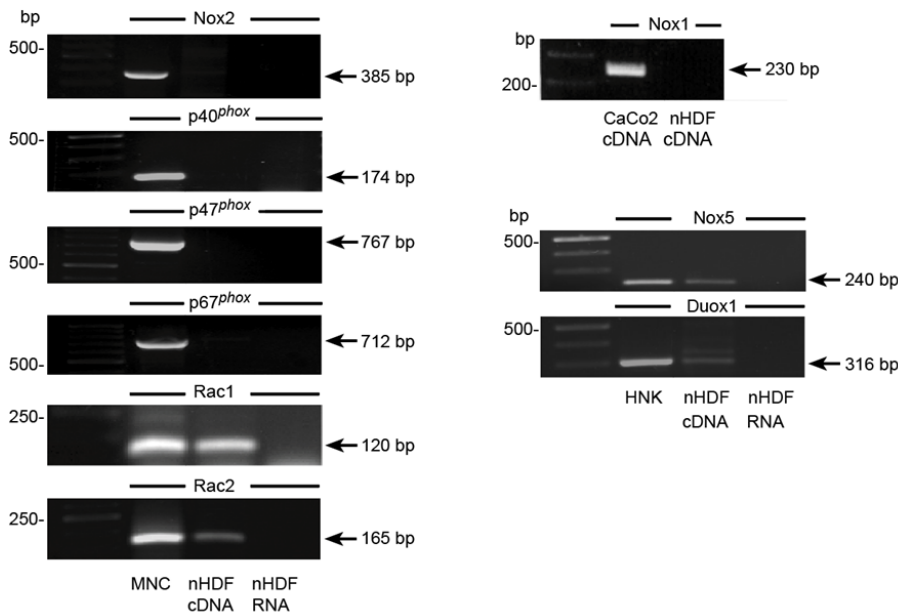


Figure 10. Expression analysis of additional Nox isoforms, adaptor proteins as well as Rac1 and Rac2 in normal nHDFs by endpoint RT-PCR analysis. Expression analysis of additional Nox isoforms, adaptor proteins as well as Rac1 and Rac2 in normal nHDFs by endpoint RT-PCR analysis. State of the art positive controls consisted of cDNA from HUVEC, normal human keratinocytes (NHKs), human peripheral blood monocytes (MNC) and the human colon carcinoma cell line CaCo2. Negative controls consisted of HDF templates without RT. Depicted are representative images from RT-PCR analyses of n=3 donors.

4.1.4. Expression of additional Nox isoform and adaptor proteins in HDFs from SSc patients

In order to get qualitative information about mRNA expression profiling of additional Nox family members in SSc HDFs (n=3 donors), their expression was characterized in HDFs from SSc patients. Notably, endpoint RT-PCR analysis revealed no presence of other Nox isoforms such as Nox1, Nox2 including its adapters p40^{phox}, p47^{phox}, p67^{phox} or Duox1 using state of the art positive and negative controls (representatively shown in **Fig. 11** for one donor). However, in accordance with the expression pattern in nHDFs and aHDFs, SSc HDFs expressed transcripts for Rac1, Rac2 and low level of Nox5.

Results

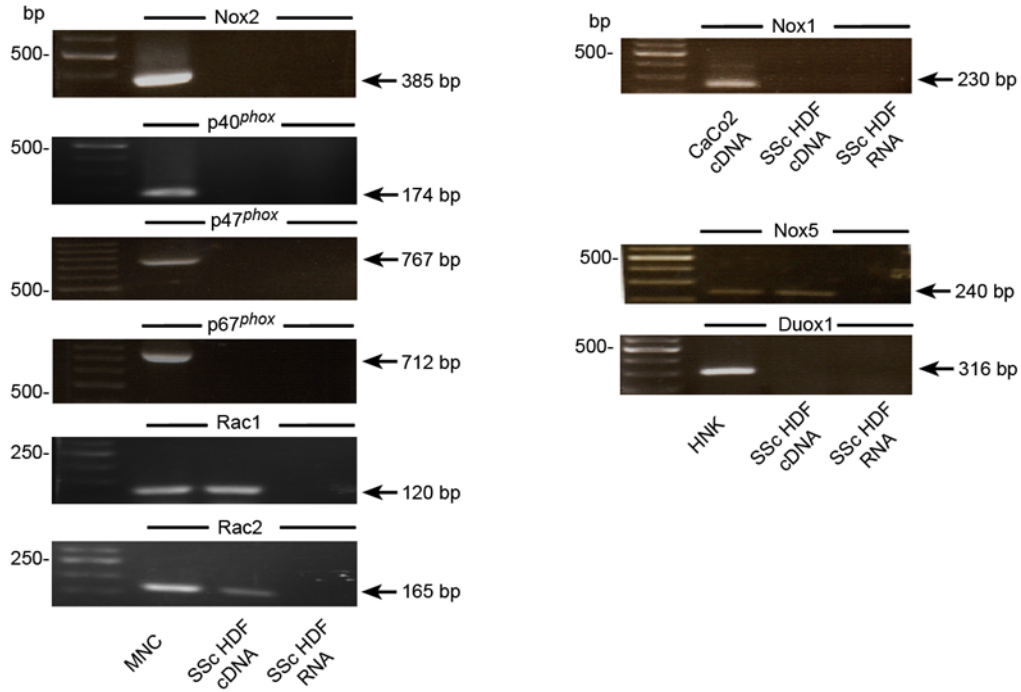


Figure 11. Expression analysis of additional Nox isoforms, adaptor proteins as well as Rac 1 and Rac2 in HDFs from patients with SSc by endpoint RT-PCR. Positive controls consisted of HUVEC, normal human keratinocytes (NHKs), human peripheral blood monocytes (MNCs) and the human colon carcinoma cell line CaCo2. Negative controls consisted of HDF templates without RT. Depicted are representative images from RT-PCR analyses of n=3 donors.

4.2. Subcellular localization of Nox4 in HDFs

Next, we investigated the subcellular localization of Nox4 within HDFs using laser scanning confocal microscopy. We used a polyclonal Nox4 antibody to examine the localization of endogenous Nox4 by immunofluorescence in nHDFs and aHDFs. Interestingly, the Nox4 protein was found to be co-localized with an endoplasmic reticulum marker, protein disulfide isomerase (PDI), as shown in yellow within the merged images (**Fig. 12**). However, there was also strong Nox4 immunostaining within the endoplasmic reticulum in aHDFs. To further validate the specificity of the Nox4 antibody, we knocked down Nox4 using small interference oligonucleotide RNA directed against Nox4 (siRNA Nox4). Nox4 protein staining was attenuated in cells treated with siRNA Nox4 compared with non-targeting siRNA (**Appendix Fig. 2**). Negative control incubated with secondary antibody or the isotope control antibody showed no reaction. To get further insights on the Nox4 localization patterns in SSc HDFs, we performed immunofluorescence analysis in 3 HDFs from SSc patients. Again, we observed colocalization of Nox4 with PDI. One representative image is shown in **Fig. 12**.

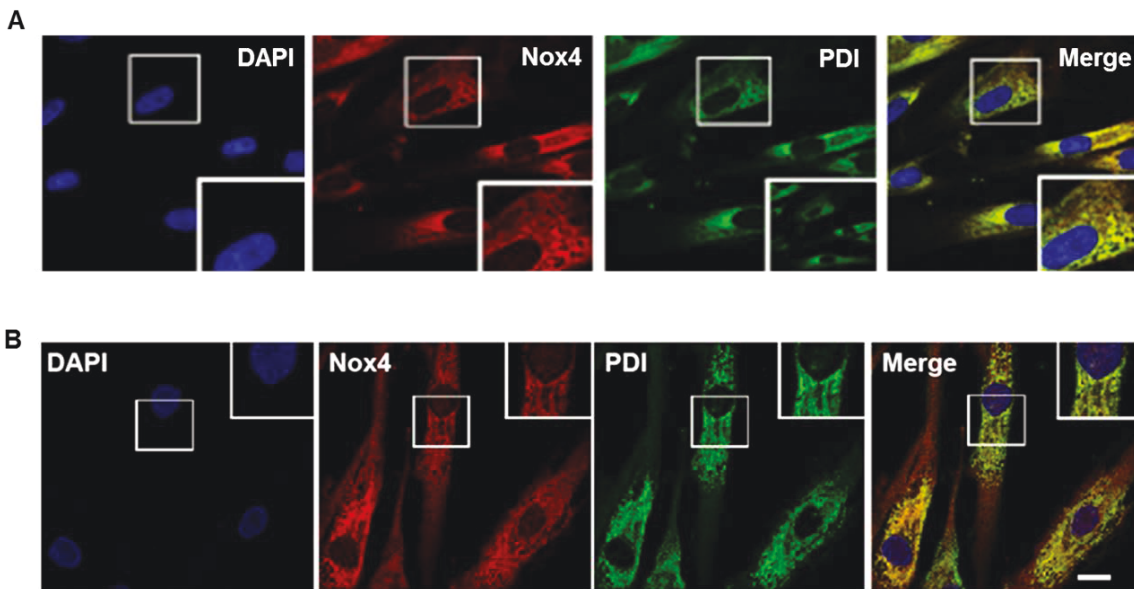


Figure 12. Subcellular localization of Nox4 in cultured HDFs. (A) Detection of Nox4 immunoreactivity in nHDFs by double immunofluorescence analysis and confocal laser-scanning microscopy. Cells were plated on gelatin-coated glass coverslips, fixed and double stained with anti-Nox4 (AlexaFluor594; red) and ER-specific marker PDI (AlexaFluor488; green). Nuclei are stained with DAPI (blue). Note colocalization of Nox4 with the ER marker PDI. Identical results were obtained in aHDFs. Co-localization is indicated by yellow color in merged images. Representative confocal fluorescence

Results

images were taken at a 63x magnification of 3 independent experiments. Scale bar is 20 μm . **(B)** Detection of Nox4 immunoreactivity in SSc HDFs by double immunofluorescence analysis and confocal laser-scanning microscopy. Nox4 colocalized with the ER marker PDI. Scale bar: 20 μm . Images are representative for n=3 donors with identical results

Since several studies reported various subcellular localization of Nox4 isoform within different organelles in different cell types, we further investigated the localization of Nox4 within mitochondria, lysosome and focal adhesion. In separate experiments, HDFs were stained with antibodies directed against either vinculin, a focal adhesion protein or against LAMP2, a marker of lysosomes and or with the mitochondrial marker MTR. Double-immunofluorescence staining did not reveal any significant co-localization of Nox4 within the mitochondria, the lysosome or focal adhesions (**Fig. 13**). Taken together, these data represent strong evidence that Nox4 localized to the ER in HDFs.

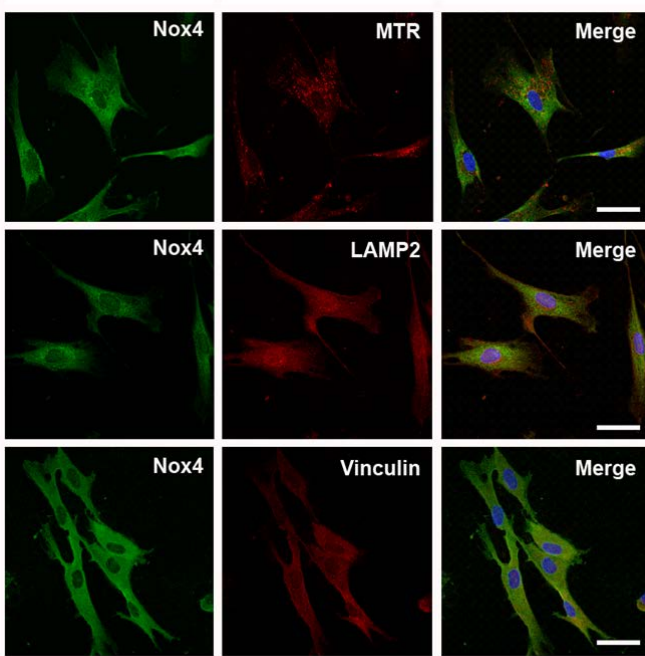


Figure 13. Nox4 did not co-localize with mitochondria, lysosomes or focal adhesion in nHDFs. Cells were double-stained with Nox4 antibody (green) and either the mitochondrial marker Mitotracker Red (red), an antibody against LAMP2 (red), or an antibody against vinculin (red). Nuclei were counterstained with DAPI (blue). Images are representative for 3 independent experiments with similar results. Scale bar: 50 μm .

4.3. Induction of Nox4 expression and NADPH oxidase activity by TGF- β_1 in HDFs

4.3.1. TGF- β_1 -upregulates Nox4 expression at mRNA level

Next, we assessed the gene expression of the Nox4 complex in HDFs in the context of fibroblast activation by the key profibrotic cytokine TGF- β_1 . Cells were treated with different doses of TGF- β_1 (0.1-10 ng/ml) for various time intervals (1- 48 hrs). Quantitative real-time PCR (qPCR) analysis revealed that TGF- β_1 dramatically up-regulated the expression of Nox4 at the mRNA level in a concentration and time-dependent manner (**Fig. 14A,B**). Remarkable significant induction of Nox4 mRNA was observed at 0.1 ng/ml by (~ 10-fold) and reached maximal level at 10 ng/ml (~ 50-fold) (**Fig. 14A**). Additionally, TGF- β_1 induced rapidly Nox4 gene expression within 4 hrs and maximal mRNA transcript level for TGF- β_1 was detected after 16 h at 10 ng/ml followed by a decrease. However, elevated Nox4 mRNA transcript levels were observed for 48 hrs (**Fig. 14B**). Indeed, treatment of aHDFs with TGF- β_1 for 16 hours likewise resulted in an increase of Nox4 mRNA (**Fig. 14C**). In contrast to the upregulating effect of TGF- β_1 on Nox4 mRNA in both nHDFs and aHDFs the mRNA expression levels of the Nox4 adaptors p22^{phox} and Poldip2 were not affected (**Fig. 14D**). Two different lot numbers of HDFs were analyzed with similar results.

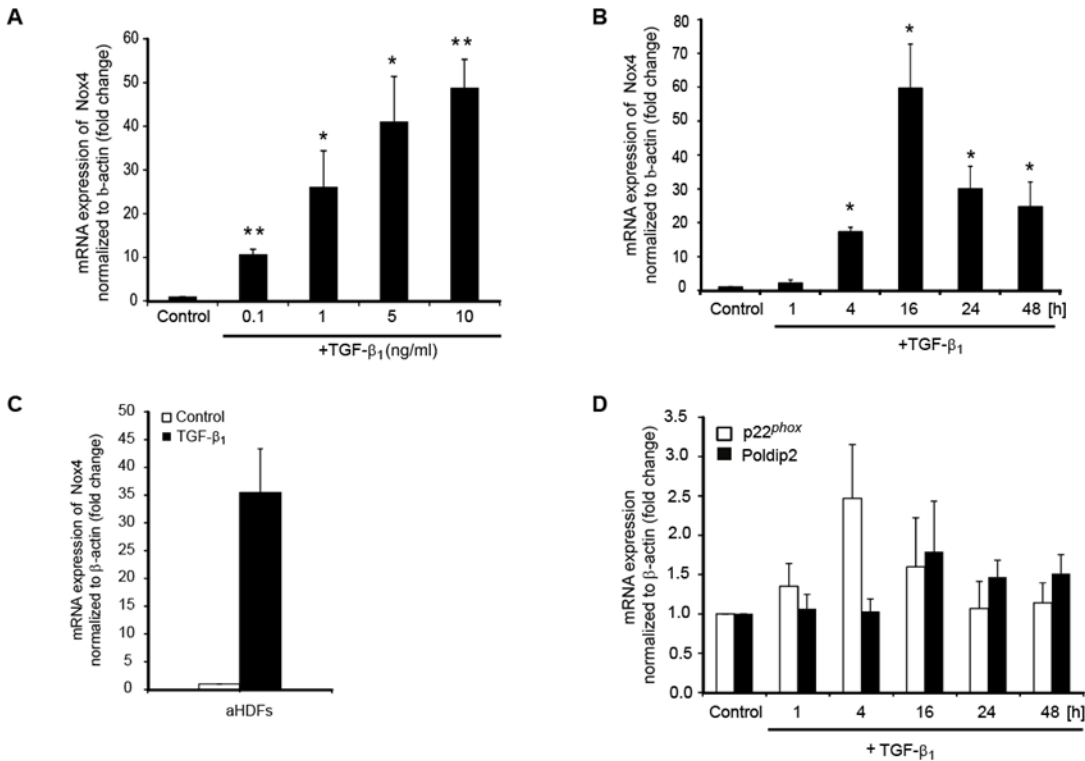


Figure 14. TGF- β_1 -induced Nox4 mRNA expression in HDFs. (A) Dose kinetics of TGF- β_1 -mediated upregulation of Nox4 mRNA expression as shown by real-time RT-PCR. Cells were treated with of TGF- β_1 for 16 hours at indicated doses. (B) Time kinetics of TGF- β_1 -mediated upregulation of Nox4 mRNA expression as shown by real-time RT-PCR. Cells were stimulated with TGF- β_1 (10 ng/ml) as indicated. $n=4$; * $p<0.05$; ** $p<0.01$ vs. control. (C) TGF- β_1 also induced Nox4 expression in aHDFs. Cells were treated with TGF- β_1 (10 ng/ml) for 16 hours followed by real-time RT-PCR analysis of Nox4 transcripts. $n=4$; * $p<0.05$ vs. control. (D) TGF- β_1 did not alter expression of p22^{phox} and Poldip2 expression in nHDFs. Cells were stimulated with TGF- β_1 (10 ng/ml) as indicated followed by real-time RT-PCR analysis. $n=4$.

4.3.2. TGF- β_1 upregulates Nox4 expression at protein level

To further determine whether TGF- β_1 also induced Nox4 expression at the protein level, cells were treated with TGF- β_1 (10 ng/ml) for different time intervals and Nox4 protein expression was analyzed with Western immunoblotting analysis using a commercial rabbit polyclonal Nox4 antibody. Notably, the Nox4 protein expression was also increased but showed later expression reached its maximum level at 16-24 hrs when compared to mRNA level, upon treatment with TGF- β_1 (10 ng/ml) (Fig. 15A). To clarify difference between the mRNA and protein level expression of Nox4 in HDFs, cells were cultured in the absence of serum for 24 hrs and then

Results

serum were readded and cells cultured for different time points. In order to investigate the basal level of Nox4 mRNA in the presence and absence of serum, we followed Nox4 mRNA levels after addition of serum. Nox4 mRNA amounts were significantly increased by more than 75 % in serum-derived nHDFs, in contrast, readdition of serum decreased the Nox4 expression to the basal level by 30% (**Fig. 15B**). Taken together, this observation needs further investigation to explain why mRNA expression and protein detection does not appear to be correlated.

Consistent with our previous results, however, we confirmed the impact of TGF- β_1 on Nox4 protein expression using an immunofluorescence approach. Again, TGF- β_1 showed increased intracytoplasmic Nox4 immunoreactivity relative to unstimulated cells (**Fig. 15C**). Negative controls incubated with secondary antibody showed no reaction

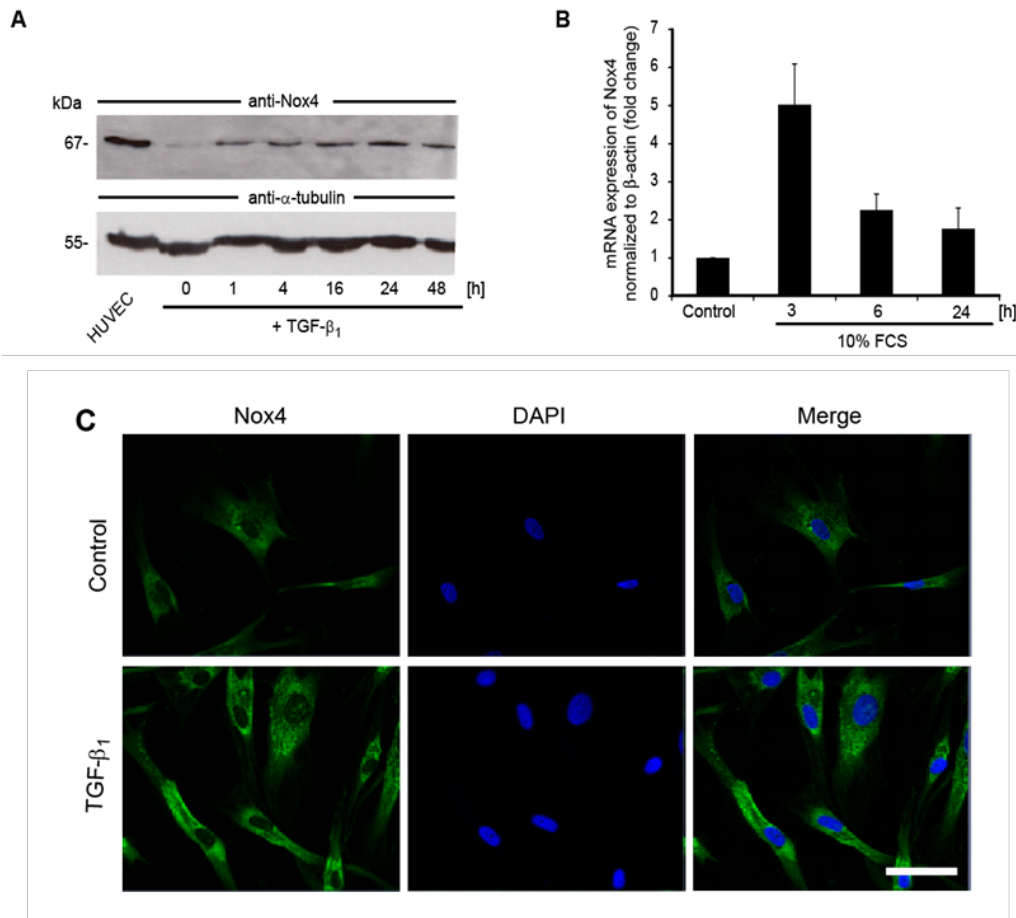


Figure 15. TGF- β_1 induces Nox4 protein expression in nHDFs. (A) Nox4 expression is induced by TGF- β_1 at protein level. nHDFs were stimulated with TGF- β_1 (10 ng/ml) for indicated time points

Results

followed by Western immunoblotting with an antibody directed against Nox4 (2 $\mu\text{g/ml}$). **(B)** Detection of Nox4 mRNA in the presence of serum. **(C)** Induction of Nox4 protein by TGF- β_1 as shown by immunofluorescence analysis (green). Cells were left untreated or stimulated with TGF- β_1 (10 ng/ml) for 16 hours. DAPI was used as nucleotracker (blue). Images are representative for 3 independent experiments with similar results. Scale bar: 50 μm .

4.3.3. TGF- β_1 enhances NADPH oxidase activity

Finally, we performed an enzymatic assay to determine if the transcriptional activation of Nox4 by TGF- β_1 leads to an increase of NADPH oxidase activity in HDFs. We specifically employed this assay since redox-sensitive fluoroprobes commonly used for measurement of oxidative stress are considered as non-specific (Kalyanaraman, Darley-Usmar et al. 2012) Therefore, cells were treated with TGF- β_1 for 24 hrs). NADPH oxidase activity was measured using lucigenin-enhanced chemiluminescence assay by addition of NADH as electron donors. Membrane fractions from nHDFs treated for 24 hours with TGF- β_1 displayed markedly enhanced NADPH oxidase activity over control (a representative result is shown in **Fig. 16**. These observations demonstrated that Nox4 (but not the other Nox4 adaptors) was a target gene for TGF- β_1 in HDFs. It should be noted that NADPH oxidase activity was present in both total cell homogenates and membrane but not in cytosolic fractions supporting the evidence that the cytosolic subunits are not essential for the functional activity of Nox4.

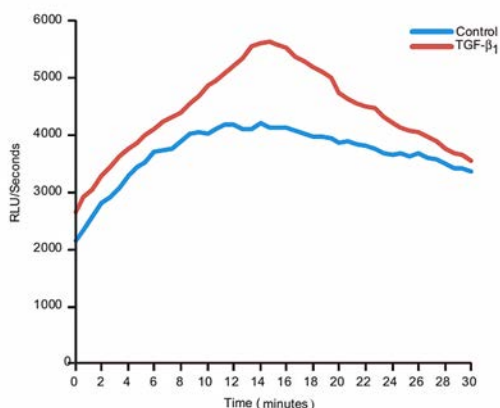


Figure 16. Increase of NADPH enzyme activity by TGF- β_1 Increase of NADPH enzyme activity by TGF- β_1 . Cells were stimulated with TGF- β_1 (10 ng/ml) for 24 hrs. Membrane fractions were incubated with lucigenin and NADH as substrates. The figure is representative of 3 independent experiments with similar results.

4.4. Functional characterization of Nox4 in TGF- β_1 -mediated activation of HDFs

In the next set of experiments, we intended to explore the role of Nox4-dependent generation of reactive oxygen species in TGF- β_1 signaling in cell culture. To exclude cytotoxic effects, we first assessed the effects of DPI and VAS2870 on cell viability in nHDFs.

4.4.1. Effect of the pharmacological inhibitor DPI on cell viability and metabolic activity in nHDFs

Harmful effects of DPI on cell viability and metabolic activity of HDFs were analyzed by XTT test and crystal violet assay, respectively. HDFs were incubated with different concentrations of DPI for 16 hrs. Then, both XTT test and crystal violet assay were performed. The results showed that DPI at concentrations ranging from (1-10 μM) were neither cytotoxic nor affected cell viability or metabolic activity of HDFs under our experimental conditions (**Fig. 17A,B**).

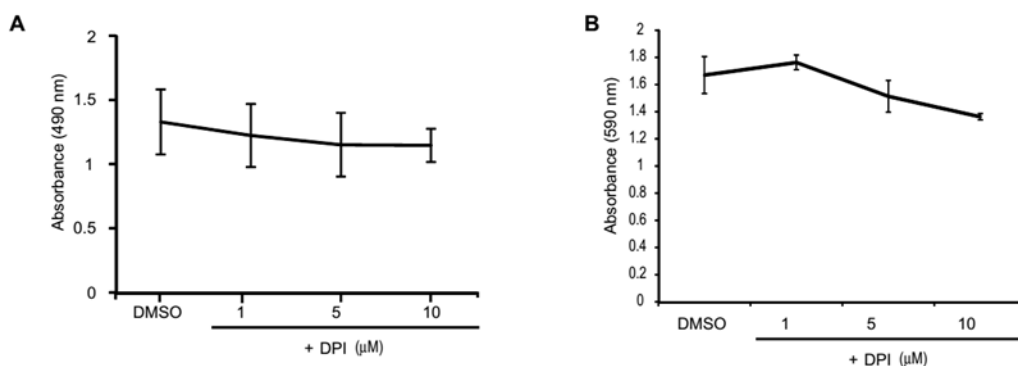


Figure 17. Effect of DPI on metabolic activity and cell viability of nHDFs as measured by crystal violet assay and XTT assay nHDF (10^5 cells /well) were seeded into 96 well plates. After serum starvation for 24 hrs, cells were incubated with different doses of DPI (1-10 μM). n=3; *p<0.05.

4.4.2. Effect of the pharmacological inhibitor VAS2870 on cell viability in nHDFs

Then, we examined the pharmacologically validated, low-molecular-weight NADPH oxidase inhibitor, VAS2870, which has been shown to exert beneficial effects in the treatment of cardiovascular diseases and has been applied in preclinical studies in both in vitro and in vivo experiments (Altenhöfer, Kleikers et al. 2012). First, cells were incubated with VAS2870 concentrations ranging from 5-50 μM , and metabolic activity and cell viability were assessed by XTT test and crystal violet assay, respectively. The results showed that VAS2870 at concentrations ranging from 5-50 μM decreased viability of HDFs

Results

by 40-50 % after 16 hrs of incubation (Fig. 18A, B). Therefore, concentrations higher than 10 μ M were not chosen for subsequent experiments, but concentrations ranging from (0.1- 2.5 μ M).

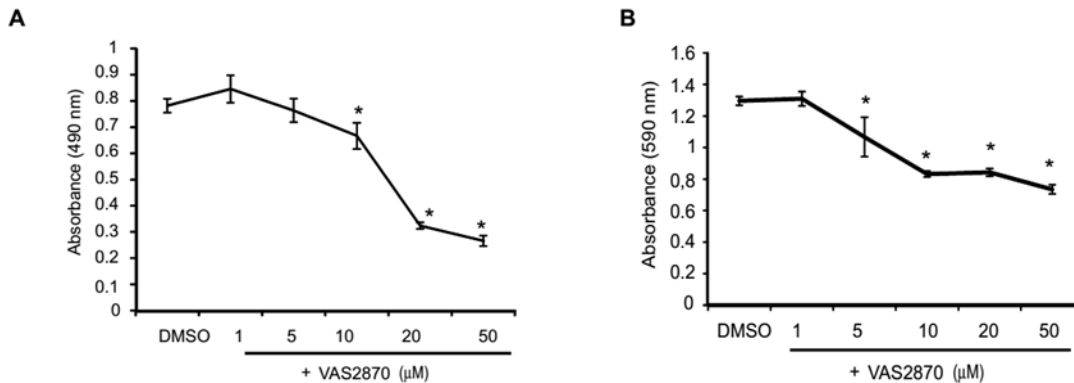


Figure 18. Effect of VAS2870 on metabolic activity and cell viability of nHDFs as measured by crystal violet assay and XTT test. nHDF (10⁵ cells /well) were seeded into 96 well plates. After serum starvation for 24 hrs, cells were incubated with different doses of VAS2870 (1-50 μ M). n=3; *p<0.05.

4.4.3. Pharmacological inhibition of NADPH oxidase by DPI reduces TGF- β ₁-mediated fibroblast activation

To explore whether Nox4 activation is involved in the cellular response of TGF- β ₁, we investigated the impact of the two established Nox inhibitors DPI, the most commonly used Nox inhibitor (Lambeth 2004), and VAS2870 on differentiation of fibroblasts into myofibroblasts which is considered a key event in fibrotic disorders (Hinz, Phan et al. 2012). First, nHDFs were pre-treated with DPI (10 μ M) and then stimulated with TGF- β ₁ for 16 hrs. Then the expression of established myofibroblast markers such as COL(I) α 1, COL(I) α 2, α -SMA, and fibronectin I was analyzed by real-time RT-PCR. **Fig. 12A** shows that expression of COL(I) α 1, COL(I) α 2, α -SMA and fibronectin I were increased after stimulation with TGF- β ₁. Pretreatment of nHDFs with DPI significantly suppressed this stimulatory effect of TGF- β ₁ not only on COL(I) α 1 and COL(I) α 2 gene expression but also on the expression of α -SMA and fibronectin 1 (**Fig. 19A**). In contrast, DPI *per se* did not have any significant effect on the basal expression of these genes in nHDFs. Collectively, these data suggest that Nox4 is involved in TGF- β ₁-mediated myofibroblasts differentiation.

To confirm these observations at the protein level, we also determined the inhibitory effect of DPI on TGF- β ₁-induced collagen type I secretion employing a procollagen type I C-terminal

Results

peptide (PICP) ELISA and assessed the expression of α -SMA and fibronectin 1 by immunofluorescence analysis. DPI neutralized both TGF- β_1 -mediated secretion of collagen type I (**Fig. 19B**) and reduced TGF- β_1 -mediated expression of both α -SMA and fibronectin 1 (**Fig. 19C**). These findings suggest that TGF- β_1 via Nox4 regulates activation of HDFs and myofibroblast differentiation.

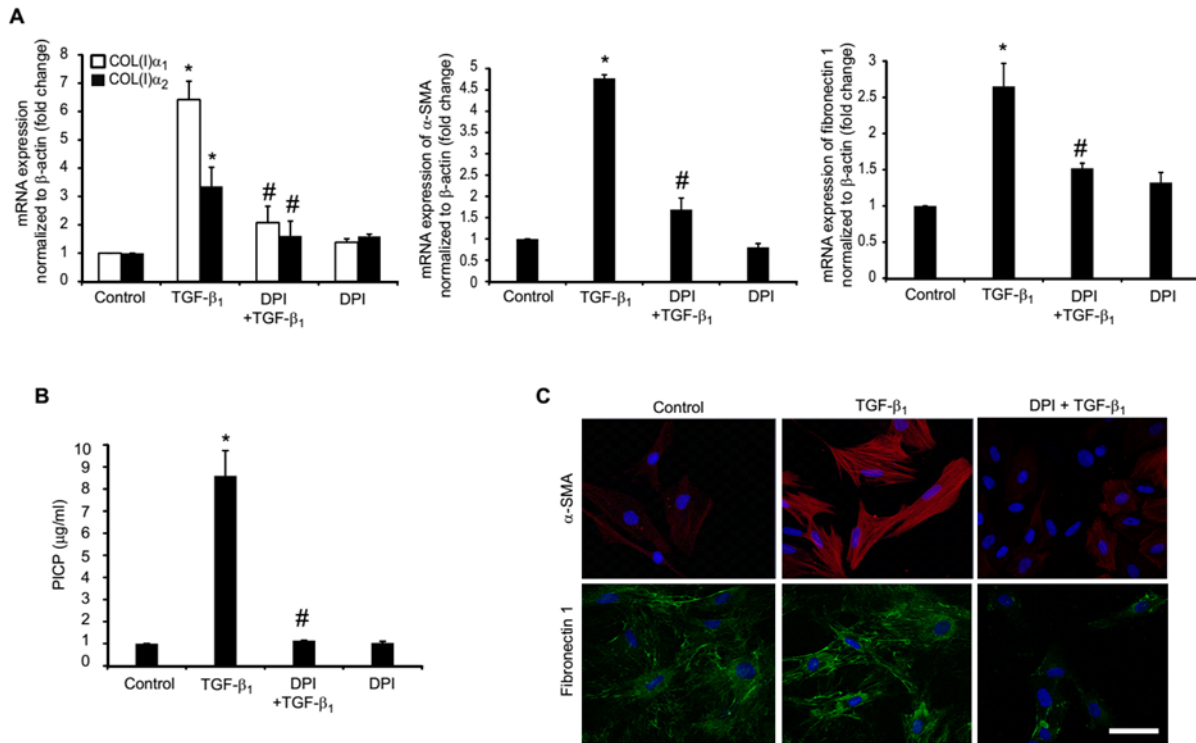


Figure 19. Effect of DPI on TGF- β_1 -mediated activation of dermal fibroblasts. (A) DPI abrogated TGF- β_1 -mediated expression of collagen type I, α -SMA and fibronectin 1. nHDFs were preincubated with DPI (10 μ M/ml) for 1 hour followed by TGF- β_1 treatment for 16 hrs and real-time RT-PCR. n=4; *p<0.05 vs. control; #p<0.05 vs. TGF- β_1 . (B) DPI abrogated TGF- β_1 -induced collagen type I secretion. nHDFs were treated with DPI as described followed by TGF- β_1 treatment for 48 hrs and PICP ELISA. n=3; *p<0.05 vs. control #p<0.05. (C) DPI inhibited TGF- β_1 -induced α -SMA and fibronectin 1 expression as shown by immunofluorescence. nHDFs were treated with DPI as described followed by TGF- β_1 treatment or 16 hrs. Nuclei were stained with DAPI. Images are representative for 3 independent experiments with similar results. Scale bar: 50 μ m.

4.4.4. VAS2870 does not reduce TGF- β_1 -mediated fibroblast activation

Then, we also investigated the effect of VAS2870 on TGF- β_1 -induced fibroblast differentiation into myofibroblasts. As shown in **Fig. 20A-C**, treatment with VAS2870 resulted in a small but not significant decrease in TGF- β_1 -mediated collagen type I expression (**Fig. 20A-C**). Further, it did not effectively abolish myofibroblast marker genes expression. VAS2870 alone had no significant effect on the basal expression of these genes in nHDFs. Taken together, these findings indicate that VAS2870 could interfere with other alternative sources of ROS, such as the mitochondrial electron chain that have not been investigated in our study, rather than NADPH oxidase.

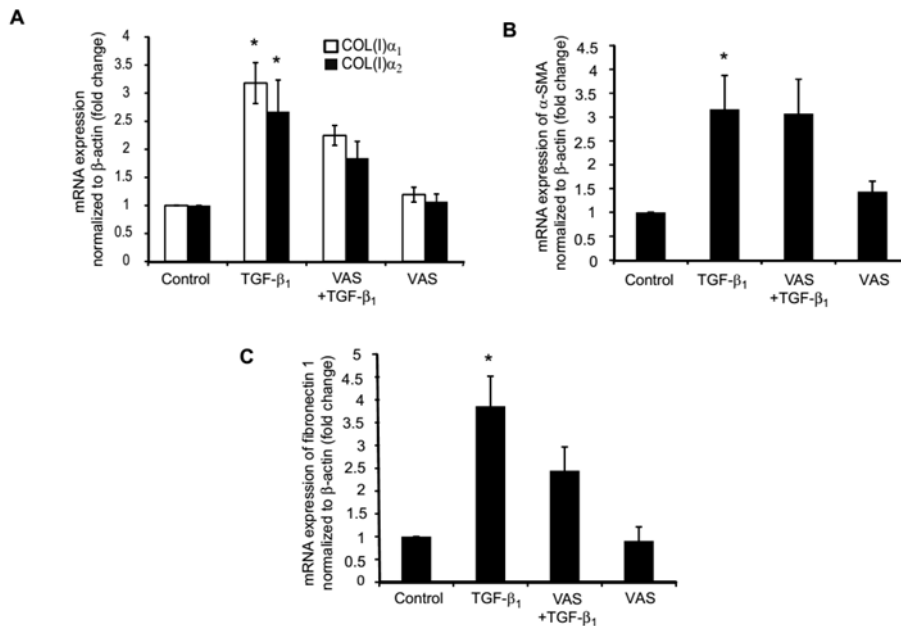


Figure 20. Effect of VAS2870 on TGF- β_1 -mediated activation of dermal fibroblasts. VAS2870 treatment could not effectively suppress collagen and myofibroblast marker genes expression. nHDFs were treated with VAS2870 (2.5 μ M) for 1 h prior to stimulation with TGF- β_1 (10 ng/ml) for 16 hrs. COL(I) α_1 , COL(I) α_2 (**A**), α -SMA (**B**) and fibronectin 1 (**C**) gene expression levels were quantified using real-time RT-PCR. n=3; *p<0.05 vs. control.

4.4.5. Genetic knockdown of Nox4 neutralizes TGF- β ₁-mediated fibroblast activation

In order to specifically confirm the role of Nox4 in both TGF- β ₁-induced collagen synthesis and myofibroblast marker gene expression, we transfected cells with either Nox4-specific siRNA or control non-targeting siRNA. Transfected cells were cultured in serum-free medium for 24 hrs and then further stimulated with TGF- β ₁ for 16 hrs. First, real-time RT PCR analysis revealed that Nox4 mRNA expression could be significantly suppressed by ~80 % compared to scrambled non-targeting control siRNA, indicating high efficiency as well as specificity of the siRNA Nox4 sequence. Second, transfection with Nox4 siRNA for 24 hours resulted in significantly reduced TGF- β ₁-inducible Nox4 mRNA levels compared to control siRNA. In accordance with our pharmacological studies using DPI, knock-down of Nox4 by siRNA markedly reduced the impact of TGF- β ₁ on collagen COL(I) α 1, COL(I) α 2, α -SMA, and fibronectin 1 gene expression (**Fig. 21A**). Interestingly, treatment of nHDFs with Nox4 siRNA further reduced basal gene expression of COL(I) α 1, COL(I) α 2, α -SMA, and fibronectin 1. This finding was not observed with nHDFs treated with DPI alone. Collectively, these data indicate that Nox4 is required for TGF- β ₁-mediated myofibroblasts differentiation and possibly for basal collagen expression and moreover expression of α -SMA and fibronectin1.

In parallel, we utilized Nox4^{-/-}-deficient murine dermal fibroblasts in order to prove the hypothesis that Nox4 acts as an intracellular mediator of fibroblast activation. If applicable it was expected that TGF- β ₁-mediated expression of collagen type I, α -SMA and fibronectin 1 should be abrogated. Indeed, TGF- β ₁ failed to upregulate gene expression of COL(I) α 1, COL(I) α 2, α -SMA, and fibronectin 1 in Nox4^{-/-}-deficient cells (**Fig. 21B**). These findings clearly provide strong evidence that endogenous Nox4 represent a crucial intrinsic mediator for TGF- β ₁-induced fibroblast activation as well as differentiation into myofibroblasts.

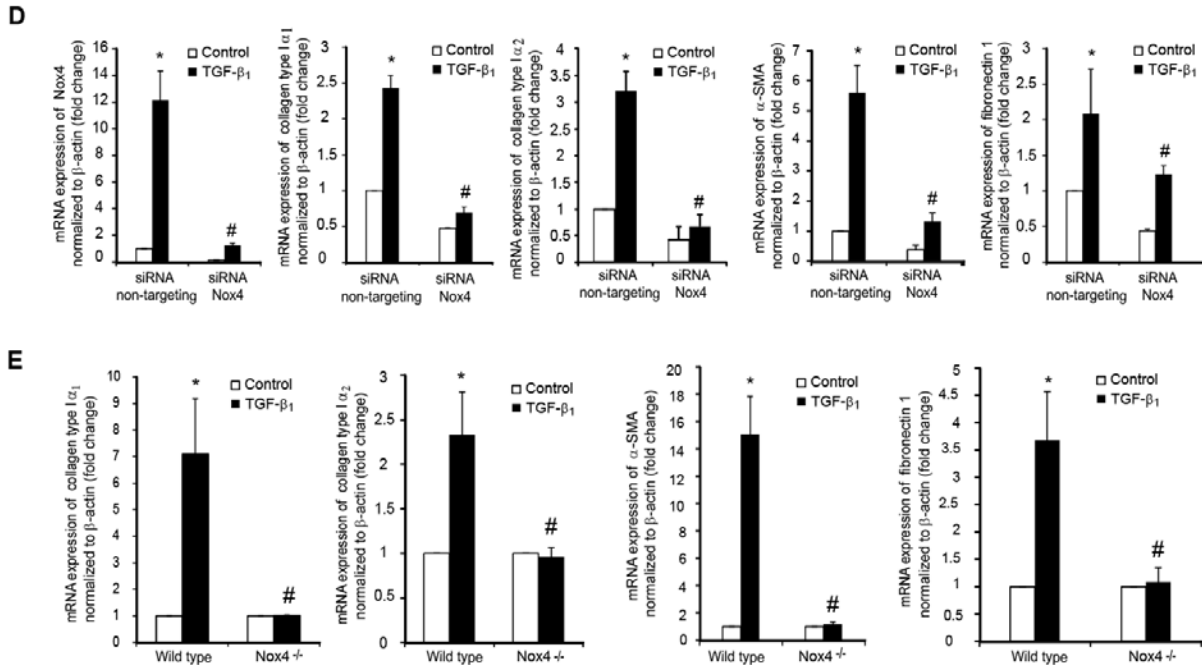


Figure 21. Effect of genetic inhibition of Nox4 on TGF-β₁-mediated activation of dermal fibroblasts. (A) Nox4 silencing by siRNA suppressed fibroblast activation by TGF-β₁. nHDFs were transfected with non-targeting siRNA or Nox4 siRNA for 48 hours followed by TGF-β₁ treatment for 16 hours and real-time RT-PCR of Nox4, COL(I)α₁, COL(I)α₂, α-SMA and fibronectin 1 transcripts was performed. Bars represent the means±SEM. n=3; *p<0.05 vs. non-targeting siRNA; #p<0.05 vs. non-targeting siRNA+TGF-β₁. (B) Nox4 gene ablation abrogated TGF-β₁-mediated collagen type I, α-SMA and fibronectin 1 expression. Murine Nox4^{-/-} or wild type dermal fibrosarcoma cells were treated with TGF-β₁ for 16 hrs followed by real-time RT-PCR. n=4; *p<0.05 vs. control. #p<0.05 vs. wild type+TGF-β₁

4.5. Regulation of Nox4 expression by TGF-β₁ in HDFs

4.5.1. *In silico* promoter analysis of the human Nox4 gene

To explore the underlying molecular mechanisms by which TGF-β₁ drives Nox4 gene expression in HDFs, we employed *in silico* promoter analysis of the human Nox4 gene. Computer based software programs (ALiBaba 2.1/TRANSFAC 8.3) were used to predict potential regulatory binding sites for transcription factors within the upstream 4.0 kb region of the human Nox4 promoter. By this informatic analysis, three putative binding sites were identified: one for nuclear factor (erythroid derived 2) like 2 (Nrf2), another for nuclear factor-κB (NF-κB), and a third one for Smad3 displaying the highest score (0.99) (**Fig. 22**). The localization of consensus sequences was counted relative to the ATG codon.

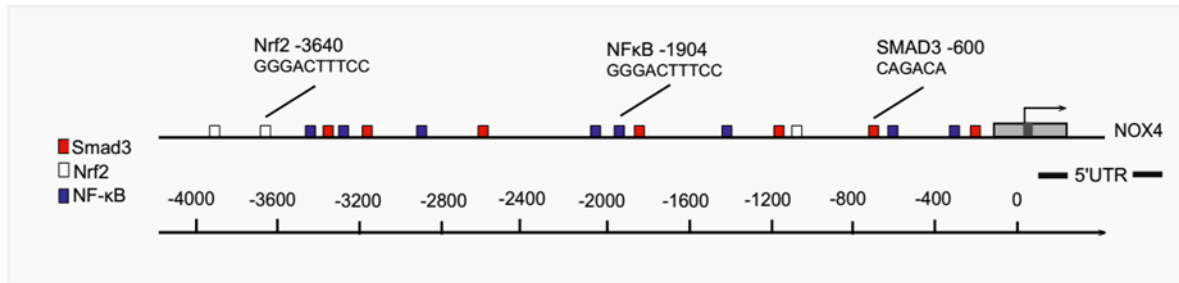


Figure 22. Mechanisms of TGF- β_1 -mediated Nox4 expression in nHDFs In silico analysis of Nox4 promoter for putative transcription factor binding sites. Each block represents a possible binding site: red bars: Smad3; white bars: Nrf2 sites; blue bars: NF- κ B sites. The numbers on the axis refer to bases upstream from the transcription start site.

4.5.2. Nox4 expression is depend on canonical smad3 signaling pathway in HDFs

To investigate whether RNA stabilization or transcriptional induction mediated the upregulating effect of TGF- β_1 on Nox4 mRNA expression, nHDFs were pretreated with the mRNA polymerase inhibitor actinomycin D for 30 min followed by stimulation with TGF- β_1 . The treatment resulted in a significant decline of Nox4 mRNA level after 16 hrs as shown by real-time RT-PCR analysis, indicating that TGF- β_1 -mediated Nox4 mRNA expression occurs via transcriptional induction (**Fig. 23A**).

It is likely that TGF- β_1 activates various intracellular signaling pathways, e. g. canonical and or non-canonical pathways (Allison, 2014). To elucidate the mechanism by which the upregulation of Nox4 induces dermal fibrosis and also to clarify whether TGF- β_1 -induced Nox4 expression was dependent on canonical Smad signaling pathway, we applied a pharmacological and genetic inhibition approach for Smad3. First, preincubation of HDFs with pharmacological specific Smad3 inhibitor SIS3 significantly alleviated TGF- β_1 -induced Nox4 expression (**Fig. 23C**). To further address the involvement of Smad3 in TGF- β_1 -induced Nox4 expression, siRNA Smad3 was applied. First, the specificity of siRNA Smad3 (25 nM), mRNA level of Smad3 was confirmed by real-time RT PCR analysis. As expected, mRNA level of Smad3 was reduced in cells transfected with Smad3 siRNA by ~70 % compared to control siRNA (**Fig. 23 B**). Second, TGF- β_1 -induced Nox4 up-regulation was partially, however significantly, attenuated by siRNA Smad3 in HDFs (**Fig. 23D**). These data was in accordance with our pervious pharmacological data.

Results

Collectively, these data indicate that Smad3 regulates TGF- β_1 -induced Nox4 upregulation in HDFs, providing further evidence that a crosstalk between NADPH oxidases and Smad mediates TGF- β_1 -induced myofibroblasts differentiation. However, we cannot exclude for certain that additional transcription factors may be also involved in the upregulation of Nox4 expression in response to TGF- β_1 .

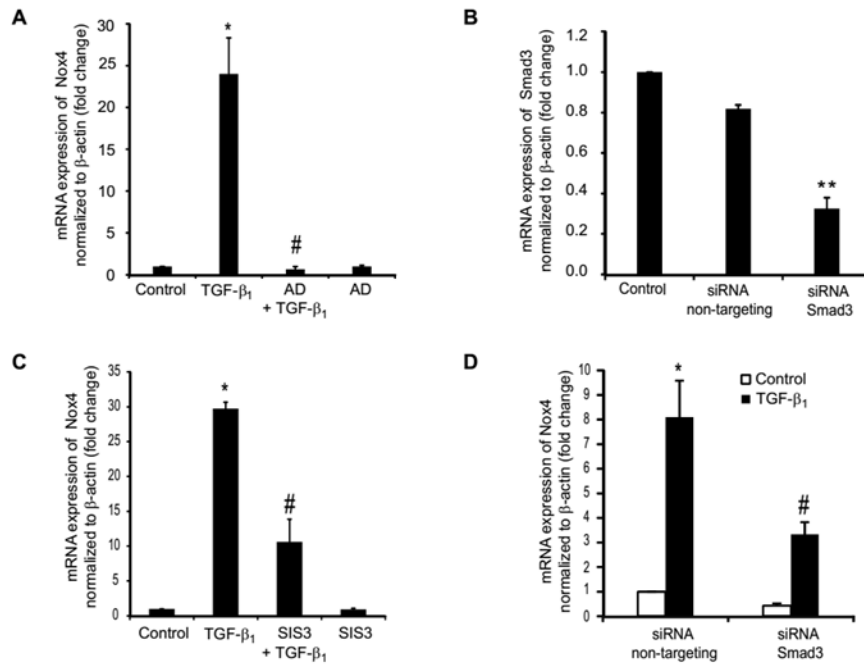


Figure 23. Mechanisms of TGF- β_1 -mediated Nox4 expression in nHDFs. (A) Nox4 was transcriptionally induced by TGF- β_1 . Prior to stimulation with TGF- β_1 (10 ng/ml) for 16 hours nHDFs were treated with 5 μ g/ml actinomycin D (AD) for 30 min. Nox4 expression was determined by real time RT-PCR. n=4; *p<0.01 vs. control; #p<0.01 vs. TGF- β_1 . (B) Suppression of Smad3 gene expression by siRNA in nHDFs. Cells were transfected with Smad3 siRNA (25 nM) or non-targeting siRNA for 48 hours followed by real-time RT-PCR analysis. n=3; **p<0.01 vs. non-targeting siRNA. (C,D) Impact of pharmacological inhibition and gene silencing of Smad3 by siRNA on TGF- β_1 -mediated Nox4 expression in nHDFs. Cells were pretreated with SIS3 (5 μ M) for 1 hr followed by stimulation with TGF- β_1 (10 ng/ml) for 16 hrs and real-time RT-PCR. n=3; *p<0.05 vs. control; *p<0.05 vs. TGF- β_1 . For Smad3 gene silencing cells were transfected with either non-targeting siRNA or Smad3 siRNA (25 nM) for 48 hours followed by stimulation with TGF- β_1 (10 ng/ml) for 16 hours and real-time RT-PCR analysis. n=3; *p<0.05 vs. non-targeting siRNA; #p<0.05 vs. non-targeting siRNA + TGF- β_1 .

4.6. Pharmacological inhibition of NADPH oxidase activity by DPI reduces cutaneous fibrosis in the bleomycin mouse model of scleroderma

Since both pharmacological inhibition of NADPH oxidase activity by DPI and Nox4-specific gene suppression strongly reduced TGF- β ₁-mediated activation of HDFs, we then utilized the bleomycin (BLM) mouse model of scleroderma to verify the effect of this agent in experimentally induced skin fibrosis. Mice were administered DPI daily by i. p. injection at a dose of 2 mg/kg/day) or vehicle control beginning immediately with BLM injection. None of the mice experienced signs of toxicity by the latter treatment. After 30 days of BLM or DPI treatment, skin biopsies were harvested from four animal groups followed by RNA extraction, assessment dermal thickness, and measurement of collagen content.

BLM increased the mRNA transcript levels of COL(I) α 1 and COL(I) α 2 compared to NaCl-treated animals as shown by real-time RT-PCR analysis (**Fig. 24A,B**). Treatment with DPI markedly reduced or even normalized the cutaneous levels of COL(I) α 1 and COL(I) α 2 gene expression in DPI treated mice compared to NaCl treated mice while it appeared to even slightly increase the mRNA levels of collagen type I α 2 compared to NaCl-treated mice. Furthermore, the effect of Nox inhibition on skin fibrosis in the scleroderma mouse model was also determined by analysis of extracellular matrix gene expression (**Fig. 24C,D**). Interestingly, DPI treatment significantly reduced BLM-induced α -SMA and fibronectin I mRNA expression compared to mice receiving BLM alone. DPI itself had no effect on the expression of the above mentioned genes.

These mRNA data were confirmed at protein level with regard to cutaneous collagen type I. as shown in **Fig. 24E**. Routine histochemical analysis likewise confirmed the anti-fibrogenic effect of DPI compared to animals treated with BLM alone (**Fig. 24 F**).

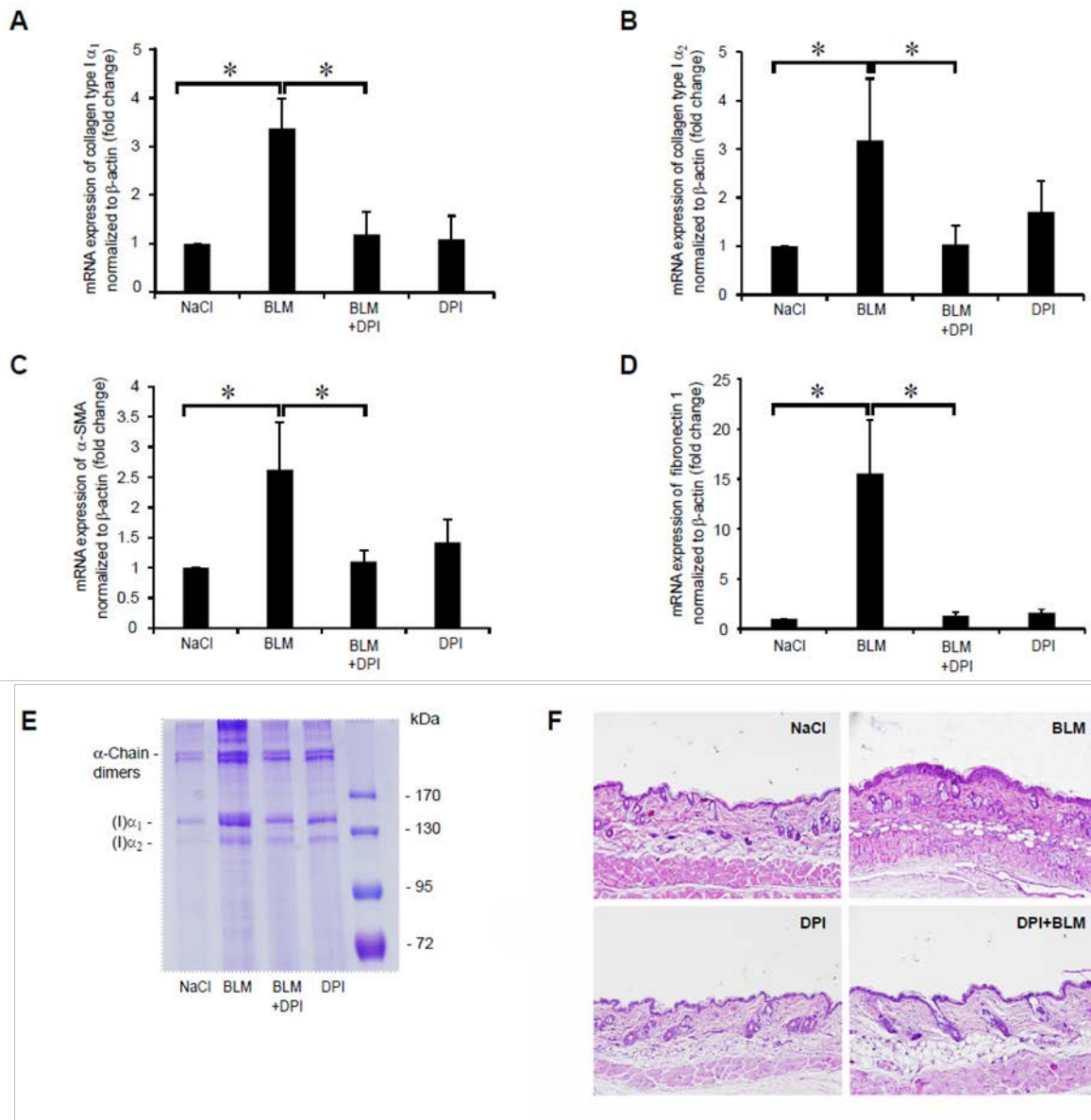


Figure 24. The NADPH oxidase inhibitor DPI attenuated BLM-induced skin fibrosis.

(A-D) C3H/HeJ mice were injected daily subcutaneously with BLM (10 μ g) alone or in combination with daily DPI (i. p., 2 mg/kg). Control mice received NaCl or DPI alone. COL(I) α_1 , COL(I) α_2 were determined in skin biopsies after 4 weeks by real-time RT-PCR analysis. n=7 mice per group; *p<0.05. (E) Determination of collagen protein content using pepsin digestion methods. Mice were treated as above, and proteins were extracted from skin samples, digested with pepsin, and separated by SDS-PAGE. Results are representative of 6 independent experiments with identical results. (F) Skin fibrosis was also assessed by routine histochemistry (H&E staining). Depicted are representative images of each treatment group with similar results. Scale bar: 100 μ m.

4.7. Nox4 is an emerging novel target for antifibrotic agents

In a final set of experiments we analyzed the effect of 3 established pharmacological agents on TGF- β_1 -induced Nox4 expression in HDF that have recently been shown to exert fibrosis-preventing properties in distinct molecular pathways. The peptide α -MSH induces canonical cAMP signaling in fibroblasts and prevents bleomycin-induced fibrosis in mice (Böhm, Raghunath et al. 2004, Kokot, Sindrilaru et al. 2009). Tropisetron elicits Ca⁺² signaling and has both antifibrotic and antifibrotic effects (Stegemann, Sindrilaru et al. 2013). Everolimus was shown to antagonize TGF- β_1 -induced collagen secretion and to suppress BLM-induced skin fibrosis (Böhm et al, in preparation). Remarkably, treatment with α -MSH suppressed TGF- β_1 -mediated Nox4 expression in a dose-dependent manner as shown by real-time RT-PCR (**Fig. 25A**) while neither tropisetron (10 μ g/ml) nor everolimus (500 nM) exerted any effects. In addition, treatment with α -MSH further attenuated the upregulatory effect of TGF- β_1 on α -SMA, fibronectin 1, COL(I) α 1, and COL(I) α 2 gene expression, providing evidence for the first time that this peptide might be involved in the regulation of Nox4 gene expression (**Fig. 25B-D**).

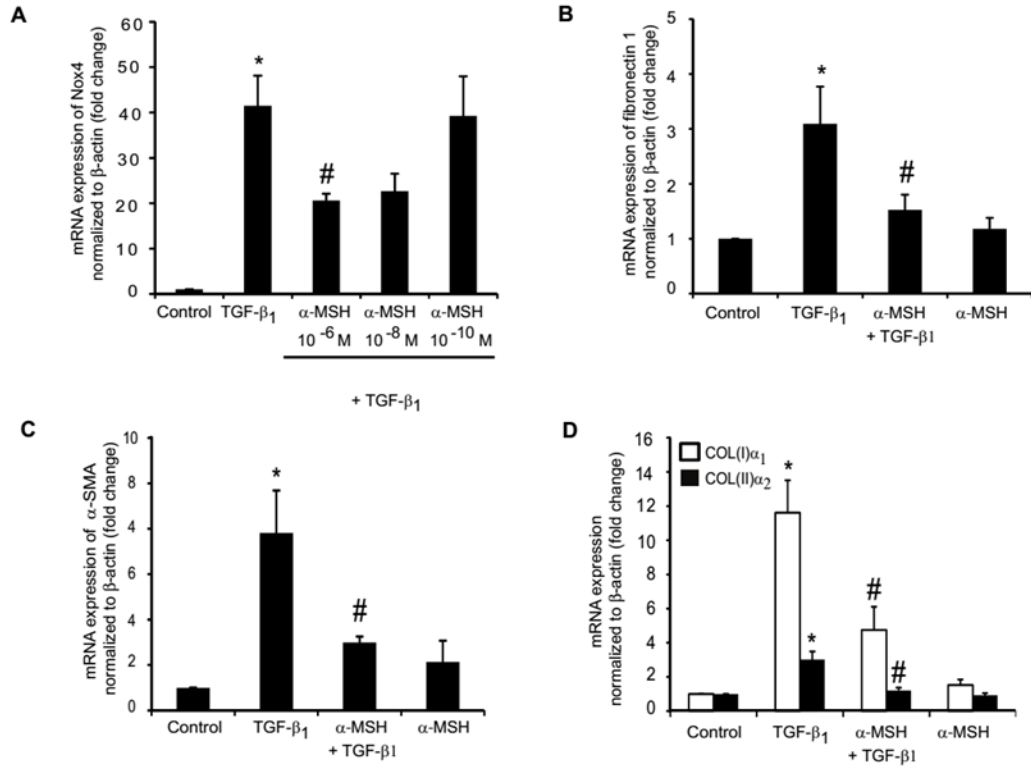


Figure 25. α -MSH suppresses TGF- β_1 -mediated Nox4, Collagen and myofibroblast marker genes expression in HDF. Cells were preincubated with α -MSH for 6 hrs as indicated followed by stimulation with TGF- β_1 (10 ng/ml) for 16 hrs. Expression of Nox4 (A), fibronectin 1 (B), α -SMA (C), collagen type I α_1 and α_2 (D) mRNA transcripts was determined by real-time RT-PCR. n=3; *p<0.05 vs. control; #p<0.01 vs. TGF- β_1 .

5. Discussion

SSc is a complex autoimmune disease with an incompletely understood pathogenesis that involves autoimmune, vascular and fibrotic damage. Several mediators including TGF- β_1 induce collagen synthesis and the excessive accumulation of extracellular matrix, making them to master regulators of pathological fibrosis. In addition, there is also accumulating evidence that abnormal expression and activity of distinct Nox isoforms are involved in the pathogenesis of some fibrotic diseases such as lung fibrosis. For example, oxidative stress has been shown to be pathogenetically relevant in SSc (Gabrielli, Svegliati et al. 2008, Gabrielli, Svegliati et al. 2012). However, the underlying molecular mechanism by which TGF- β_1 and oxidative stress-generating intracellular enzymes contribute to SSc pathogenesis remains largely unexplored, in particular in relevant skin cells such as HDFs. Therefore, the present thesis has been performed to study the role of oxidative stress-generating intracellular enzymes in the context of TGF- β_1 signaling within fibrotic disorders.

5.1. Nox4 is abundant in SSc HDFs

First, we investigated the expression of various Nox isoforms in HDFs from both healthy individuals and individuals suffering from SSc. We found that Nox4 mRNA expression was relatively abundant in normal HDFs as well as in diseased cells. These findings are in accordance with previous studies exploring Nox4 in kidney fibroblasts (Geiszt, Kopp et al. 2000), cardiac fibroblasts (Rocic and Lucchesi 2005), lung fibroblasts (Hecker, Vittal et al. 2009), pulmonary fibroblasts (Amara, Goven et al. 2010) and renal fibroblasts (Kern, Mair et al. 2014). In contrast to previous studies of Sambo (Sambo, Baroni et al. 2001) and (Spadoni, Svegliati Baroni et al. 2015) we were unable to detect the prototypic Nox isoform Nox2, its cytosolic proteins, or its other cytosolic components in normal and SSc HDFs. Similarly, we did not detect transcripts for Nox1 in both normal and diseased HDFs. Therefore, further studies are required to clarify these discrepancies. Additionally, we could show that healthy HDFs express Nox5, Duox1 and the small GTPases Rac1 and Rac2. A very recent study demonstrated that inactivation of Nox4/5 reduced the indirect harmful effect caused by ROS production and radiation-induced DNA damage in human primary fibroblasts, although the interplay between Nox4 and Nox5 enzymatic activities in ROS production remained unclear (Weyemi, Redon et al. 2015). Notably, we could

not detect Duox1 in our SSc HDFs. To our knowledge the expression of Duox1 has not been reported earlier, thus the functional relevance of the previous observation is not clear to date and requires further investigations.

Our data showed differential expression of Nox4 at mRNA and protein levels in both adult HDFs and SSc HDF. There was no significant difference at Nox4 mRNA level while Nox4 protein was abundant in SSc HDFs. Differential expression was not detected for p22^{phox} and Poldip2. It cannot be excluded that larger sample sizes might reveal statistically higher Nox4 expression (at the mRNA level) in SSc HDFs than normal HDFs. However, it is well established that changes at gene expression levels do not frequently correlate with corresponding changes at protein level. In addition, various regulatory mechanisms might occur during gene expression, such as transcriptional, post-transcriptional, and translational modification. With respect to these data we conclude that gene expression levels do not necessarily reflect protein levels, especially for enzymatic proteins (like Nox4) that must undergo post-translational modifications and structural or configuration changes at the catalytic core (Maier, Guell et al. 2009, Weake and Workman 2010). We also speculate that the latter difference might be related to differences in experimental culture conditions and/or donor variability.

Our principal finding that Nox4 protein is highly expressed in SSc HDFs than control cells is consistent with recent studies demonstrating an increased in situ immunoreactivity of Nox4 in patients with idiopathic lung fibrosis (Hecker, Vittal et al. 2009) and enhanced Nox4 expression in pulmonary fibroblasts from patients with idiopathic pulmonary fibrosis (IPF) (Amara, Goven et al. 2010). Interestingly, overexpression of Nox4 has been linked to pathological tissue remodeling and fibrosis in different organ systems including the heart (Ago, Kuroda et al. 2010, Aoyama, Paik et al. 2012), liver (Aoyama, Paik et al. 2012) and kidney (Sedeek, Gutsol et al. 2013). Furthermore, treatment of HDFs with serum decreased Nox4 expression at the mRNA level in a time dependent-manner. Interestingly, the Jiang group showed a negative correlation between steady state level of Nox4 mRNA and the serum treatment in endothelial cells (Peshavariya, Jiang et al. 2009). Additionally, in pancreatic cancer cells both Nox4 protein expression and ROS production were increased after the addition of serum to culture medium. The authors proposed that serum could be a powerful inducer of Nox4 protein expression and it needs to be considered in future studies concerning Nox4 expression. Thus, the precise role of

serum in regulation of Nox4 expression in HDFs is apparently not clear and needs further investigations.

5.2. Nox4 is colocalized with endoplasmic reticulum in HDFs

Many studies have shown that Nox4 is localized in different compartments in various cell types which influence its functions including enzyme activity, the type of ROS produced and downstream signaling mechanisms. Therefore, we investigated the intracellular localization of Nox4 in healthy and diseased HDFs. Through laser scanning confocal microscopy, we found that Nox4 is localized in the endoplasmic reticulum but not in other cellular compartments such as focal adhesions, mitochondria, and lysosomes. In other studies, Nox4 expression was found in different organelles. For example, in vascular smooth muscle cells, Nox4 was close to focal adhesions (Hilenski, Clempus et al. 2004); in transfected HEK293 cells, it was found in the ER (Martyn, Frederick et al. 2006, Chen, Kirber et al. 2008) or in plasma membranes (Lee, Qiao et al. 2010). Conversely, in a different study with vascular smooth muscle cells and endothelial cells, Nox4 was reported to be localized in the nucleus (Hilenski, Clempus et al. 2004) (Kuroda, Nakagawa et al. 2005). Additionally, in somatic cells, Nox4 was detected in mitochondria (Block, Gorin et al. 2009).

Even in the same cell type, different studies have found Nox4 in different locations. This may be at least a consequence of Nox4 having yet unknown interaction partners or is due to different Nox4 antibodies used in these studies that exhibit various affinities and (cross) reactivates. Indeed, Nox4 was demonstrated to relocate from focal adhesions to stress fibers during differentiation in vascular smooth muscle cells (Clempus, Sorescu et al. 2007). Based on these findings, another hypothesis might be that changes in Nox4 localization correlate with the functional or pathological state of cells (Weyemi, Caillou et al. 2010). Here, we found that Nox4 co-localized with the regulatory protein PDI in the ER in nHFDs and SSc fibroblasts and this might suggest that Nox4 is restricted to the ER in nHDFs.

Based on our observation, we suggest that a cross talk between NADPH oxidase and ER signaling might exist and that PDI might regulate Nox4 activation in HDFs. Notably, Nox4 activation in response to ER stress has been shown in different studies (Laurindo, Fernandes et al. 2008, Santos, Tanaka et al. 2009, Loughlin and Artlett 2010, Amanso, Debbas et al. 2011). In addition, it is thought currently that ER stress has a profibrotic role. In a previous study using a

rat model of cardiac fibrosis, tunicamycin-induced ER stress along with bleomycin-induced fibrosis increased the expression of PDI and cardiac fibrosis. This finding suggests that activation of ER stress could affect fibrotic remodeling (Ayala, Montenegro et al. 2012). Furthermore, recent evidence revealed a close association between the ER stress and cutaneous systemic sclerosis which might have a direct impact in TGF- β_1 response in myofibroblast activation through induction of ROS production.

Since Nox4 is the only detectable isoform in HDFs, its activation might link ER stress and oxidative stress to the TGF- β_1 -induced fibroblast activation and eventually development of fibrosis. In fact, there are number of recent published papers that link directly or indirectly Nox-derived ROS to ER stress. According to our findings, Nox4 is up-regulated upon TGF- β_1 stimulation leading to oxidative stress which could trigger the unfolded protein response (UPR) signaling that results in ROS production from the ER-resident Nox4 generating a vicious cycle. During this process, PDI will activate and promote Nox4 activation to produce hydrogen peroxide which subsequently contribute to activation and differentiation of fibroblast into myofibroblasts and ultimately lead to fibrosis (Santos, Nabeebaccus et al. 2014), yet, the order remains to be determined. Therefore, this organelle might be an important location where Nox4 produces its main ROS product, hydrogen peroxide. One of the limitation of this study is that we did not investigate the effect of the physical interaction between PDI and Nox4, however we postulate that Nox4 itself might represent a source of ER-generated ROS and PDI might promote the oxidative stress in HDFs by maintaining the Nox4 activity. Thus, PDI might be a novel regulator of Nox4 signaling in HDFs contributing to oxidative stress in SSc and further studies are required to prove our speculations. Thus, the understanding of such association could facilitate further identification the comprehensive mechanism of PDI-Nox activation and its potential contribution in fibrotic disorders which remains to be investigated. With better understanding of the ROS pathobiology in human cells, it should be possible to develop a specific targeted Nox inhibitor or ER-targeted antioxidants which could be used in a combined therapy.

5.3. Nox4 expression is regulated by TGF- β_1 in HDFs

In the present study we showed that TGF- β_1 strongly induces Nox4 expression, which in turn mediates fibroblast activation and synthesis of ECM components. The induction of Nox4 expression in response to TGF- β_1 is consistent with previous findings (Cucoranu, Clempus et al. 2005, Hecker, Vittal et al. 2009, Bondi, Manickam et al. 2010, Michaeloudes 2011) (Barnes and Gorin 2011). However, we were unable to detect a modulatory effect of TGF- β_1 upon the expression of its associated proteins p22^{phox} and Poldip2. This is in contrast to findings by (Manickam, Patel et al. 2014) who demonstrated a role for Poldip2 in TGF- β_1 -induced Nox4-dependent ROS production in kidney fibroblasts and subsequent myofibroblast activation. Another study also revealed that Nox4 and p22^{phox} were concomitantly increased at the protein level in the kidneys of diabetic rats (Etoh, Inoguchi et al. 2003). However, endogenous factors such as p22^{phox} and Poldip2 might not need to be upregulated to the same expression level as Nox4 to coordinate ROS production. Thus, instead of influencing affect Nox4 expression or subcellular localization, these associated proteins might only affect Nox4 stabilization and activity (Lyle, Deshpande et al. 2009).

Although it is well known that TGF- β_1 promotes collagen expression and differentiation of fibroblasts into myofibroblasts, which are responsible for ECM production leading to fibrotic disorders (Takagawa, Lakos et al. 2003, Lakos, Takagawa et al. 2004), little is known about the signaling mechanisms that mediate this response. To prove the role of Nox4 in TGF- β_1 -mediated dermal fibrosis, two in vitro approaches were used to inhibit Nox4 activity: a pharmacological approach using the NADPH oxidase inhibitor DPI and a genetic approach using specific siRNA for Nox4. Overall, inhibiting Nox4 significantly attenuated not only collagen expression but also expression of myofibroblasts marker genes such as fibronectin I and α -SMA in response to TGF- β_1 . For example, when Nox4 was inhibited by DPI, enhanced activity of NADPH oxidase was significantly diminished in subcellular fractions. Additionally, in murine Nox4-deficient dermal fibrosarcoma cells derived from Nox4 knockout mice, TGF- β_1 had almost no stimulatory effect on collagen synthesis and the expression of myofibroblasts marker genes. These findings are in agreement with previous reports demonstrating a similar effect of genetic ablation of Nox4 in TGF- β_1 -mediated induction of collagen and extracellular matrix proteins in

lung fibroblasts (Hecker, Vittal et al. 2009), adventitial fibroblasts (Amara, Goven et al. 2010) and kidney fibroblasts (Bondi, Manickam et al. 2010). Taken together, we propose that Nox4 acts as a potent mediator in the downstream profibrotic signaling of TGF- β_1 in HDFs, one of the main effector cells involved in the development of fibrotic lesions in SSc.

5.4. Nox4 expression is regulated by the Smad2/3 pathway in HDFs

To elucidate the molecular mechanism by which Nox4 modulates TGF- β_1 -mediated fibroblast activation, we investigated the canonical TGF- β_1 -dependent Smad2/3 pathway. Smad2/3 are involved in both the induction of Nox4 and the proliferation of lung fibroblasts (Hecker, Vittal et al. 2009), pulmonary vascular smooth muscle cells (Sturrock, Cahill et al. 2006) and endothelial cells (Peshavariya, Chan et al. 2014). In addition, there is evidence that several transcription factors, such as Smad3, Nrf2, NF- κ B and AP1 potentially coordinate in the regulation of Nox expression and function (Manea, Manea et al. 2008, Manea, Tanase et al. 2010, Siuda, Zechner et al. 2012, Bai, Hock et al. 2014). Therefore, Smad3 was inhibited either pharmacologically by SIS3, a smad3 specific inhibitor, or genetically by using specific siRNA for Smad3. Smad inhibition led to a partial but significantly reduction in TGF- β_1 -mediated Nox4 expression. This observation is sustained by the findings that TGF- β_1 signaling via Smad2/3 was important in the transformation of fibroblasts to myofibroblasts and Nox4 was shown to be important in this signaling process (Cucoranu, Clempus et al. 2005). That previous study also showed that ROS production through Nox4 activation in response to TGF- β_1 caused persistent Smad3 activation through a feed-forward mechanism. Nonetheless, activation of Nox4 amplifies the H₂O₂ signal, which activates the TGF- β_1 signaling pathway through a feedback mechanism (Thannickal 1995, Thannickal and Fanburg 1995, Murakami, Ichinohe et al. 2013). Although TGF- β_1 was originally thought to exert its function through activation of the Smad pathway, recent studies have shown that TGF- β_1 counteracts other Smad-independent signaling pathways, such as MAPK pathways that involve p38, ERK, and JNK. For instance, both TGF- β_1 -induced canonical Smad2 and non-canonical ERK1/2 pathways regulated Nox4 expression in microvascular endothelial cells (Jain, Rivera et al. 2013). Although these data provide further evidence that Nox4 mediates myofibroblasts activation via TGF- β_1 /Smad3 signaling, we cannot exclude for certain that other pathways might also be involved.

5.5. Nox4 inhibition prevented experimentally induced skin fibrosis in the bleomycin mouse model of scleroderma

To demonstrate the *in vivo* relevance of our *in vitro* findings, we used an established mouse model of SSc. Herein, dermal fibrosis is induced by daily subcutaneous injections of BLM (Yamamoto, Takagawa et al. 1999). We found that pharmacological inhibition of NADPH oxidase activity by DPI prevented experimentally induced skin fibrosis in the BLM mouse model of scleroderma. These results are consistent with a previous study by Hecker et al. 2009, who showed that Nox4 inhibition (through *in vivo* DPI administration and *in vivo* siRNA treatment) suppressed BLM-induced lung fibrosis. Further evidence is given by two other *in vivo* studies showing that Nox4 is involved in local TGF- β_1 -stimulated collagen accumulation (Chan, Peshavariya et al. 2013), and BLM administration in p47^{phox} knockout mice lead to markedly suppressed collagen deposition in lungs (Manoury, Nenan et al. 2005). Interestingly, a recent study demonstrated that Nox4 mRNA and protein expression was increased by BLM and reversed by preincubation with roflmilast N-oxide (RNO), the active metabolite of roflmilast (Vecchio, Acquaviva et al. 2013). In summary, the *in vivo* reports together with our *in vivo*- and *in vitro* findings indicate that anti-fibrotic agents could be beneficial for treating fibrotic disorders in humans, in particular for SSc.

5.6. α -MSH suppressed TGF- β_1 -mediated Nox4 gene expression in HDFs

We finally showed that the peptide α -MSH attenuated TGF- β_1 -mediated Nox4 induction in a dose dependent manner when preincubated before addition of stimulants. Additionally, α -MSH could also attenuate the expression of collagen, fibronectin I and α -SMA in response to TGF- β_1 . This result is in agreement with a previous study by (Böhm, Raghunath et al. 2004) who showed that α -MSH reduced TGF- β_1 -mediated collagen synthesis via the melanocortin-1 receptor (MC-1R) *in vitro*. *In vivo*, α -MSH was found to attenuate skin fibrosis in the bleomycin scleroderma mouse model (Kokot, Sindrilaru et al. 2009). However, in MC-1R-deficient mice, bleomycin-induced fibrosis is aggravated, suggesting that this receptor has a pathogenic role in fibrotic Conditions (Böhm and Stegemann 2014). Phase II trials with a superpotent α -MSH analogue have already been conducted for treating a number of skin diseases, including inflammatory disorders (Böhm, Ehrchen et al. 2014). Most recently, a superpotent α -MSH analogue was approved for treating the orphan disease erythropoetic protoporphyria (Luger and Böhm 2015).

Our finding therefore supports and further extends previous findings in which α -MSH reduced BLM-induced intracellular accumulation of ROS in vitro (Kokot, Sindrilaru et al. 2009). It is likely that its suppressive effect is mediated by induction of anti-oxidative enzymes and/or transcription factors regulating those enzymes.

Finally, an important perspective would be to determine the mechanism by which α -MSH decreases Nox4 gene transcription. α -MSH can upregulate the expression of superoxide dismutase 2 and heme oxygenase-1(HO-1) in HDFs. HO-1 expression is under the control of Nrf2. It is a crucial transcriptional regulator of antioxidant genes, and it binds to antioxidant response elements (AREs), which are present in many cytoprotective genes. Nrf2 is expressed in human skin cells such as human dermal fibroblasts, and normal human keratinocytes; moreover, in human skin the expression of Nrf2 expression and Nrf-dependent genes is upregulated by α -MSH. Interestingly, a cross talk between NADPH oxidase and Nrf2 has been suggested in endothelial cells. In one study, Nrf2 knockdown by short hairpin RNAs increased Nox4 expression (Goettsch, Rauner et al. 2011). Kovac recently suggested a negative feedback regulatory mechanism between Nox4 and Nrf2 (Kovac, Angelova et al. 2015). Moreover, previous studies reported that Nrf2 is decreased in patients with idiopathic pulmonary fibrosis (Artaud-Macari, Goven et al. 2013) whereas Nox4 expression is upregulated (Amara, Goven et al. 2010). These observations might in part explain the sustained redox imbalance which in turn promotes persistent myofibroblasts and fibrosis. Taken together with the above mentioned studies, we hypothesized that Nrf2, via upregulation by α -MSH, may antagonize the stimulatory effect of TGF- β_1 on Nox4 in HDFs.

Taken together, the findings obtained in this doctoral thesis provide evidence that Nox4 represents an intracellular nodal point that orchestrates collagen synthesis, differentiation of dermal fibroblasts into a profibrotic myofibroblast phenotype, and thus dermal fibrosis as summarized in (**Fig. 26**). These data also indicate that Nox4 could become an important novel target for future therapy of SSc and related fibrotic diseases.

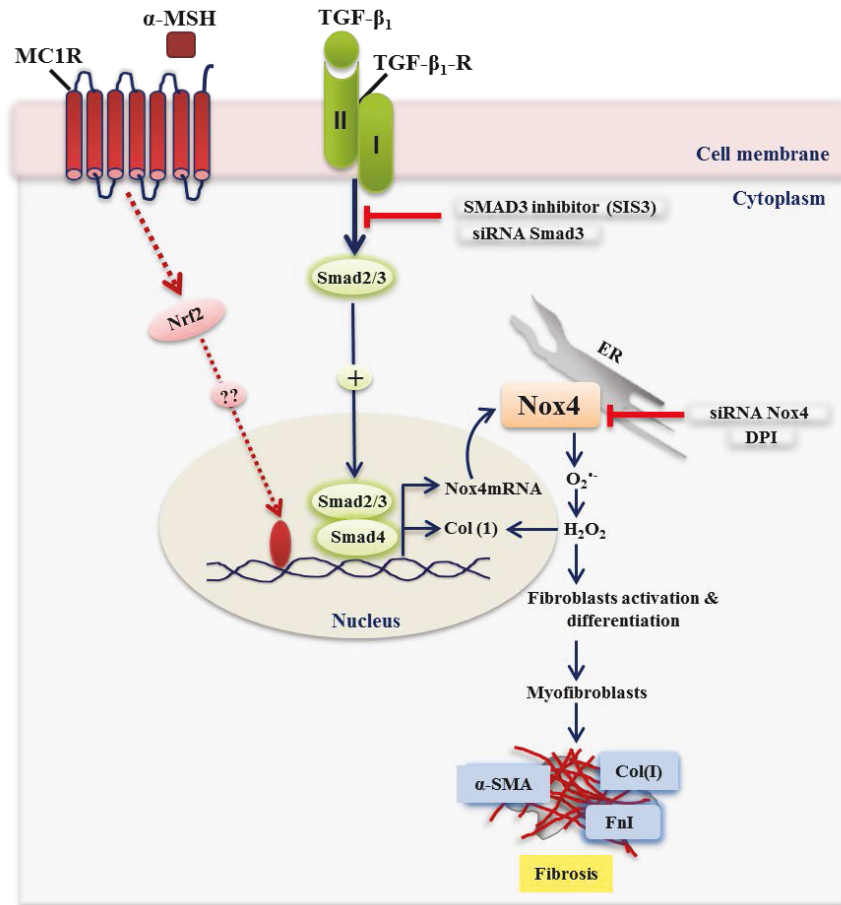


Figure 26. Schematic illustration of the proposed interaction between TGF-β₁-mediated Nox4 induction, α-MSH-signaling, collagen expression and fibroblast activation.

Upon stimulation with TGF-β₁, it binds to and activates the TGF-β₁ receptor followed by phosphorylation of Smad2 and Smad3 forming complex with Smad4. Activated complex translocates to the nucleus, bind to the promoter of target genes like Nox4 and collagen I and activate their transcription. Then, Nox4 produces ROS (mainly H₂O₂) in the ER which acts as a signaling molecule to promote the activation and differentiation of fibroblasts into myofibroblasts. These events can be diminished by inhibition of Smad3 either genetically by Smad3siRNA or pharmacologically by the SIS3 inhibitor. Similarly, inactivation of Nox4 either transcriptionally by Nox4siRNA or pharmacological by DPI inhibitor can suppress myofibroblasts activation; collagen synthesis and expression of fibronectin 1 and α-SMA that subsequently prevent fibrosis. These data indicates that Nox4 acts downstream of Smad3 in HDFs. In addition, α-MSH attenuates TGF-β₁-induced Nox4 expression and Nrf2 might negatively regulate the stimulatory effect of TGF-β₁ on Nox4. TGF-β₁-R, TGF-β₁ receptor; COL(I), collagen type I; FN 1, fibronectin 1; MC1R, melanocortin-1 receptor; α-MSH, alpha melanocyte stimulating hormone; ER, endoplasmic reticulum.

6. Conclusion & Future perspectives

The present study provides evidence that targeting Nox4 may represent an effective therapeutic strategy for the treatment of fibrotic disorders in SSc patients. We could demonstrate that:

- 1) Nox4 is the singular detectable Nox protein in both normal and SSc human dermal fibroblasts (HDFs).
- 2) TGF- β_1 strongly induced Nox4 gene expression in a Smad3-dependent manner.
- 3) Genetic silencing of Nox4 abrogated the promoting effect of TGF- β_1 on collagen synthesis and myofibroblasts differentiation
- 4) The non-selective NADPH oxidase inhibitor DPI significantly suppressed skin fibrosis in the bleomycin mouse model of scleroderma.
- 5) Treatment with α -MSH attenuated TGF- β_1 -mediated Nox4 expression as well as the upregulatory effect of TGF- β_1 on α -SMA, fibronectin 1, COL(I) α_1 , and COL(I) α_2 gene expression.

These data strongly indicate that pharmacological targeting of Nox4 may represent a novel strategy for the treatment of scleroderma. Therefore, both modulation of Nox4 enzyme activity and reduction / suppression of the oxidative stress in patients with SSc with highly Nox4-specific inhibitors could have more beneficial effects for SSc patients than the non-selective scavenging of ROS by administration of antioxidants.

Future perspectives

Recent studies using models of liver and lung fibrosis further sustain the potential therapeutic use of a new first-in- small-molecule Nox1/4 inhibitor GKT137831 in the treatment of a broad range of fibrotic diseases (Hecker, Logsdon et al. 2014, Lan, Kisseleva et al. 2015, Zhao, Viswanadhapalli et al. 2015). GKT137831 is the most recent Nox1/4 inhibitor designed by Genkyotex. It displays high oral bioavailability, lacks off-target effects and shows a good safety profile *in vivo*. Currently, it is tested in phase II clinical studies, and very promising results have been reported for patients with diabetic kidney disease. In collaboration with Genkyotex, we are

therefore interested in investigating whether GKT137831 counteracts fibroblast activation of normal and diseased cells alone and in combination with the profibrotic cytokine TGF- β_1 . Interestingly, our preliminary data demonstrate that GKT137831 significantly attenuated TGF- β_1 -induced collagen synthesis in nHDFs suggesting that Nox4 specifically contributes to myofibroblasts differentiation (**Section 7**). The next stage would be to explore the potential therapeutic effects of GKT137831 *in vivo*, for example, whether GKT137831 prevents bleomycin-induced skin fibrosis and is also capable of reversing an already established fibrosis of the skin. One of the major obstacles hindering the development of anti-fibrotic therapies is the lack of disease specific biomarkers that can be used to identify local and systemic oxidative stress in patients with SSc. Therefore, we intend to analyze the expression of Nox4 as well as other suitable biomarkers as biomarkers for a dysregulated ROS production in skin biopsies of SSc patients,

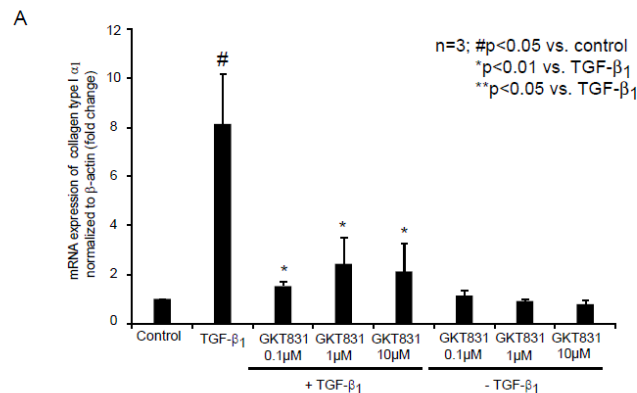
Due to the complexity of Nox4 biology the generation of Nox4-specific antibodies is strongly required. Through histological assessment of clinical samples for Nox4 expression utilizing that antibodies might allow the identification of abnormalities in specific skin diseases, in particular the identification of specific isoform dysfunction.

Further studies should intend to explore whether PDI has a direct effect on Nox4 activity in HDFs and whether knockdown of PDI interferes with Nox4 downstream profibrotic signaling. It is also worthwhile to investigate the molecular mechanism by which α -MSH attenuates TGF- β_1 -induced Nox4 expression. Further insights into the molecular mechanism by which Nox4 interacts with partner proteins may facilitate the development of next generation Nox inhibitors.

Finally, further *in vivo* studies (e.g. knock down of Nox4 by siRNA in the BLM mouse model or use of Nox4^{-/-} mice) are required to definitely validate the benefit of Nox inhibition on skin fibrosis as demonstrated in the BLM mouse model of scleroderma and to ensure that Nox4 definitely control dermal fibrosis. Answers to these questions could move the field of Nox biology towards a better understanding of the onset and progression of skin diseases and might provide novel targets for therapeutic interventions.

7. Pharmacological inhibition of Nox4 by GKT137831 reduces TGF- β_1 -mediated fibroblast activation

The role of Nox4 in nHDFs was evaluated using a first-in-class small-molecule of Nox1/4 inhibitor GKT137831. HDFs were pre-treated with GKT137831 at different doses (0.1-10 μ M) and then stimulated with TGF- β_1 for 16 hrs. Then the expression of established myofibroblasts marker genes such as COL(I) α_1 , COL(I) α_2 , α -SMA, and fibronectin I was analyzed by real-time RT-PCR. **Fig. 18A-D** shows that the expression of COL(I) α_1 , COL(I) α_2 , α -SMA and fibronectin 1 were increased after stimulation with TGF- β_1 . Pretreatment of nHDFs with GKT137831 significantly attenuated this stimulatory effect of TGF- β_1 not only on COL(I) α_1 and COL(I) α_2 gene expression but also expression of α -SMA and fibronectin 1. In contrast, GKT137831 *per se* did not have any significant effect on the basal expression of these genes in nHDFs. Notably, GKT137831 when tested at 20-50 μ M did not show any significant inhibition of TGF- β_1 -target genes. Taken together, these findings indicate that Nox4 specifically regulates activation of HDFs and Nox4-dependent ROS generation are involved in collagen production. To confirm these observations at protein level, we are currently investigating the inhibitory effect of GKT137831 on TGF- β_1 -induced collagen type I secretion employing a procollagen type I C-terminal peptide (PICP) ELISA and will assess the expression of α -SMA and fibronectin 1 by immunofluorescence analysis.



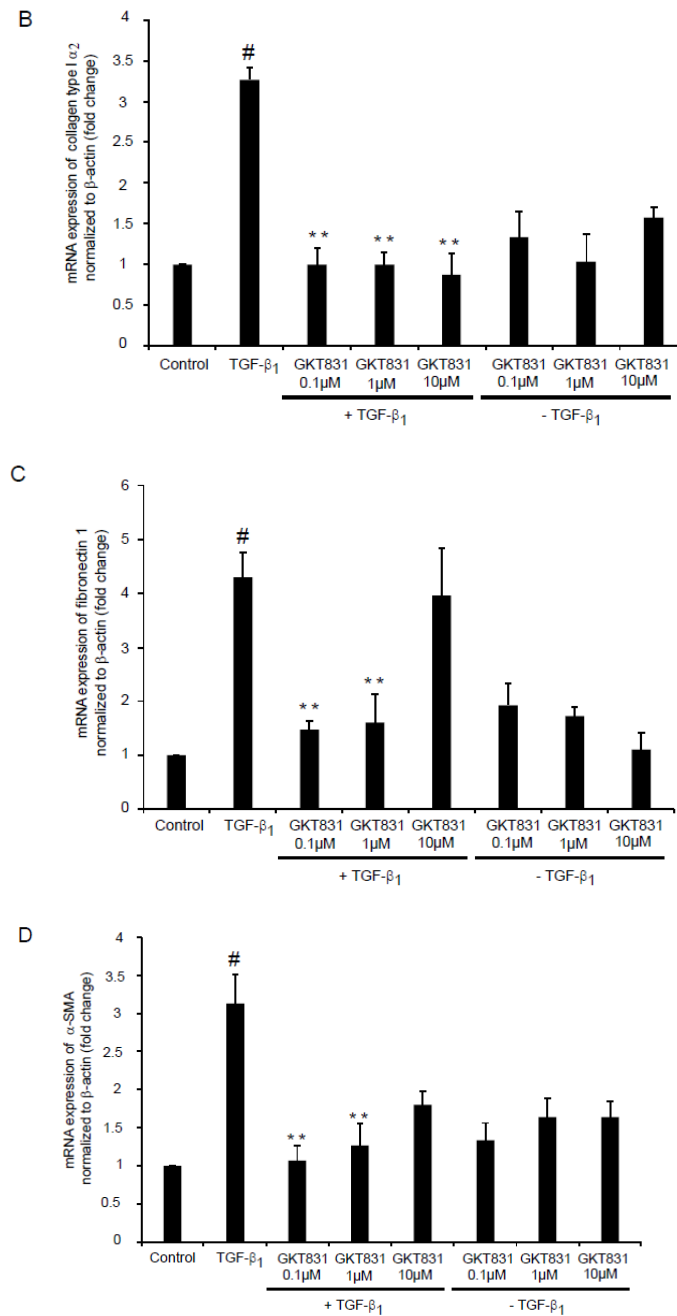


Figure 27. Effect of pharmacological inhibition of Nox4 via GKT137831 on TGF-β₁ mediated activation of dermal fibroblasts. (A-D) GKT137831 abrogated TGF-β₁-mediated expression of COL(I)α₁, COL(I) α₂, α-SMA and fibronectin I. nHDFs were preincubated with GKT137831 (0.1-10 μM) for 1 hour followed by TGF-β₁ (10ng/ml) treatment for 16 hrs and real-time RT-PCR. n=3; #p<0.05 vs. control; *p<0.01 vs. TGF-β₁ and **p<0.05 vs. TGF-β₁.

8. References

Abdelrahman, M., E. Mazzone, M. Bauer, I. Bauer, S. Delbosco, J. P. Cristol, N. S. Patel, S. Cuzzocrea and C. Thiemeermann (2005). Inhibitors of NADPH oxidase reduce the organ injury in hemorrhagic shock. *Shock* 23(2): 107-114.

Abid, M. R., K. C. Spokes, S. C. Shih and W. C. Aird (2007). NADPH oxidase activity selectively modulates vascular endothelial growth factor signaling pathways. *J Biol Chem* 282(48): 35373-35385.

Ago, T., J. Kuroda, J. Pain, C. Fu, H. Li and J. Sadoshima (2010). Upregulation of Nox4 by hypertrophic stimuli promotes apoptosis and mitochondrial dysfunction in cardiac myocytes. *Circ Res* 106(7): 1253-1264.

Akhmetshina, A., K. Palumbo, C. Dees, C. Bergmann, P. Venalis, P. Zerr, A. Horn, T. Kireva, C. Beyer, J. Zwerina, H. Schneider, A. Sadowski, M. O. Riener, O. A. MacDougald, O. Distler, G. Schett and J. H. Distler (2012). Activation of canonical Wnt signalling is required for TGF-beta-mediated fibrosis. *Nat Commun* 3: 735.

Altenhöfer, S., P. M. Kleikers, K. Radermacher, P. Scheurer, J. J. Rob Hermans, P. Schiffers, H. Ho, K. Wingler and H. H. W. Schmidt (2012). The NOX toolbox: validating the role of NADPH oxidases in physiology and disease. *Cellular and Molecular Life Sciences* 69(14): 2327-2343.

Amanso, A. M., V. Debbas and F. R. Laurindo (2011). Proteasome inhibition represses unfolded protein response and Nox4, sensitizing vascular cells to endoplasmic reticulum stress-induced death. *PLoS One* 6(1): e14591.

Amara, N., D. Goven, F. Prost, R. Muloway, B. Crestani and J. Boczkowski (2010). NOX4/NADPH oxidase expression is increased in pulmonary fibroblasts from patients with idiopathic pulmonary fibrosis and mediates TGFbeta1-induced fibroblast differentiation into myofibroblasts. *Thorax* 65(8): 733-738.

Ambasta, R. K., P. Kumar, K. K. Griendling, H. H. Schmidt, R. Busse and R. P. Brandes (2004). Direct interaction of the novel Nox proteins with p22^{phox} is required for the formation of a functionally active NADPH oxidase. *J Biol Chem* 279(44): 45935-45941.

Anilkumar, N., G. San Jose, I. Sawyer, C. X. Santos, C. Sand, A. C. Brewer, D. Warren and A. M. Shah (2013). A 28-kDa splice variant of NADPH oxidase-4 is nuclear-localized and involved in redox signaling in vascular cells. *Arterioscler Thromb Vasc Biol* 33(4): e104-112.

Anilkumar, N., R. Weber, M. Zhang, A. Brewer and A. M. Shah (2008). Nox4 and nox2 NADPH oxidases mediate distinct cellular redox signaling responses to agonist stimulation. *Arterioscler Thromb Vasc Biol* 28(7): 1347-1354.

Aoyama, T., Y. H. Paik, S. Watanabe, B. Laleu, F. Gaggini, L. Fioraso-Cartier, S. Molango, F. Heitz, C. Merlot, C. Szyndralewicz, P. Page and D. A. Brenner (2012). Nicotinamide adenine

References

dinucleotide phosphate oxidase in experimental liver fibrosis: GKT137831 as a novel potential therapeutic agent. *Hepatology* 56(6): 2316-2327.

Armitage, M. E., K. Wingler, H. H. Schmidt and M. La (2009). Translating the oxidative stress hypothesis into the clinic: NOX versus NOS. *J Mol Med (Berl)* 87(11): 1071-1076.

Artaud-Macari, E., D. Goven, S. Brayer, A. Hamimi, V. Besnard, J. Marchal-Somme, Z. E. Ali, B. Crestani, S. Kerdine-Romer, A. Boutten and M. Bonay (2013). Nuclear factor erythroid 2-related factor 2 nuclear translocation induces myofibroblastic dedifferentiation in idiopathic pulmonary fibrosis. *Antioxid Redox Signal* 18(1): 66-79.

Ayala, P., J. Montenegro, R. Vivar, A. Letelier, P. A. Urroz, M. Copaja, D. Pivet, C. Humeres, R. Troncoso, J. M. Vicencio, S. Lavandero and G. Diaz-Araya (2012). Attenuation of endoplasmic reticulum stress using the chemical chaperone 4-phenylbutyric acid prevents cardiac fibrosis induced by isoproterenol. *Exp Mol Pathol* 92(1): 97-104.

Babalola, O., A. Mamalis, H. Lev-Tov and J. Jagdeo (2014). NADPH oxidase enzymes in skin fibrosis: molecular targets and therapeutic agents. *Arch Dermatol Res* 306(4): 313-330.

Bae, Y. S., H. Oh, S. G. Rhee and Y. D. Yoo (2011). Regulation of Reactive Oxygen Species Generation in Cell Signaling. *Molecules and Cells* 32(6): 491-509.

Bai, G., T. D. Hock, N. Logsdon, Y. Zhou and V. J. Thannickal (2014). A far-upstream AP-1/Smad binding box regulates human NOX4 promoter activation by transforming growth factor-beta. *Gene* 540(1): 62-67.

Banfi, B., B. Malgrange, J. Knisz, K. Steger, M. Dubois-Dauphin and K. H. Krause (2004). NOX3, a superoxide-generating NADPH oxidase of the inner ear. *J Biol Chem* 279(44): 46065-46072.

Barnes, J. L. and Y. Gorin (2011). Myofibroblast differentiation during fibrosis: role of NAD(P)H oxidases. *Kidney Int* 79(9): 944-956.

Bartsch, C., M. M. Bekhite, A. Wolheim, M. Richter, C. Ruhe, B. Wissuwa, A. Marciniak, J. Muller, R. Heller, H. R. Figulla, H. Sauer and M. Wartenberg (2011). NADPH oxidase and eNOS control cardiomyogenesis in mouse embryonic stem cells on ascorbic acid treatment. *Free Radic Biol Med* 51(2): 432-443.

Bedard, K. and K. H. Krause (2007). The NOX family of ROS-generating NADPH oxidases: physiology and pathophysiology. *Physiol Rev* 87(1): 245-313.

Bedard, K., B. Lardy and K. H. Krause (2007). NOX family NADPH oxidases: not just in mammals. *Biochimie* 89(9): 1107-1112.

Bellini, A. and S. Mattoli (2007). The role of the fibrocyte, a bone marrow-derived mesenchymal progenitor, in reactive and reparative fibroses. *Lab Invest* 87(9): 858-870.

References

- Bhandary, B., A. Marahatta, H.-R. Kim and H.-J. Chae (2012). An Involvement of Oxidative Stress in Endoplasmic Reticulum Stress and Its Associated Diseases. *International Journal of Molecular Sciences* 14(1): 434.
- Bhattacharyya, S., J. Wei and J. Varga (2011). Understanding fibrosis in systemic sclerosis: shifting paradigms, emerging opportunities. *Nature reviews. Rheumatology* 8(1): 42-54.
- Bickers, D. R. and M. Athar (2006). Oxidative stress in the pathogenesis of skin disease. *J Invest Dermatol* 126(12): 2565-2575.
- Block, K., Y. Gorin and H. E. Abboud (2009). Subcellular localization of Nox4 and regulation in diabetes." *Proc Natl Acad Sci U S A* 106(34): 14385-14390.
- Böhm, M., J. Ehrchen and T. A. Luger (2014). Beneficial effects of the melanocortin analogue Nle4-D-Phe7- α -MSH in acne vulgaris. *Journal of the European Academy of Dermatology and Venereology* 28(1): 108-111.
- Böhm, M., M. Raghunath, C. Sunderkötter, M. Schiller, S. Ständer, T. Brzoska, T. Cauvet, H. B. Schiöth, T. Schwarz and T. A. Luger (2004). Collagen Metabolism Is a Novel Target of the Neuropeptide α -Melanocyte-stimulating Hormone. *Journal of Biological Chemistry* 279(8): 6959-6966.
- Böhm, M. and A. Stegemann (2014). Bleomycin-induced fibrosis in MC1 signalling-deficient C57BL/6J-Mc1re/e mice further supports a modulating role for melanocortins in collagen synthesis of the skin. *Experimental Dermatology* 23(6): 431-433.
- Bondi, C. D., N. Manickam, D. Y. Lee, K. Block, Y. Gorin, H. E. Abboud and J. L. Barnes (2010). NAD(P)H oxidase mediates TGF-beta1-induced activation of kidney myofibroblasts. *J Am Soc Nephrol* 21(1): 93-102.
- Boudreau, H. E., S. U. Emerson, A. Korzeniowska, M. A. Jendrysik and T. L. Leto (2009). Hepatitis C virus (HCV) proteins induce NADPH oxidase 4 expression in a transforming growth factor beta-dependent manner: a new contributor to HCV-induced oxidative stress. *J Virol* 83(24): 12934-12946.
- Bradford, M. M. (1976). A rapid and sensitive method for the quantitation of microgram quantities of protein utilizing the principle of protein-dye binding. *Anal Biochem* 72: 248-254.
- Brar, S. S., T. P. Kennedy, A. B. Sturrock, T. P. Huecksteadt, M. T. Quinn, A. R. Whorton and J. R. Hoidal (2002). An NAD(P)H oxidase regulates growth and transcription in melanoma cells. *Am J Physiol Cell Physiol* 282(6): C1212-1224.
- Brown, D. I. and K. K. Griending (2009). Nox proteins in signal transduction. *Free Radic Biol Med* 47(9): 1239-1253.

References

- Carneseccchi, S., C. Deffert, Y. Donati, O. Basset, B. Hinz, O. Preynat-Seauve, C. Guichard, J. L. Arbiser, B. Banfi, J. C. Pache, C. Barazzzone-Argiroffo and K. H. Krause (2011). A key role for NOX4 in epithelial cell death during development of lung fibrosis. *Antioxid Redox Signal* 15(3): 607-619.
- Chaisson, N. F. and P. M. Hassoun (2013). Systemic sclerosis-associated pulmonary arterial hypertension. *Chest* 144(4): 1346-1356.
- Chamulitrat, W., W. Stremmel, T. Kawahara, K. Rokutan, H. Fujii, K. Wingler, H. H. Schmidt and R. Schmidt (2004). A constitutive NADPH oxidase-like system containing gp91phox homologs in human keratinocytes. *J Invest Dermatol* 122(4): 1000-1009.
- Chan, E. C., H. M. Peshavariya, G. S. Liu, F. Jiang, S. Y. Lim and G. J. Dusting (2013). Nox4 modulates collagen production stimulated by transforming growth factor beta1 in vivo and in vitro. *Biochem Biophys Res Commun* 430(3): 918-925.
- Chapman, H. A. (2011). Epithelial-mesenchymal interactions in pulmonary fibrosis. *Annu Rev Physiol* 73: 413-435.
- Chen, K., M. T. Kirber, H. Xiao, Y. Yang and J. F. Keaney, Jr. (2008). Regulation of ROS signal transduction by NADPH oxidase 4 localization. *J Cell Biol* 181(7): 1129-1139.
- Cho, H. Y., S. P. Reddy, M. Yamamoto and S. R. Kleeberger (2004). The transcription factor NRF2 protects against pulmonary fibrosis. *Faseb j* 18(11): 1258-1260.
- Chung, H. S., S.-B. Wang, V. Venkatraman, C. I. Murray and J. E. Van Eyk (2013). Cysteine Oxidative Posttranslational Modifications: Emerging Regulation in the Cardiovascular System. *Circulation Research* 112(2): 382-392.
- Ciofu, O. and J. Lykkesfeldt (2014). Antioxidant supplementation for lung disease in cystic fibrosis. *Cochrane Database Syst Rev* 8: Cd007020.
- Clempus, R. E., D. Sorescu, A. E. Dikalova, L. Pounkova, P. Jo, G. P. Sorescu, H. H. Schmidt, B. Lassegue and K. K. Griendling (2007). Nox4 is required for maintenance of the differentiated vascular smooth muscle cell phenotype. *Arterioscler Thromb Vasc Biol* 27(1): 42-48.
- Cross, A. R. and A. W. Segal (2004). The NADPH oxidase of professional phagocytes--prototypic of the NOX electron transport chain systems. *Biochim Biophys Acta* 1657(1): 1-22.
- Cucoranu, I., R. Clempus, A. Dikalova, P. J. Phelan, S. Ariyan, S. Dikalov and D. Sorescu (2005). NAD(P)H oxidase 4 mediates transforming growth factor-beta1-induced differentiation of cardiac fibroblasts into myofibroblasts. *Circ Res* 97(9): 900-907.
- De Felice, B., R. R. Wilson and M. Nacca (2009). Telomere shortening may be associated with human keloids. *BMC Med Genet* 10: 110.

References

- Delanian, S. and J. L. Lefaix (2004). The radiation-induced fibroatrophic process: therapeutic perspective via the antioxidant pathway. *Radiother Oncol* 73(2): 119-131.
- Denton, C. P., C. M. Black and D. J. Abraham (2006). Mechanisms and consequences of fibrosis in systemic sclerosis. *Nat Clin Pract Rheumatol* 2(3): 134-144.
- Denton, C. P., P. A. Merkel, D. E. Furst, D. Khanna, P. Emery, V. M. Hsu, N. Silliman, J. Streisand, J. Powell, A. Åkesson, J. Coppock, F. v. d. Hoogen, A. Herrick, M. D. Mayes, D. Veale, J. Haas, S. Ledbetter, J. H. Korn, C. M. Black, J. R. Seibold and C. on Behalf Of The Cat-192 Study Group The Scleroderma Clinical Trials (2007). Recombinant human anti-transforming growth factor β 1 antibody therapy in systemic sclerosis: A multicenter, randomized, placebo-controlled phase I/II trial of CAT-192. *Arthritis & Rheumatism* 56(1): 323-333.
- Desmouliere, A., A. Geinoz, F. Gabbiani and G. Gabbiani (1993). Transforming growth factor-beta 1 induces alpha-smooth muscle actin expression in granulation tissue myofibroblasts and in quiescent and growing cultured fibroblasts. *J Cell Biol* 122(1): 103-111.
- Di Marco, E., S. P. Gray, P. Chew, C. Koulis, A. Ziegler, C. Szyndralewicz, R. M. Touyz, H. H. Schmidt, M. E. Cooper, R. Slattery and K. A. Jandeleit-Dahm (2014). Pharmacological inhibition of NOX reduces atherosclerotic lesions, vascular ROS and immune-inflammatory responses in diabetic Apoe(-/-) mice. *Diabetologia* 57(3): 633-642.
- Diaz, B., G. Shani, I. Pass, D. Anderson, M. Quintavalle and S. A. Courtneidge (2009). Tks5-dependent, nox-mediated generation of reactive oxygen species is necessary for invadopodia formation. *Sci Signal* 2(88): ra53.
- Diebold, I., A. Petry, J. Hess and A. Gorkach (2010). The NADPH oxidase subunit NOX4 is a new target gene of the hypoxia-inducible factor-1. *Mol Biol Cell* 21(12): 2087-2096.
- Ding, Y., Z. J. Chen, S. Liu, D. Che, M. Vetter and C. H. Chang (2005). Inhibition of Nox-4 activity by plumbagin, a plant-derived bioactive naphthoquinone. *J Pharm Pharmacol* 57(1): 111-116.
- Dooley, A., X. Shi-Wen, N. Aden, T. Tranah, N. Desai, C. P. Denton, D. J. Abraham and R. Bruckdorfer (2010). Modulation of collagen type I, fibronectin and dermal fibroblast function and activity, in systemic sclerosis by the antioxidant epigallocatechin-3-gallate. *Rheumatology (Oxford)* 49(11): 2024-2036.
- Dotor, J. and J. Pablos (2008). Topical Application of TGF- β 1 Peptide Inhibitors for the Therapy of Skin Fibrosis. *Transforming Growth Factor- β in Cancer Therapy, Volume I*, Humana Press: 693-702.
- Drose, S. and U. Brandt (2012). Molecular mechanisms of superoxide production by the mitochondrial respiratory chain. *Adv Exp Med Biol* 748: 145-169.

References

Drummond, G. R., S. Selemidis, K. K. Griendling and C. G. Sobey (2011). Combating oxidative stress in vascular disease: NADPH oxidases as therapeutic targets. *Nature Reviews. Drug Discovery* 10(6): 453-471.

Etoh, T., T. Inoguchi, M. Kakimoto, N. Sonoda, K. Kobayashi, J. Kuroda, H. Sumimoto and H. Nawata (2003). Increased expression of NAD(P)H oxidase subunits, NOX4 and p22phox, in the kidney of streptozotocin-induced diabetic rats and its reversibility by interventive insulin treatment. *Diabetologia* 46(10): 1428-1437.

Failli, P., L. Palmieri, C. D'Alfonso, L. Giovannelli, S. Generini, A. D. Rosso, A. Pignone, N. Stanflin, S. Orsi, L. Zilletti and M. Matucci-Cerinic (2002). Effect of N-acetyl-L-cysteine on peroxynitrite and superoxide anion production of lung alveolar macrophages in systemic sclerosis. *Nitric Oxide* 7(4): 277-282.

Finkel, T. and N. J. Holbrook (2000). Oxidants, oxidative stress and the biology of ageing. *Nature* 408(6809): 239-247.

Fragiadaki, M. and R. M. Mason (2011). Epithelial-mesenchymal transition in renal fibrosis - evidence for and against. *Int J Exp Pathol* 92(3): 143-150.

Gabrielli, A., S. Svegliati, G. Moroncini and D. Amico (2012). New insights into the role of oxidative stress in scleroderma fibrosis. *Open Rheumatol J* 6: 87-95.

Gabrielli, A., S. Svegliati, G. Moroncini, G. Pomponio, M. Santillo and E. V. Avvedimento (2008). Oxidative stress and the pathogenesis of scleroderma: the Murrell's hypothesis revisited. *Semin Immunopathol* 30(3): 329-337.

Galli, F., A. Battistoni, R. Gambari, A. Pompella, A. Bragonzi, F. Pilolli, L. Iuliano, M. Piroddi, M. C. Dehecchi and G. Cabrini (2012). Oxidative stress and antioxidant therapy in cystic fibrosis. *Biochim Biophys Acta* 1822(5): 690-713.

Geiszt, M. (2006). NADPH oxidases: new kids on the block. *Cardiovasc Res* 71(2): 289-299.

Geiszt, M., J. B. Kopp, P. Varnai and T. L. Leto (2000). Identification of renox, an NAD(P)H oxidase in kidney. *Proc Natl Acad Sci U S A* 97(14): 8010-8014.

Gianni, D., N. Taulet, H. Zhang, C. DerMardirossian, J. Kister, L. Martinez, W. R. Roush, S. J. Brown, G. M. Bokoch and H. Rosen (2010). A novel and specific NADPH oxidase-1 (Nox1) small-molecule inhibitor blocks the formation of functional invadopodia in human colon cancer cells. *ACS Chem Biol* 5(10): 981-993.

Giri, S. N., D. M. Hyde and M. A. Hollinger (1993). Effect of antibody to transforming growth factor beta on bleomycin induced accumulation of lung collagen in mice. *Thorax* 48(10): 959-966.

References

- Goettsch, C., M. Rauner, C. Hamann, K. Sinnigen, U. Hempel, S. R. Bornstein and L. C. Hofbauer (2011). Nuclear factor of activated T cells mediates oxidised LDL-induced calcification of vascular smooth muscle cells. *Diabetologia* 54(10): 2690-2701.
- Gorin, Y., J. M. Ricono, N. H. Kim, B. Bhandari, G. G. Choudhury and H. E. Abboud (2003). Nox4 mediates angiotensin II-induced activation of Akt/protein kinase B in mesangial cells. *Am J Physiol Renal Physiol* 285(2): F219-229.
- Goyal, P., N. Weissmann, F. Rose, F. Grimminger, H. J. Schafers, W. Seeger and J. Hanze (2005). Identification of novel Nox4 splice variants with impact on ROS levels in A549 cells. *Biochem Biophys Res Commun* 329(1): 32-39.
- Grange, L., M. V. Nguyen, B. Lardy, M. Derouazi, Y. Campion, C. Trocme, M. H. Paclet, P. Gaudin and F. Morel (2006). NAD(P)H oxidase activity of Nox4 in chondrocytes is both inducible and involved in collagenase expression. *Antioxid Redox Signal* 8(9-10): 1485-1496.
- Green, D. E., T. C. Murphy, B. Y. Kang, J. M. Kleinhenz, C. Szyndralewicz, P. Page, R. L. Sutliff and C. M. Hart (2012). The Nox4 inhibitor GKT137831 attenuates hypoxia-induced pulmonary vascular cell proliferation. *Am J Respir Cell Mol Biol* 47(5): 718-726.
- Grygiel-Gorniak, B. and M. Puszczewicz (2014). Oxidative damage and antioxidative therapy in systemic sclerosis. *Mediators Inflamm* 2014: 389582.
- Guo, S. and X. Chen (2015). The human Nox4: gene, structure, physiological function and pathological significance. *J Drug Target*: 1-9.
- Hahm, K. B., Y. H. Im, C. Lee, W. T. Parks, Y. J. Bang, J. E. Green and S. J. Kim (2000). Loss of TGF-beta signaling contributes to autoimmune pancreatitis. *J Clin Invest* 105(8): 1057-1065.
- Hecker, L., J. Cheng and V. J. Thannickal (2012). Targeting NOX enzymes in pulmonary fibrosis. *Cellular and molecular life sciences : CMLS* 69(14): 2365-2371.
- Hecker, L., N. J. Logsdon, D. Kurundkar, A. Kurundkar, K. Bernard, T. Hock, E. Meldrum, Y. Y. Sanders and V. J. Thannickal (2014). Reversal of persistent fibrosis in aging by targeting Nox4-Nrf2 redox imbalance. *Sci Transl Med* 6(231): 231ra247.
- Hecker, L., R. Vittal, T. Jones, R. Jagirdar, T. R. Luckhardt, J. C. Horowitz, S. Pennathur, F. J. Martinez and V. J. Thannickal (2009). NADPH oxidase-4 mediates myofibroblast activation and fibrogenic responses to lung injury. *Nat Med* 15(9): 1077-1081.
- Hilenski, L. L., R. E. Clempus, M. T. Quinn, J. D. Lambeth and K. K. Griendling (2004). Distinct subcellular localizations of Nox1 and Nox4 in vascular smooth muscle cells. *Arterioscler Thromb Vasc Biol* 24(4): 677-683.

References

- Hinz, B., S. H. Phan, V. J. Thannickal, M. Prunotto, A. Desmouliere, J. Varga, O. De Wever, M. Mareel and G. Gabbiani (2012). Recent developments in myofibroblast biology: paradigms for connective tissue remodeling. *Am J Pathol* 180(4): 1340-1355.
- Hneino, M., A. Francois, V. Buard, G. Tarlet, R. Abderrahmani, K. Blirando, P. A. Hoodless, M. Benderitter and F. Milliat (2012). The TGF-beta/Smad repressor TG-interacting factor 1 (TGIF1) plays a role in radiation-induced intestinal injury independently of a Smad signaling pathway. *PLoS One* 7(5): e35672.
- Holmstrom, K. M. and T. Finkel (2014). Cellular mechanisms and physiological consequences of redox-dependent signalling. *Nat Rev Mol Cell Biol* 15(6): 411-421.
- Hunzelmann, N. and J. Brinckmann (2010). What are the new milestones in the pathogenesis of systemic sclerosis? *Annals of the Rheumatic Diseases* 69(Suppl 1): i52-i56.
- Hybertson, B. M., B. Gao, S. K. Bose and J. M. McCord (2011). Oxidative stress in health and disease: The therapeutic potential of Nrf2 activation. *Molecular Aspects of Medicine* 32(4-6): 234-246.
- Ihn, H., K. Yamane and K. Tamaki (2005). Increased Phosphorylation and Activation of Mitogen-Activated Protein Kinase p38 in Scleroderma Fibroblasts. *J Investig Dermatol* 125(2): 247-255.
- Ikeda, R., K. Ishii, Y. Hoshikawa, J. Azumi, Y. Arakaki, T. Yasui, S. Matsuura, Y. Matsumi, Y. Kono, Y. Mizuta, A. Kurimasa, I. Hisatome, S. L. Friedman, H. Kawasaki and G. Shiota (2011). Reactive oxygen species and NADPH oxidase 4 induced by transforming growth factor beta1 are the therapeutic targets of polyenylphosphatidylcholine in the suppression of human hepatic stellate cell activation. *Inflamm Res* 60(6): 597-604.
- Ikushima, H. and K. Miyazono (2010). TGFbeta signalling: a complex web in cancer progression. *Nat Rev Cancer* 10(6): 415-424.
- Ismail, S., A. Sturrock, P. Wu, B. Cahill, K. Norman, T. Huecksteadt, K. Sanders, T. Kennedy and J. Hoidal (2009). NOX4 mediates hypoxia-induced proliferation of human pulmonary artery smooth muscle cells: the role of autocrine production of transforming growth factor-beta1 and insulin-like growth factor binding protein-3. *Am J Physiol Lung Cell Mol Physiol* 296(3): L489-499.
- Jain, M., S. Rivera, E. A. Monclus, L. Synenki, A. Zirk, J. Eisenbart, C. Feghali-Bostwick, G. M. Mutlu, G. R. Budinger and N. S. Chandel (2013). Mitochondrial reactive oxygen species regulate transforming growth factor-beta signaling. *J Biol Chem* 288(2): 770-777.
- Janiszewski, M., L. R. Lopes, A. O. Carmo, M. A. Pedro, R. P. Brandes, C. X. Santos and F. R. Laurindo (2005). Regulation of NAD(P)H oxidase by associated protein disulfide isomerase in vascular smooth muscle cells. *J Biol Chem* 280(49): 40813-40819.

References

Jiang, F., G.-S. Liu, G. J. Dusting and E. C. Chan (2014). NADPH oxidase-dependent redox signaling in TGF- β -mediated fibrotic responses. *Redox Biology* 2: 267-272.

Jiang, J. X., X. Chen, N. Serizawa, C. Szyndralewicz, P. Page, K. Schroder, R. P. Brandes, S. Devaraj and N. J. Torok (2012). Liver fibrosis and hepatocyte apoptosis are attenuated by GKT137831, a novel NOX4/NOX1 inhibitor in vivo. *Free Radic Biol Med* 53(2): 289-296.

Jinnin, M. (2010). Mechanisms of skin fibrosis in systemic sclerosis. *J Dermatol* 37(1): 11-25.

Kalyanaraman, B., V. Darley-USmar, K. J. Davies, P. A. Dennery, H. J. Forman, M. B. Grisham, G. E. Mann, K. Moore, L. J. Roberts, 2nd and H. Ischiropoulos (2012). Measuring reactive oxygen and nitrogen species with fluorescent probes: challenges and limitations. *Free Radic Biol Med* 52(1): 1-6.

Kanda, Y., T. Hinata, S. W. Kang and Y. Watanabe (2011). Reactive oxygen species mediate adipocyte differentiation in mesenchymal stem cells. *Life Sci* 89(7-8): 250-258.

Katsumoto, T. R., M. L. Whitfield and M. K. Connolly (2011). The pathogenesis of systemic sclerosis. *Annu Rev Pathol* 6: 509-537.

Katsuyama, M., H. Hirai, K. Iwata, M. Ibi, K. Matsuno, M. Matsumoto and C. Yabe-Nishimura (2011). Sp3 transcription factor is crucial for transcriptional activation of the human NOX4 gene. *FEBS J* 278(6): 964-972.

Kawahara, T. and J. D. Lambeth (2007). Molecular evolution of Phox-related regulatory subunits for NADPH oxidase enzymes. *BMC Evol Biol* 7: 178.

Kern, G., S. M. Mair, S. J. Noppert, P. Jennings, H. Schramek, M. Rudnicki, G. A. Mueller, G. Mayer and C. Koppelstaetter (2014). Tacrolimus increases Nox4 expression in human renal fibroblasts and induces fibrosis-related genes by aberrant TGF-beta receptor signalling. *PLoS One* 9(5): e96377.

Kikuchi, N., Y. Ishii, Y. Morishima, Y. Yageta, N. Haraguchi, K. Itoh, M. Yamamoto and N. Hizawa (2010). Nrf2 protects against pulmonary fibrosis by regulating the lung oxidant level and Th1/Th2 balance. *Respiratory Research* 11(1): 31-31.

Kim, H. J., C. H. Kim, J. H. Ryu, J. H. Joo, S. N. Lee, M. J. Kim, J. G. Lee, Y. S. Bae and J. H. Yoon (2011). Crosstalk between platelet-derived growth factor-induced Nox4 activation and MUC8 gene overexpression in human airway epithelial cells. *Free Radic Biol Med* 50(9): 1039-1052.

Kisseleva, T. and D. A. Brenner (2008). Mechanisms of fibrogenesis. *Exp Biol Med* (Maywood) 233(2): 109-122.

Kleinschnitz, C., H. Grund, K. Wingler, M. E. Armitage, E. Jones, M. Mittal, D. Barit, T. Schwarz, C. Geis, P. Kraft, K. Barthel, M. K. Schuhmann, A. M. Herrmann, S. G. Meuth, G.

References

- Stoll, S. Meurer, A. Schrewe, L. Becker, V. Gailus-Durner, H. Fuchs, T. Klopstock, M. H. de Angelis, K. Jandeleit-Dahm, A. M. Shah, N. Weissmann and H. H. Schmidt (2010). Post-stroke inhibition of induced NADPH oxidase type 4 prevents oxidative stress and neurodegeneration. *PLoS Biol* 8(9).
- Kokot, A., A. Sindrilaru, M. Schiller, C. Sunderkotter, C. Kerkhoff, B. Eckes, K. Scharffetter-Kochanek, T. A. Luger and M. Bohm (2009). alpha-melanocyte-stimulating hormone suppresses bleomycin-induced collagen synthesis and reduces tissue fibrosis in a mouse model of scleroderma: melanocortin peptides as a novel treatment strategy for scleroderma? *Arthritis Rheum* 60(2): 592-603.
- Konior, A., A. Schramm, M. Czesnikiewicz-Guzik and T. J. Guzik (2014). NADPH oxidases in vascular pathology. *Antioxid Redox Signal* 20(17): 2794-2814.
- Kovac, S., P. R. Angelova, K. M. Holmstrom, Y. Zhang, A. T. Dinkova-Kostova and A. Y. Abramov (2015). Nrf2 regulates ROS production by mitochondria and NADPH oxidase. *Biochim Biophys Acta* 1850(4): 794-801.
- Kuroda, J., K. Nakagawa, T. Yamasaki, K. Nakamura, R. Takeya, F. Kuribayashi, S. Imajoh-Ohmi, K. Igarashi, Y. Shibata, K. Sueishi and H. Sumimoto (2005). The superoxide-producing NAD(P)H oxidase Nox4 in the nucleus of human vascular endothelial cells. *Genes Cells* 10(12): 1139-1151.
- Kuwahara, F., H. Kai, K. Tokuda, M. Takeya, A. Takeshita, K. Egashira and T. Imaizumi (2004). Hypertensive myocardial fibrosis and diastolic dysfunction: another model of inflammation? *Hypertension* 43(4): 739-745.
- Lakos, G., S. Takagawa, S. J. Chen, A. M. Ferreira, G. Han, K. Masuda, X. J. Wang, L. A. DiPietro and J. Varga (2004). Targeted disruption of TGF-beta/Smad3 signaling modulates skin fibrosis in a mouse model of scleroderma. *Am J Pathol* 165(1): 203-217.
- Lambeth, J. D. (2004). NOX enzymes and the biology of reactive oxygen. *Nat Rev Immunol* 4(3): 181-189.
- Lambeth, J. D. and A. S. Neish (2014). Nox enzymes and new thinking on reactive oxygen: a double-edged sword revisited. *Annu Rev Pathol* 9: 119-145.
- Lan, T., T. Kisseleva and D. A. Brenner (2015). Deficiency of NOX1 or NOX4 Prevents Liver Inflammation and Fibrosis in Mice through Inhibition of Hepatic Stellate Cell Activation. *PLoS One* 10(7): e0129743.
- Lassegue, B. and K. K. Griendling (2010). NADPH oxidases: functions and pathologies in the vasculature. *Arterioscler Thromb Vasc Biol* 30(4): 653-661.

References

- Laurindo, F. R., D. C. Fernandes, A. M. Amanso, L. R. Lopes and C. X. Santos (2008). Novel role of protein disulfide isomerase in the regulation of NADPH oxidase activity: pathophysiological implications in vascular diseases. *Antioxid Redox Signal* 10(6): 1101-1113.
- Leask, A. and D. J. Abraham (2004). TGF- β signaling and the fibrotic response. *The FASEB Journal* 18(7): 816-827.
- Lee, C. F., M. Qiao, K. Schroder, Q. Zhao and R. Asmis (2010). Nox4 is a novel inducible source of reactive oxygen species in monocytes and macrophages and mediates oxidized low density lipoprotein-induced macrophage death. *Circ Res* 106(9): 1489-1497.
- Levin, I., J. Petrasek and G. Szabo (2012). The Presence of p47phox in Liver Parenchymal Cells is a Key Mediator in the Pathogenesis of Alcoholic Liver Steatosis. *Alcoholism, clinical and experimental research* 36(8): 1397-1406.
- Li, J.-M. and A. M. Shah (2003). Mechanism of Endothelial Cell NADPH Oxidase Activation by Angiotensin II: ROLE OF THE p47 phox SUBUNIT. *Journal of Biological Chemistry* 278(14): 12094-12100.
- Li, S., S. S. Tabar, V. Malec, B. G. Eul, W. Klepetko, N. Weissmann, F. Grimminger, W. Seeger, F. Rose and J. Hanze (2008). NOX4 regulates ROS levels under normoxic and hypoxic conditions, triggers proliferation, and inhibits apoptosis in pulmonary artery adventitial fibroblasts. *Antioxid Redox Signal* 10(10): 1687-1698.
- Liu, H., R. Colavitti, I. I. Rovira and T. Finkel (2005). Redox-Dependent Transcriptional Regulation. *Circulation Research* 97(10): 967-974.
- Liu, R. M. and K. A. Gaston Pravia (2010). Oxidative stress and glutathione in TGF-beta-mediated fibrogenesis. *Free Radic Biol Med* 48(1): 1-15.
- Loughlin, D. T. and C. M. Artlett (2010). Precursor of advanced glycation end products mediates ER-stress-induced caspase-3 activation of human dermal fibroblasts through NAD(P)H oxidase 4. *PLoS One* 5(6): e11093.
- Lyle, A. N., N. N. Deshpande, Y. Taniyama, B. Seidel-Rogol, L. Pounkova, P. Du, C. Papaharalambus, B. Lassegue and K. K. Griendling (2009). Poldip2, a novel regulator of Nox4 and cytoskeletal integrity in vascular smooth muscle cells. *Circ Res* 105(3): 249-259.
- Maghzal, G. J., K. H. Krause, R. Stocker and V. Jaquet (2012). Detection of reactive oxygen species derived from the family of NOX NADPH oxidases. *Free Radic Biol Med* 53(10): 1903-1918.
- Maier, T., M. Guell and L. Serrano (2009). Correlation of mRNA and protein in complex biological samples. *FEBS Lett* 583(24): 3966-3973.

References

- Maitre, A., M. Hours, V. Bonneterre, J. Arnaud, M. T. Arslan, P. Carpentier, A. Bergeret and R. de Gaudemaris (2004). Systemic sclerosis and occupational risk factors: role of solvents and cleaning products. *J Rheumatol* 31(12): 2395-2401.
- Manea, A., S. A. Manea, A. V. Gafencu, M. Raicu and M. Simionescu (2008). AP-1-dependent transcriptional regulation of NADPH oxidase in human aortic smooth muscle cells: role of p22phox subunit. *Arterioscler Thromb Vasc Biol* 28(5): 878-885.
- Manea, A., L. I. Tanase, M. Raicu and M. Simionescu (2010). Jak/STAT signaling pathway regulates nox1 and nox4-based NADPH oxidase in human aortic smooth muscle cells. *Arterioscler Thromb Vasc Biol* 30(1): 105-112.
- Manea, A., L. I. Tanase, M. Raicu and M. Simionescu (2010). Transcriptional regulation of NADPH oxidase isoforms, Nox1 and Nox4, by nuclear factor-kappaB in human aortic smooth muscle cells. *Biochem Biophys Res Commun* 396(4): 901-907.
- Manickam, N., M. Patel, K. K. Griendling, Y. Gorin and J. L. Barnes (2014). RhoA/Rho kinase mediates TGF-beta1-induced kidney myofibroblast activation through Poldip2/Nox4-derived reactive oxygen species. *Am J Physiol Renal Physiol* 307(2): F159-171.
- Manoury, B., S. Nenan, O. Leclerc, I. Guenon, E. Boichot, J.-M. Planquois, C. P. Bertrand and V. Lagente (2005). The absence of reactive oxygen species production protects mice against bleomycin-induced pulmonary fibrosis. *Respiratory Research* 6(1): 11-11.
- Martyn, K. D., L. M. Frederick, K. von Loehneysen, M. C. Dinauer and U. G. Knaus (2006). Functional analysis of Nox4 reveals unique characteristics compared to other NADPH oxidases. *Cell Signal* 18(1): 69-82.
- Marut, W. K., N. Kavian, A. Servettaz, C. Nicco, L. A. Ba, M. Doering, C. Chereau, C. Jacob, B. Weill and F. Batteux (2012). The organotelluride catalyst (PHTe)(2)NQ prevents HOCl-induced systemic sclerosis in mouse. *J Invest Dermatol* 132(4): 1125-1132.
- Massague, J. (2012). TGF-beta signalling in context. *Nat Rev Mol Cell Biol* 13(10): 616-630.
- Mathai, S. K., M. Gulati, X. Peng, T. R. Russell, A. C. Shaw, A. N. Rubinowitz, L. A. Murray, J. M. Siner, D. E. Antin-Ozerkis, R. R. Montgomery, R. A. Reilkoff, R. J. Bucala and E. L. Herzog (2010). Circulating monocytes from systemic sclerosis patients with interstitial lung disease show an enhanced profibrotic phenotype. *Lab Invest* 90(6): 812-823.
- Matsushima, S., J. Kuroda, T. Ago, P. Zhai, J. Y. Park, L. H. Xie, B. Tian and J. Sadoshima (2013). Increased oxidative stress in the nucleus caused by Nox4 mediates oxidation of HDAC4 and cardiac hypertrophy. *Circ Res* 112(4): 651-663.
- Mayes, M. D., J. V. Lacey, Jr., J. Beebe-Dimmer, B. W. Gillespie, B. Cooper, T. J. Laing and D. Schottenfeld (2003). Prevalence, incidence, survival, and disease characteristics of systemic sclerosis in a large US population. *Arthritis Rheum* 48(8): 2246-2255.

References

- McCann, S. K., G. J. Dusting and C. L. Roulston (2008). Early increase of Nox4 NADPH oxidase and superoxide generation following endothelin-1-induced stroke in conscious rats. *J Neurosci Res* 86(11): 2524-2534.
- Michaeloudes, C. (2011). TGF- β_1 regulates Nox4, MnSOD and catalase expression, and IL-6 release in airway smooth muscle cells. *Am J Physiol Lung Cell Mol Physiol*.
- Moon, S.-K., S.-K. Kang and C.-H. Kim (2006). Reactive oxygen species mediates disialoganglioside GD3-induced inhibition of ERK1/2 and matrix metalloproteinase-9 expression in vascular smooth muscle cells. *The FASEB Journal* 20(9): 1387-1395.
- Mori, Y., S. J. Chen and J. Varga (2003). Expression and regulation of intracellular SMAD signaling in scleroderma skin fibroblasts. *Arthritis Rheum* 48(7): 1964-1978.
- Moustakas, A. and C. H. Heldin (2009). The regulation of TGFbeta signal transduction. *Development* 136(22): 3699-3714.
- Murakami, K., Y. Ichinohe, M. Koike, N. Sasaoka, S. Iemura, T. Natsume and A. Kakizuka (2013). VCP Is an integral component of a novel feedback mechanism that controls intracellular localization of catalase and H₂O₂ Levels. *PLoS One* 8(2): e56012.
- Murrell, D. F. (1993). A radical proposal for the pathogenesis of scleroderma. *J Am Acad Dermatol* 28(1): 78-85.
- Nisimoto, Y., B. A. Diebold, D. Cosentino-Gomes and J. D. Lambeth (2014). Nox4: a hydrogen peroxide-generating oxygen sensor. *Biochemistry* 53(31): 5111-5120.
- Nozik-Grayck, E., H. B. Suliman and C. A. Piantadosi (2005). Extracellular superoxide dismutase. *Int J Biochem Cell Biol* 37(12): 2466-2471.
- O'Sullivan, B. and W. Levin (2003). Late radiation-related fibrosis: pathogenesis, manifestations, and current management. *Semin Radiat Oncol* 13(3): 274-289.
- Pendyala, S., J. Moitra, S. Kalari, S. R. Kleeberger, Y. Zhao, S. P. Reddy, J. G. Garcia and V. Natarajan (2011). Nrf2 regulates hyperoxia-induced Nox4 expression in human lung endothelium: identification of functional antioxidant response elements on the Nox4 promoter. *Free Radic Biol Med* 50(12): 1749-1759.
- Pendyala, S. and V. Natarajan (2010). Redox regulation of Nox proteins. *Respir Physiol Neurobiol* 174(3): 265-271.
- Peshavariya, H., F. Jiang, C. J. Taylor, S. Selemidis, C. W. Chang and G. J. Dusting (2009). Translation-linked mRNA destabilization accompanying serum-induced Nox4 expression in human endothelial cells. *Antioxid Redox Signal* 11(10): 2399-2408.

References

- Peshavariya, H. M., E. C. Chan, G. S. Liu, F. Jiang and G. J. Dusting (2014). Transforming growth factor-beta1 requires NADPH oxidase 4 for angiogenesis in vitro and in vivo. *J Cell Mol Med* 18(6): 1172-1183.
- Piccoli, C., R. Ria, R. Scrima, O. Cela, A. D'Aprile, D. Boffoli, F. Falzetti, A. Tabilio and N. Capitanio (2005). Characterization of mitochondrial and extra-mitochondrial oxygen consuming reactions in human hematopoietic stem cells. Novel evidence of the occurrence of NAD(P)H oxidase activity. *J Biol Chem* 280(28): 26467-26476.
- Pini, A., R. Shemesh, C. S. Samuel, R. A. D. Bathgate, A. Zauberman, C. Hermesh, A. Wool, D. Bani and G. Rotman (2010). Prevention of Bleomycin-Induced Pulmonary Fibrosis by a Novel Antifibrotic Peptide with Relaxin-Like Activity. *Journal of Pharmacology and Experimental Therapeutics* 335(3): 589-599.
- Piwkowska, A., D. Rogacka, I. Audzeyenka, M. Jankowski and S. Angielski (2011). High glucose concentration affects the oxidant-antioxidant balance in cultured mouse podocytes. *J Cell Biochem* 112(6): 1661-1672.
- Rahman, K. (2007). Studies on free radicals, antioxidants, and co-factors. *Clin Interv Aging* 2(2): 219-236.
- Rajkumar, V. S., X. Shiwen, M. Bostrom, P. Leoni, J. Muddle, M. Ivarsson, B. Gerdin, C. P. Denton, G. Bou-Gharios, C. M. Black and D. J. Abraham (2006). Platelet-derived growth factor-beta receptor activation is essential for fibroblast and pericyte recruitment during cutaneous wound healing. *Am J Pathol* 169(6): 2254-2265.
- Rajkumar, V. S., C. Sundberg, D. J. Abraham, K. Rubin and C. M. Black (1999). Activation of microvascular pericytes in autoimmune Raynaud's phenomenon and systemic sclerosis. *Arthritis Rheum* 42(5): 930-941.
- Razzaque, M. S. and T. Taguchi (2003). Pulmonary fibrosis: cellular and molecular events. *Pathol Int* 53(3): 133-145.
- Rinnerthaler, M., J. Bischof, M. K. Streubel, A. Trost and K. Richter (2015). Oxidative stress in aging human skin. *Biomolecules* 5(2): 545-589.
- Rizvi, F., T. Heimann and W. J. O'Brien (2012). Expression of NADPH oxidase (NOX)5 in rabbit corneal stromal cells. *PLoS One* 7(4): e34440.
- Rocic, P. and P. A. Lucchesi (2005). NAD(P)H Oxidases and TGF- β -Induced Cardiac Fibroblast Differentiation: Nox-4 Gets Smad. *Circulation Research* 97(9): 850-852.
- Rodino-Janeiro, B. K., B. Paradela-Dobarro, M. I. Castineiras-Landeira, S. Raposeiras-Roubin, J. R. Gonzalez-Juanatey and E. Alvarez (2013). Current status of NADPH oxidase research in cardiovascular pharmacology. *Vasc Health Risk Manag* 9: 401-428.

- Rotzer, D., M. Roth, M. Lutz, D. Lindemann, W. Sebald and P. Knaus (2001). Type III TGF-beta receptor-independent signalling of TGF-beta2 via TbetaRII-B, an alternatively spliced TGF-beta type II receptor. *Embo j* 20(3): 480-490.
- Sakai, N. and A. M. Tager (2013). Fibrosis of Two: Epithelial Cell-Fibroblast Interactions in Pulmonary Fibrosis. *Biochimica et biophysica acta* 1832(7): 911-921.
- Sambo, P., S. S. Baroni, M. Luchetti, P. Paroncini, S. Dusi, G. Orlandini and A. Gabrielli (2001). Oxidative stress in scleroderma: maintenance of scleroderma fibroblast phenotype by the constitutive up-regulation of reactive oxygen species generation through the NADPH oxidase complex pathway. *Arthritis Rheum* 44(11): 2653-2664.
- Sanders, Y. Y., H. Liu, G. Liu and V. J. Thannickal (2015). Epigenetic mechanisms regulate NADPH oxidase-4 expression in cellular senescence. *Free Radic Biol Med* 79: 197-205.
- Santos, C. X., A. A. Nabeebaccus, A. M. Shah, L. L. Camargo, S. V. Filho and L. R. Lopes (2014). Endoplasmic reticulum stress and Nox-mediated reactive oxygen species signaling in the peripheral vasculature: potential role in hypertension. *Antioxid Redox Signal* 20(1): 121-134.
- Santos, C. X., L. Y. Tanaka, J. Wosniak and F. R. Laurindo (2009). Mechanisms and implications of reactive oxygen species generation during the unfolded protein response: roles of endoplasmic reticulum oxidoreductases, mitochondrial electron transport, and NADPH oxidase. *Antioxid Redox Signal* 11(10): 2409-2427.
- Sargent, J. L., A. Milano, S. Bhattacharyya, J. Varga, M. K. Connolly, H. Y. Chang and M. L. Whitfield (2009). A TGF- β_1 Responsive Gene Signature Is Associated with a Subset of Diffuse Scleroderma with Increased Disease Severity. *J Invest Dermatol* 130(3): 694-705.
- Saw, C. L., A. Yang, M.-T. Huang, Y. Liu, J. Lee, T. Khor, Z.-Y. Su, L. Shu, Y. Lu, A. Conney and A.-N. Kong (2014). Nrf2 null enhances UVB-induced skin inflammation and extracellular matrix damages. *Cell & Bioscience* 4(1): 39.
- Scandalios, J. G. (2005). Oxidative stress: molecular perception and transduction of signals triggering antioxidant gene defenses. *Braz J Med Biol Res* 38(7): 995-1014.
- Schramm, A., P. Matusik, G. Osmenda and T. J. Guzik (2012). Targeting NADPH oxidases in vascular pharmacology. *Vascul Pharmacol* 56(5-6): 216-231.
- Schramm, A., P. Matusik, G. Osmenda and T. J. Guzik (2012). Targeting NADPH oxidases in vascular pharmacology. *Vascular pharmacology* 56(5-6): 216-231.
- Schröder, K., M. Zhang, S. Benkhoff, A. Mieth, R. Pliquett, J. Kosowski, C. Kruse, P. Luedike, U. R. Michaelis, N. Weissmann, S. Dimmeler, A. M. Shah and R. P. Brandes (2012). Nox4 is a protective reactive oxygen species generating vascular NADPH oxidase. *Circ Res* 110(9): 1217-1225.

References

- Sedeek, M., G. Callera, A. Montezano, A. Gutsol, F. Heitz, C. Szyndralewicz, P. Page, C. R. Kennedy, K. D. Burns, R. M. Touyz and R. L. Hebert (2010). "Critical role of Nox4-based NADPH oxidase in glucose-induced oxidative stress in the kidney: implications in type 2 diabetic nephropathy." *Am J Physiol Renal Physiol* 299(6): F1348-1358.
- Sedeek, M., A. Gutsol, A. C. Montezano, D. Burger, A. Nguyen Dinh Cat, C. R. Kennedy, K. D. Burns, M. E. Cooper, K. Jandeleit-Dahm, P. Page, C. Szyndralewicz, F. Heitz, R. L. Hebert and R. M. Touyz (2013). Renoprotective effects of a novel Nox1/4 inhibitor in a mouse model of Type 2 diabetes. *Clin Sci (Lond)* 124(3): 191-202.
- Servettaz, A., P. Guilpain, C. Goulvestre, C. Chereau, C. Hercend, C. Nicco, L. Guillevin, B. Weill, L. Mouthon and F. Batteux (2007). Radical oxygen species production induced by advanced oxidation protein products predicts clinical evolution and response to treatment in systemic sclerosis. *Ann Rheum Dis* 66(9): 1202-1209.
- Sfrent-Cornateanu, R., C. Mihai, I. Stoian, D. Lixandru, C. Bara and E. Moldoveanu (2008). Antioxidant defense capacity in scleroderma patients. *Clin Chem Lab Med* 46(6): 836-841.
- Siuda, D., U. Zechner, N. El Hajj, D. Prawitt, D. Langer, N. Xia, S. Horke, A. Pautz, H. Kleinert, U. Forstermann and H. Li (2012). Transcriptional regulation of Nox4 by histone deacetylases in human endothelial cells. *Basic Res Cardiol* 107(5): 283.
- Spadoni, T., S. Svegliati Baroni, D. Amico, L. Albani, G. Moroncini, E. V. Avvedimento and A. Gabrielli (2015). A reactive oxygen species-mediated loop maintains increased expression of NADPH oxidases 2 and 4 in skin fibroblasts from patients with systemic sclerosis. *Arthritis Rheumatol* 67(6): 1611-1622.
- Stegemann, A., A. Sindrilaru, B. Eckes, A. del Rey, A. Heinick, J. S. Schulte, F. U. Muller, S. A. Grando, B. L. Fiebich, K. Scharffetter-Kochanek, T. A. Luger and M. Böhm (2013). Tropisetron suppresses collagen synthesis in skin fibroblasts via alpha7 nicotinic acetylcholine receptor and attenuates fibrosis in a scleroderma mouse model. *Arthritis Rheum* 65(3): 792-804.
- Stern, E. P. and C. P. Denton (2015). The Pathogenesis of Systemic Sclerosis. *Rheum Dis Clin North Am* 41(3): 367-382.
- Stuehr, D. J., O. A. Fasehun, N. S. Kwon, S. S. Gross, J. A. Gonzalez, R. Levi and C. F. Nathan (1991). Inhibition of macrophage and endothelial cell nitric oxide synthase by diphenylethylidenehydrazine and its analogs. *Faseb j* 5(1): 98-103.
- Sturrock, A., B. Cahill, K. Norman, T. P. Huecksteadt, K. Hill, K. Sanders, S. V. Karwande, J. C. Stringham, D. A. Bull, M. Gleich, T. P. Kennedy and J. R. Hoidal (2006). Transforming growth factor-beta1 induces Nox4 NAD(P)H oxidase and reactive oxygen species-dependent proliferation in human pulmonary artery smooth muscle cells. *Am J Physiol Lung Cell Mol Physiol* 290(4): L661-1673.

References

- t Hart, B. A., J. M. Simons, S. Knaan-Shanzer, N. P. Bakker and R. P. Labadie (1990). Antiarthritic activity of the newly developed neutrophil oxidative burst antagonist apocynin. *Free Radic Biol Med* 9(2): 127-131.
- Takac, I., K. Schröder, L. Zhang, B. Lardy, N. Anilkumar, J. D. Lambeth, A. M. Shah, F. Morel and R. P. Brandes (2011). The E-loop is involved in hydrogen peroxide formation by the NADPH oxidase Nox4. *J Biol Chem* 286(15): 13304-13313.
- Takagawa, S., G. Lakos, Y. Mori, T. Yamamoto, K. Nishioka and J. Varga (2003). Sustained activation of fibroblast transforming growth factor-beta/Smad signaling in a murine model of scleroderma. *J Invest Dermatol* 121(1): 41-50.
- Tamby, M. C., Y. Chanseaud, L. Guillevin and L. Mouthon (2003). New insights into the pathogenesis of systemic sclerosis. *Autoimmun Rev* 2(3): 152-157.
- Tejada-Simon, M. V., F. Serrano, L. E. Villasana, B. I. Kanterewicz, G. Y. Wu, M. T. Quinn and E. Klann (2005). Synaptic localization of a functional NADPH oxidase in the mouse hippocampus. *Mol Cell Neurosci* 29(1): 97-106.
- Ten Dijke, P. and H. M. Arthur (2007). Extracellular control of TGFbeta signalling in vascular development and disease. *Nat Rev Mol Cell Biol* 8(11): 857-869.
- Ten Freyhaus, H., M. Huntgeburth, K. Wingler, J. Schnitker, A. T. Baumer, M. Vantler, M. M. Bekhite, M. Wartenberg, H. Sauer and S. Rosenkranz (2006). Novel Nox inhibitor VAS2870 attenuates PDGF-dependent smooth muscle cell chemotaxis, but not proliferation. *Cardiovasc Res* 71(2): 331-341.
- Thannickal, V. J. and B. L. Fanburg (1995). Activation of an H₂O₂-generating NADH oxidase in human lung fibroblasts by transforming growth factor beta 1. *J Biol Chem* 270(51): 30334-30338.
- Towbin, H., T. Staehelin and J. Gordon (1979). Electrophoretic transfer of proteins from polyacrylamide gels to nitrocellulose sheets: procedure and some applications. *Proc Natl Acad Sci U S A* 76(9): 4350-4354.
- Tsai, M. H. and M. J. Jiang (2010). Reactive oxygen species are involved in regulating alpha1-adrenoceptor-activated vascular smooth muscle contraction. *J Biomed Sci* 17: 67.
- Tsou, P. S., B. Balogh, A. J. Pinney, G. Zakhem, A. Lozier, M. A. Amin, W. A. Stinson, E. Schiopu, D. Khanna, D. A. Fox and A. E. Koch (2014). Lipoic acid plays a role in scleroderma: insights obtained from scleroderma dermal fibroblasts. *Arthritis Res Ther* 16(5): 411.
- Ushio-Fukai, M. (2008). Compartmentalization of Redox Signaling Through NADPH Oxidase-Derived ROS. *Antioxidants & Redox Signaling* 11(6): 1289-1299.

References

- Valko, M., D. Leibfritz, J. Moncol, M. T. Cronin, M. Mazur and J. Telser (2007). "Free radicals and antioxidants in normal physiological functions and human disease. *Int J Biochem Cell Biol* 39(1): 44-84.
- van der Rest, M. and R. Garrone (1991). Collagen family of proteins." *Faseb j* 5(13): 2814-2823.
- Van Laar, J. M. and J. Varga (2015). The immunopathology of systemic sclerosis. *Semin Immunopathol*.
- Varga, J. and D. Abraham (2007). Systemic sclerosis: a prototypic multisystem fibrotic disorder. *J Clin Invest* 117(3): 557-567.
- Varga, Z. V., K. Kupai, G. Szucs, R. Gaspar, J. Paloczi, N. Farago, A. Zvara, L. G. Puskas, Z. Razga, L. Tiszlavicz, P. Bencsik, A. Gorbe, C. Csonka, P. Ferdinandy and T. Csont (2013). MicroRNA-25-dependent up-regulation of NADPH oxidase 4 (NOX4) mediates hypercholesterolemia-induced oxidative/nitrative stress and subsequent dysfunction in the heart. *J Mol Cell Cardiol* 62: 111-121.
- Vecchio, D., A. Acquaviva, B. Arezzini, H. Tenor, P. A. Martorana and C. Gardi (2013). Downregulation of NOX4 expression by roflumilast N-oxide reduces markers of fibrosis in lung fibroblasts. *Mediators Inflamm* 2013: 745984.
- Verrecchia, F., A. Mauviel and D. Farge (2006). Transforming growth factor-beta signaling through the Smad proteins: role in systemic sclerosis. *Autoimmun Rev* 5(8): 563-569.
- Viswanath, V., M. M. Phiske and V. V. Gopalani (2013). Systemic sclerosis: current concepts in pathogenesis and therapeutic aspects of dermatological manifestations. *Indian J Dermatol* 58(4): 255-268.
- Vives-Bauza, C., A. Starkov and E. Garcia-Arumi (2007). Measurements of the antioxidant enzyme activities of superoxide dismutase, catalase, and glutathione peroxidase. *Methods Cell Biol* 80: 379-393.
- von Lohneysen, K., D. Noack, A. J. Jesaitis, M. C. Dinauer and U. G. Knaus (2008). Mutational analysis reveals distinct features of the Nox4-p22 phox complex. *J Biol Chem* 283(50): 35273-35282.
- Wan, K. C. and J. H. Evans (1999). Free radical involvement in hypertrophic scar formation. *Free Radic Biol Med* 26(5-6): 603-608.
- Wan, K. C., H. T. Wu, H. P. Chan and L. K. Hung (2002). Effects of antioxidants on pyridinoline cross-link formation in culture supernatants of fibroblasts from normal skin and hypertrophic scars. *Clin Exp Dermatol* 27(6): 507-512.
- Weake, V. M. and J. L. Workman (2010). Inducible gene expression: diverse regulatory mechanisms. *Nat Rev Genet* 11(6): 426-437.

References

- Wells, R. G. (2010). The epithelial-to-mesenchymal transition in liver fibrosis: here today, gone tomorrow? *Hepatology* 51(3): 737-740.
- Weyemi, U., B. Caillou, M. Talbot, R. Ameziane-El-Hassani, L. Lacroix, O. Lagent-Chevallier, A. Al Ghuzlan, D. Roos, J. M. Bidart, A. Virion, M. Schlumberger and C. Dupuy (2010). Intracellular expression of reactive oxygen species-generating NADPH oxidase NOX4 in normal and cancer thyroid tissues. *Endocr Relat Cancer* 17(1): 27-37.
- Weyemi, U., C. E. Redon, T. Aziz, R. Choudhuri, D. Maeda, P. R. Parekh, M. Y. Bonner, J. L. Arbiser and W. M. Bonner (2015). Inactivation of NADPH Oxidases NOX4 and NOX5 Protects Human Primary Fibroblasts from Ionizing Radiation-Induced DNA Damage. *Radiation Research* 183(3): 262-270.
- Wind, S., K. Beuerlein, T. Eucker, H. Muller, P. Scheurer, M. E. Armitage, H. Ho, H. H. Schmidt and K. Wingler (2010). Comparative pharmacology of chemically distinct NADPH oxidase inhibitors. *Br J Pharmacol* 161(4): 885-898.
- Winterbourn, C. C. and M. B. Hampton (2008). Thiol chemistry and specificity in redox signaling. *Free Radic Biol Med* 45(5): 549-561.
- Yamamoto, T. (2006). Bleomycin and the skin. *British Journal of Dermatology* 155(5): 869-875.
- Yamamoto, T. (2010). Animal model of systemic sclerosis. *J Dermatol* 37(1): 26-41.
- Yamamoto, T., B. Eckes and T. Krieg (2000). Bleomycin increases steady-state levels of type I collagen, fibronectin and decorin mRNAs in human skin fibroblasts. *Archives of Dermatological Research* 292(11): 556-561.
- Yamamoto, T. and I. Katayama (2011). Vascular changes in bleomycin-induced scleroderma. *Int J Rheumatol* 2011: 270938.
- Yamamoto, T. and K. Nishioka (2005). Cellular and molecular mechanisms of bleomycin-induced murine scleroderma: current update and future perspective. *Exp Dermatol* 14(2): 81-95.
- Yamamoto, T., S. Takagawa, I. Katayama, K. Yamazaki, Y. Hamazaki, H. Shinkai and K. Nishioka (1999). Animal model of sclerotic skin. I: Local injections of bleomycin induce sclerotic skin mimicking scleroderma. *J Invest Dermatol* 112(4): 456-462.
- Yamane, K., H. Ihn, M. Kubo and K. Tamaki (2002). Increased transcriptional activities of transforming growth factor beta receptors in scleroderma fibroblasts. *Arthritis Rheum* 46(9): 2421-2428.
- Yang, S., Y. Zhang, W. Ries and L. Key (2004). Expression of Nox4 in osteoclasts. *J Cell Biochem* 92(2): 238-248.

References

Yarnold, J. and M. C. Brotons (2010). Pathogenetic mechanisms in radiation fibrosis. *Radiother Oncol* 97(1): 149-161.

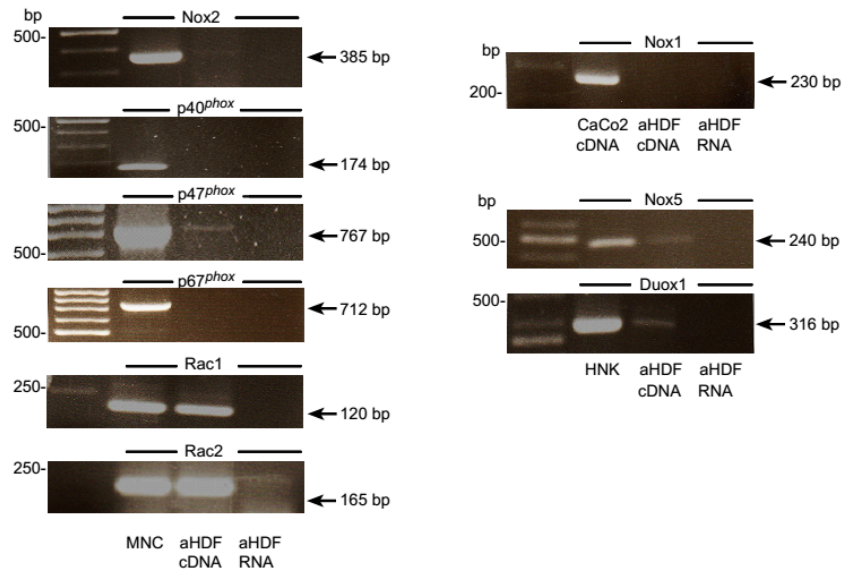
Yildirim, Z., M. Kotuk, M. Iraz, I. Kuku, R. Ulu, F. Armutcu and S. Ozen (2005). Attenuation of bleomycin-induced lung fibrosis by oral sulfhydryl containing antioxidants in rats: erdosteine and N-acetylcysteine. *Pulm Pharmacol Ther* 18(5): 367-373.

Yoshida, L. S. and S. Tsunawaki (2008). Expression of NADPH oxidases and enhanced H₂O₂-generating activity in human coronary artery endothelial cells upon induction with tumor necrosis factor- α . *Int Immunopharmacol* 8(10): 1377-1385.

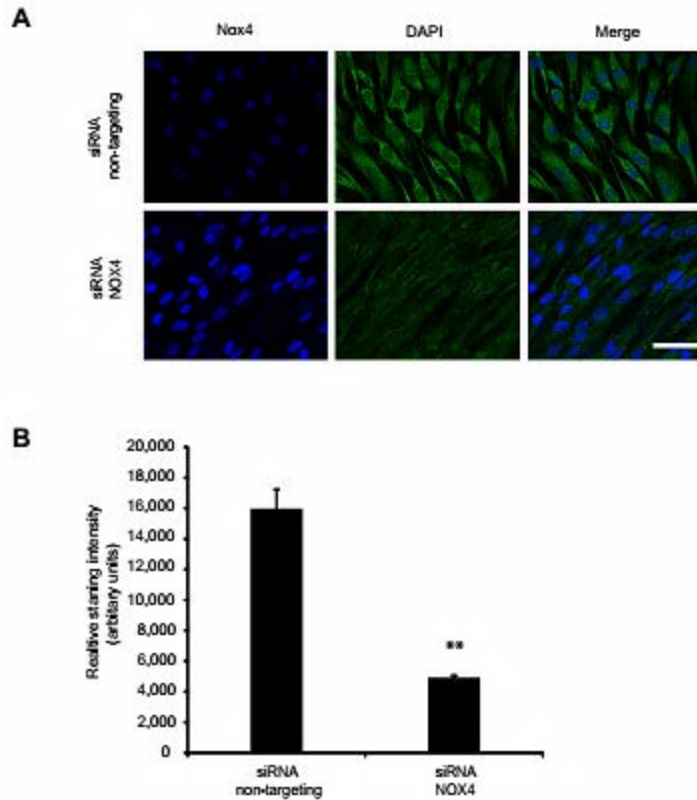
Yoshiko, Y., K. Hirao and N. Maeda (2002). Differentiation in C(2)C(12) myoblasts depends on the expression of endogenous IGFs and not serum depletion. *Am J Physiol Cell Physiol* 283(4): C1278-1286.

Zhang, L., O. R. Sheppard, A. M. Shah and A. C. Brewer (2008). Positive regulation of the NADPH oxidase NOX4 promoter in vascular smooth muscle cells by E2F. *Free Radic Biol Med* 45(5): 679-685.

Zhao, Q. D., S. Viswanadhapalli, P. Williams, Q. Shi, C. Tan, X. Yi, B. Bhandari and H. E. Abboud (2015). NADPH oxidase 4 induces cardiac fibrosis and hypertrophy through activating Akt/mTOR and NF κ B signaling pathways. *Circulation* 131(7): 643-655.



Appendix Figure 1. Expression analysis of additional Nox isoforms, adaptor proteins as well as Rac1 and Rac2 in normal adult HDFs by endpoint RT-PCR analysis. Expression analysis of additional Nox isoforms, adaptor proteins as well as Rac1 and Rac2 in normal nHDFs by endpoint RT-PCR analysis. State of the art positive controls consisted of cDNA from HUVEC, normal human keratinocytes (NHKs), human peripheral blood monocytes (MNC) and the human colon carcinoma cell line CaCo2. Negative controls consisted of HDF templates without RT. Depicted are representative images from RT-PCR analyses of n=3 donors.



Appendix Figure 2. Confirmation the specificity of Nox4 antibody. (A) nHDFs were transfected with non-targeting siRNA or Nox4 siRNA for 48 hours followed by fixation and immunofluorescence staining with anti-Nox4 (AlexaFluor488; green). (B) Relative staining intensity was evaluated using Image J software. Images are representative for 3 independent experiments with similar results. Scale bar: 50 μ m. Bars represent the means \pm SEM. n=3; *p<0.05 vs. non-targeting siRNA.

Name Heba Dosoki
Geburtsdatum 24.09.1983
Staatsangehörigkeit Egyptian
Eltern Father. Salah Eldeen Dosoki
Mother. Neamat Elabrashy
E-mail hebasalah40@gmail.com

Schulbildung

1990-1994 The primary school “Omar Makram” (Alexandria, Egypt)
1994-1997 The preparatory school “Ibn Khaldoon” (Alexandria, Egypt)
1997-2000 The secondary school “Isis” (Alexandria, Egypt)

Studium

2000-2004 Bachelor of Science in Biology, Faculty of science, Alexandria University, Egypt
2005 Visiting the Pre-Master courses at Faculty of science, Alexandria University, Egypt
2005-2008 Master of Science in Microbiology, Faculty of science, Alexandria University, Egypt, with the title (Effect of some Local Probiotics on Immunological and Biological Systems of Experimental Animals)
2008-2009 Acquisition of the academic degree M.Sc. (Microbiology). Assistant lecturer, Department of Microbiology, Faculty of Science, Alexandria University, Egypt
March 2010 Acquisition of the DAAD full-PhD scholarship (GERLS)
March -June 2010 German courses at Goethe-Institute Alexandria (Alexandria, Egypt)
October2010-March 2011 German courses at Goethe-Institute (Göttingen, Germany)

Promotionsstudium

Since April2011 Ph.D student, Department of Dermatology (**Prof. Dr.med.Markus Böhm**), University of Münster, Münster, Germany with the title. “ **The Role of NADPH Oxidase in the Pathogenesis of Systemic Sclerosis**”.

Publications

Poster presentations

- Dosoki H**, Stegemann A, Weiß N, Luger T, Kerkhoff C, Böhm M. Nox4 - an emerging target for the future treatment Of Scleroderma? International Investigative Dermatology May 8-11, 2013, Edinburgh, UK.
- Dosoki H**, Stegemann A, Weiß N, Luger T, Kerkhoff C, Böhm M. Nox4 - an intrinsic mediator of transforming growth factor-beta1-induced fibroblast activation and a target for the neuropeptide alpha-melanocyte-stimulating hormone. 40th Annual meeting of the Arbeitsgemeinschaft Dermatologische Forschung (ADF), March 13-15, 2014, Köln, Germany.
- Dosoki H**, Stegemann A, Weiß N, Luger T, Kerkhoff C, Böhm M. Nox4 - an intrinsic mediator of transforming growth factor-beta1-induced fibroblast activation and a target for the neuropeptide alpha-melanocyte-stimulating hormone. Annual Meeting of the German Society for Matrix Biology (GSMB), March 20-22, 2014, Regensburg, Germany.
- Dosoki H**, Stegemann A, Weiß N, Luger T, Kerkhoff C, Böhm M. Nox4 - an emerging target for the future treatment Of Scleroderma?. Gordon Research Conference "NOX Family NADPH Oxidases", May 17-23, 2014, Italy.
- Dosoki H**, Stegemann A, Taha M, Schnittler H, Hashimoto K, Kudla J, Luger TA, Kerkhoff C, Böhm M. The NADPH oxidase isoform Nox4 controls TGF-beta1-mediated activation of human dermal fibroblasts - a promising new target for the treatment of systemic sclerosis? International Investigative Dermatology September 10-13, 2014, Copenhagen, Denmark.
- Dosoki H**, Stegemann A, Taha M, Schnittler H, Hashimoto K, Kudla J, Luger TA, Kerkhoff C, Böhm M. The NADPH oxidase isoform Nox4 controls TGF-beta1-mediated activation of human dermal fibroblasts - a promising new target for the treatment of systemic sclerosis? 41th Annual meeting of the Arbeitsgemeinschaft Dermatologische Forschung (ADF), March 5-7, 2015, ULM, Germany.

Oral presentations

- Dosoki H**, A. Stegemann, N. Weiß, T. Luger, C. Kerkhoff, M. Böhm. Nox4 - an intrinsic mediator of transforming growth factor-beta1-induced fibroblast activation and a target for the neuropeptide alpha-melanocyte-stimulating hormone. 40th Annual meeting of the Arbeitsgemeinschaft Dermatologische Forschung (ADF), Köln, March 13-15, 2014.

Publications

- Böhm M, **Dosoki H**, Kerkhoff C. Is Nox4 a key regulator of the activated state of fibroblasts in systemic sclerosis? *Exp Dermatol* 2014; 23: 679-81.
- Dosoki H**, Stegemann A, Taha M, Schnittler H, Luger TA, Schröder K, Distler J, Kerkhoff K, Böhm M. Nox4 is a crucial mediator of TGF- β 1-induced collagen synthesis and myofibroblast activation of dermal fibroblasts. *Arthritis Rheum*, in revision.

Münster, den (.....)

(Unterschrift.....)

